Development of an Integrated Risk Analysis System (ARCTRA) for Runoff Related Heavy Metal Contaminant in Unsaturated Zone

Ziyang Zhang

A Thesis

In

the Department

of

Building, Civil and Environmental Engineering

Presented in Partial Fulfillment of the Requirements

For the Degree of

Master of Applied Science (Civil Engineering) at

Concordia University

Montreal, Quebec, Canada

November, 2017

CONCORDIA UNIVERSITY

School of Graduate Studies

This is to certify that the thesis prepared

By: Ziyang Zhang

Entitled: Development of an Integrated Risk Analysis System (ARCTRA) for Runoff Related Heavy Metal Contaminant in Unsaturated Zone

and submitted in partial fulfillment of the requirements for the degree of

Master of Applied Science (Civil Engineering)

complies with the regulations of the University and meets the accepted standards with respect to originality and quality.

Signed by the final examining committee:

_____ Chair

Dr. C. Mulligan

_____ External of Program

Dr. M. Y. Chen

_____ Examiner

Dr. S. Rahaman

_____ Examiner

Dr. C. Mulligan

_____ Thesis Supervisor

Dr. Z. Chen

Approved by _____

Chair of Department or Graduate Program Director

_____ 2017 _____

Dean of Faculty

ABSTRACT

Development of an Integrated Risk Analysis System (ARCTRA) for Runoff Related Heavy Metal Contaminant in Unsaturated Zone

Ziyang Zhang

An integrated analytical runoff and contaminant transport risk analysis system (ARCTRA) is developed for assessing the environmental risks associated with heavy metal transport in the unsaturated zone. The ARCTRA system considers three processes: rainfall runoff, soil erosion and solute transport in soil. A corresponding analytical solution is applied for each process. Particularly, a Monte Carlo simulation is integrated to quantify the uncertainties associated with key model parameters after model sensitivity analysis. Moreover, the Fuzzy Set risk assessment method is employed to quantify incomplete-type uncertainties associated with the site conditions, environmental quality guidelines and health impact criteria based on the Monte Carlo Probability Simulation. Fuzzy membership functions are established considering the environmental-guideline-based risk (ER) and health risk (HR) to obtain a generalized risk level through a fuzzy rule base. An integrated risk value can be then obtained to evaluate and rank the risk level of a contaminated site. Finally, a user interface was developed for the ARCTRA system based on the VB program code in Excel to facilitate technology transfer and to provide a user-friendly system to assist in the processing of input and calculation of results. The ARCTRA system developed in this

study can be used to systematically assess the heavy metal in the unsaturated zone caused by rainfall-runoff process and support effective management of the contaminated site.

The developed ARCTRA system was verified through compassion analysis against existing models. Specifically, the rainfall-runoff section was compared with the PCSWMM model which simulates the runoff formation under given rainfall conditions. In the soil erosion part, an analytic solution from the Hairsine-Rose model was studied to conduct a comparative analysis of the concentration of heavy metal dissolved in the surface runoff. And, the ARCTRA module for analyzing transport of contaminants in the soil is examined against the STANMOD and the HYDRUS model. Two real cases were studied in this thesis. Pb and Zn were studied in the case studies. The results of the ARCTRA and other existing models were obtained based on the real case data and compared with monitoring data. The model verification and validation indicates the developed ARCTRA system is useful in assessing the risks of heavy metals in the soil caused by the rainfall-runoff process.

Acknowledgment

First of all, I would like to express my appreciation to my supervisor, Dr. Z. Chen sincerely, for his continuous support and generous, careful suggestion in my whole Master studies. Dr. Chen always listens to my idea and process of study patiently and give me feedback, advice and encouragement timely. Not only he teaches me a lot in doing research with persistence, but also he shows me how to accomplish my study and daily life. Therefore, his support are greatly helpful for my future career and these invaluable assets are also benefit enormously in my entire life.

Moreover, also thanks to my colleagues in our research group and my friends, for their valuable and helpful assistance in any aspects of my research and studies. They give me sufficient encouragement and more inspiration.

I extend my deep gratitude to my father, my mother and other relatives for their unconditional mortal support and solitude. Without their support and standing by me all the time, I cannot overcome the difficult time I encountered during the whole studies.

Table of Contents

List of Figures

List of Tables

List of Symbols

a: The soil detachability [ML^{-3}]

A: The surface area of subcatchment [L^2]

AT: Averaging time [T]

BW: Average body weight [M]

c: The dissolved chemical concentration at the soil surface [ML^{-3}]

c_r: The dissolved contaminant concentration in surface runoff [ML^{-3}]

C_e: The solute concentration in the exchange layer [ML^{-3}]

C_s: The soil quality standard [MM^{-1}]

C_w: The solute concentration in runoff water [ML^{-3}]

CDI: The chronic daily intake [$MM^{-1}T^{-1}$]

CW: The pollutant concentration in soil [MM^{-1}]

d: The depth of water over the subcatchment [L]

d_e: The depth of the exchange layer [L]

d_s: The depression storage depth[L]

D: The dispersion coefficient [L^2T^{-1}]

D_0:The ionic or molecular diffusion coefficient in pure water [L^2T^{-1}]

Ds: Diffusivity [L^2T^{-1}]

D_x and D_y: The dispersion coefficients in the x- and y- directions [L^2T^{-1}] respectively and X is the position in the flow direction

e_r: The rainfall-induced water transfer rate [LT^{-1}]

ED: Average exposure duration [T]

EF: Exposure frequency [TT^{-1}]

f: The rainfall rate [LT^{-1}]

g: The acceleration due to gravity [L^2T^{-1}]

h: The depth of surface runoff [L]

i: The infiltration rate [LT^{-1}]

IR: Human ingestion rate [$MM^{-1}T^{-1}$],

J: The solute mass flux density [L^2T^{-1}]

k: The convective mass transfer coefficient [LT^{-1}]

K: The unsaturated hydraulic conductivity function [LT^{-1}]

K_d: The distribution coefficient of the solute between liquid and solid phases [LM^{-3}]

Kr: The relative hydraulic conductivity [LT^{-1}]

Ks: The saturated hydraulic conductivity [LT^{-1}]

M: The initial input of contaminant [MT^{-1}]

N: Manning's surface roughness coefficient for overland flow []

P: Probability []

q: The surface runoff flow rate per unit width [L^2T^{-1}]

Q: The runoff volumetric flow rate [L^3T^{-1}]

Qr: The runoff water flux [L^3T^{-1}]

R: The retardation factor []

Re: Reynolds' number []

s: The uniform soil slope []

t: time [T]

t_e: Equilibrium time [T]

v: The kinematic velocity of water [LT^{-1}]

W: The subcatchment width [L]

x: The axis along the slope [L]

α_L : Dispersivity [L]

θ: The volumetric content [L^3L^{-3}]

β: The angle between the flow direction and the vertical axis []

ρ_b : The soil bulk density [ML^{-3}]

λ : The tortuosity factor []

τ : The mean residence time of a runoff water element in the field [T]

μ: First-order rate coefficient for decay [T^{-1}]

μ_{er} : A final membership of environmental-guideline-based risk []

μ_{g} : The function of guideline membership grade []

μ_{gr} : The generalized risk membership grade []

μ_{hr} : The health risk membership grade []

List of Abbreviation and Acronyms

3DADE: 3-Dimensional Advection-Dispersion Equation

ADE: Advection-Dispersion Equation

ARCTRA: The Analytical Runoff and Contaminant Transport Risk Analysis System

ARR: Australian Rainfall and Runoff

CCME: Canadian Council of Ministers of the Environment

CDF: Cumulative Distribution Function

ER: Environmental-guideline-based Risk

ERA: Environmental-guideline-based Risk Assessment

GIN: Groundwater Information Network

GIS: Geographic Information System

GRL: Generalized risk Level

HI: Health Index

H-R: Hairsine-Rose

HR: Health Risk

HRA: Health Risk Assessment

HYSIM: Hydrological Simulation Model

IFD: Intensity-Frequency-Duration

MCS: Monte Carlo Simulation

MEF: Ministry of the Environment, Finland

NOAA: National Oceanic and Atmospheric Administration

NSC: National Safety Council

PDF: Probability Density Function

PRMS: Precipitation Runoff Modeling System

RfD: Reference Dose

RPRT: Politique de Protection des Sols et de Réhabilitation des Terrains Contaminés

SF: Slope Factor

STANMOD: Studio of Analytical Models

SWMM: Storm Water Management Model

UNESCO: United Nations Educational Scientific and Cultural Organizations

USEPA: United States Environmental Protection Agency

USGS: United States Geological Survey

VB: Visual Basic

1. INTRODUCTION

1.1 Background

Heavy metals are dense metals which can be found naturally in soil at low concentrations. However, heavy metals can accumulate in soil and surface water as a consequence of industrial activities such as mining and the disposal of heavy metal waste products (Khan et al., 2008). These industrial activities can result in the contamination of soil by heavy metals such as lead (Pb), chromium (Cr), zinc (Zn), cadmium (Cd) and copper (Cu), which can remain in the soil for an extended period. Heavy metal contamination may represent a hazard to humans and the ecosystem via bioaccumulation, through the food chain as well as by direct ingestion or contact with contaminated soil or groundwater (McLaughlin et al., 2000). For example, the direct ingestion of Pb-contaminated soil or dust may lead to poisoning (plumbism) or even death. When exposed to lead, adults usually experience loss of memory, nausea, insomnia, anorexia and weakness of the joints (NSC, 2009). Zn toxicity in human includes vomiting, dehydration, drowsiness, lethargy, electrolytic imbalance, abdominal pain, nausea, lack of muscular coordination and renal failure. Chronic doses of Zn increase the risk of developing anemia and pancreatic damage and possibly enhance the symptoms of Alzheimer's disease (Plum et al., 2010).

When contaminants such as heavy metals are disposed of at the soil surface, they can be transported into the soil and groundwater by dispersion and diffusion. However, as urban flooding has increased, rainfall-runoff has also become a significant pathway

for heavy metal transport in soil. Surface runoff floods can be formed when both the soil and the urban drainage systems have insufficient capacity to handle high-intensity rainfall. As the rainfall-runoff accumulates at the soil surface, it etches the soil and absorbs its particles as well as its contaminants. As a result, the heavy metals dissolve into the runoff and form solute which is transported into the soil and subterranean water through infiltration. Pollution via runoff in urban areas can be regarded as non-point source pollution because it sometimes enters water bodies directly without storm drain systems. Therefore, pollution by runoff has the potential to contaminate soil, groundwater and surface water. It is important to research the process of chemical fate and transport through runoff.

Various types of uncertainties in the transport process, such as chemical characteristics and physical parameters, are also considered in this study. The uncertainties are expressed as probability distributions of uncertainties of randomness done by Monte Carlo Simulation (Darbra et al., 2008). A risk assessment method based on fuzzy set theory is also developed to quantify the risk of the study area site. Fuzzy set theory is widely used to generate acceptable quantitative results associated with environmental guidelines.

1.2 Objectives

The purpose of this thesis is to develop an integrated ARCTRA system to simulate the soil erosion caused by heavy metals via rainfall-runoff and relative solute transport processes. Meanwhile, several existing models are also applied for comparison and

validation of the ARCTRA system. The detailed objectives of this research are as follows:

(1) To study the integration of the three relative processes: rainfall-runoff, the dissolution (or desorption) of heavy metal from the contaminated surface and the transport of heavy metals in the soil.

(2) To develop an integrated ARCTRA system with analytical solutions to examine the fate and transport of heavy metal in the unsaturated zone after rainfall-runoff process.

(3) To integrate the analytical solutions in ARCTRA system handling rainfall-runoff, contaminant transport in runoff and soil, the ARCTRA system is combined with non-classical risk assessment analysis, including Monte Carlo Simulation and fuzzy set theory.

(4) To test and improve the ARCTRA system by compassion analysis against existing models. The PCSWMM model, the Hairsine-Rose soil erosion model and the HYDRUS model are employed as a comparison analysis method. To validate both the models and the ARCTRA system, the results were verified by comparison with the literature data.

1.3 Thesis Organization

This thesis is organized into the following six chapters:

Chapter 1 presents a general introduction about heavy metal contamination, fate

and transport modeling process of chemical as well as the research objectives.

Chapter 2 gives the literature review about recent studies of chemical transport in soil by runoff, including rainfall-runoff formation, soil erosion and solute transport, and the effect of non-point source pollution by runoff in surface water, soil and groundwater.

Chapter 3 explains the methodology of the thesis, including the introduction of applied models for comparison, the governing equations and development of ARCTRA system, including the Monte Carlo Simulation and fuzzy set theory for risk assessment system.

Chapter 4 presents the first case study with existing models in the thesis study, including the area description, model application and results, comparison, discussion and Monte Carlo Simulation. Part of the ARCTRA system was applied in this case study and compared with the existing models.

Chapter 5 presents the second case study which the integrated ARCTRA system and existing models were applied. The results of ARCTRA system were compared with the existing models with detailed analysis and the case study was further extended by Monte Carlo Simulation and Fuzzy Set Risk Assessment.

Chapter 6 concludes the results of this thesis, presents a list of contributions and suggestions for future studies.

2. LITERATURE REVIEW

2.1 Modeling of Chemical Transport in Soil with Runoff

2.1.1 Surface runoff

Surface runoff can be regarded as free water movement overland with the influence of gravity forces, which appears in river or water body nearby. Runoff can be described as a part of water circulation that flows over land instead of being absorbed into groundwater or evaporating. Runoff is part of the precipitation, snowmelt, or irrigation water at the soil surface. A variety of factors can affect runoff, including rainfall amount, permeability, vegetation and slope (USGS, 2008). For example, a surface with high absorption ability has high permeability, and a surface with low absorption ability has low permeability.

The two main effects of runoff are erosion and pollution. Runoff can collect things from soil surface, transport them and deposit off in downstream. Moreover, urbanization leads to increased impervious surfaces such as pavement and buildings, which do not allow water to infiltrate into the soil to the aquifer (Frazer, 2005). Surface runoff influences surface water, groundwater and soil through transport of pollutants into these systems. Ultimately these impacts translate into human health risk, ecosystem disturbance and damage to water resources. When contaminants are dissolved or suspended in runoff, it creates water pollution. This pollutant load can reach various receiving systems such as soil, rivers, lakes and oceans.

Many efforts have been paid for developing analytical solution to estimate the formation of rainfall-runoff. Kinematic Wave Model and Green Ampt solution based

on Richard's Equation are the most common models for rainfall-runoff. Hjelmfelt (1981) obtained an analytical solution of the kinematic wave model for constant rainfall intensity in time and space. Mizumura (1992, 2006) developed analytical solutions of the kinematic wave model for time- and space-varying excess rainfall. The solutions are obtained considering rainfall variation and infiltration (Smith and Goodrich, 2000; Govindaraju et al., 2001; Morbidelli et al., 2006).

Many models and software have been developed to simulate the rainfall-runoff activities, such as Precipitation Runoff Modeling System (PRMS) (Markstrom et al., 2015) and HYSIM (Hydrological Simulation Model) (UNESCO, 1975). Among which, Storm Water Management Model (SWMM) by USEPA is considered the most popular. PCSWMM is a commercial software which automatically maintains standard US EPA SWMM5 model from GIS data combing with a complete GIS system tailored to urban drainage modeling which supports most projections, datum, and ellipsoids. PCSWMM is a distributed model, which means that a study area can be subdivided into any number of irregular subcatchments considering the land cover, and soil characteristics have on runoff generation. Each subcatchment can be further divided into three areas: an impervious area with depression (detention) storage or without depression storage and a previous area with depression storage.

2.1.2 Soil contamination erosion by surface runoff

When runoff flows along the ground surface, it can transport soil contaminants, causing non-point source pollution (Mackenzie and Masten, 2008). In the case of the overland runoff, there are two ways by which heavy metals at the soil surface can be transformed

into solution form by precipitation: (1) dissolution of heavy metals in solid form and (2) desorption of adsorbed or absorbed heavy metals from the soil. The solute transfer from the soil surface to the runoff flow is difficult to predict because many complex processes are occurring simultaneously. These processes include the transfer of solutes from the soil surface via (1) diffusion by the concentration gradient, (2) the ejection of solution from the soil surface by rainfall, (3) the erosion, by rainfall and surface runoff, of sediment with adsorbed chemicals and (4) the adsorption-desorption of the adsorbing chemicals.

Lots of effort has been made towards developing simulation models for the prediction of solute transfer from the soil surface to surface runoff. These models effectually consider the processes and factors which affect surface runoff and solute transfer. Other processes that occur rapidly, such as precipitation–dissolution and biogeochemical reactions, can be neglected. The two traditional models used in consideration of chemical transport from soil to surface runoff are the mixing-layer approach and the interfacial diffusion-controlled approach. The mixing-layer model is probably the most commonly-used model for chemical transport in soil (Shigaki et al., 2007; Tong et al., 2016; Yang et al., 2017). This theory assumes that the transport is controlled by a mixing-layer just below the soil surface in which rainfall runoff water and the soil solution mix instantaneously and there is no substantial transfer of chemicals to the mixing layer from below, meaning diffusion is negligible. To reduce the model's mathematical complexity, this study applies an extension of the deposited layer (Hairsine and Rose, 1991) which assumes that the exchange rate is controlled by

raindrops and the effects of diffusion are neglected. Moreover, the exchange rate k_m is replaced by the variable transfer rate, the raindrop-induced water transfer rate, which was developed by Gao et al. (2004).

2.1.3 Contaminant transport in soil

The three core processes to consider in the process of solute transport in the soil are molecular diffusion, hydrodynamic dispersion and advection. Diffusion is a result of the random movement of chemical molecules, which causes the solute to move from a position with a higher concentration to one with a lower concentration. Diffusive transport can be described using Fick's law. Dispersion transport of solutes results from the unbalanced distribution of water flow velocities within and between different soil pores. Advective transport attributes to solute transported with the moving fluid in both the liquid and gas phases (Essaid et al., 2015). However, advective transport in the gaseous phase is often ignored as its contributions in many applications are negligible compared with those of diffusion.

Several mathematical models have been adopted to describe and predict the transport of heavy metals in soil. Earlier scholars used to assume that solute transport was solely due to dispersion (Liu et al., 2006). They considered retardation factors and dispersion coefficients of chemicals by using linear adsorption with convection-dispersion equations. Numerical models are available to account for soil complexity and accommodate complicated boundary conditions. Finite difference methods have typically been applied to solve flow and transport equations, which were studied by several researchers: Li et al. (2005), Carlier et al. (2006), Godongwana et al. (2015) and

Chung et al. (2015). For example, Hydrus-1D is a numerical model for analysis of water flow and solute transport in unsaturated, partially saturated, or saturated porous media. HYDRUS model numerically solves the Richards' equation for saturated-unsaturated water flow and Fickian-based advection-dispersion equations for solute transport. HYDRUS supports both constant and varying concentration flux boundary conditions for solute transport. The dispersion coefficient includes terms reflecting the effects of molecular diffusion and tortuosity.

Several analytical solutions for the transport of chemicals in soil were also developed by van Genuchten (1981). The governing equations include parameters considering linear equilibrium adsorption, zero-order production and first-order decay. Guyonnet and Neville (2004) evaluated the analytical solutions for calculating three-dimensional solute transport with decay for a vertical plane source at a constant concentration. Other researchers such as Shackelford and Lee (2005), Srinivasan et al. (2007) and Zhang (2013) also conducted related studies. For intense, the STANMOD (STudio of analytical MODels) model includes the 3DADE code (Leij and Bradford, 1994) for estimating analytical solutions of three-dimensional equilibrium solute transport in the subsurface. The analytical solutions assume steady unidirectional water flow in porous media which have unified flow and transport properties. The transport equation contains solute transport terms by advection and dispersion as well as for solute retardation and first-order decay. The 3DADE code can be applied to solve problems wherein the concentration is calculated as a function of time and space for particular model parameters.

2.2 Heavy Metal Pollution by Runoff

2.2.1 Surface runoff pollution - non-point pollution

Urban areas are the main sites of non-point source pollution due to a lot of paved surfaces. Paved surfaces, such as concrete are impervious for water to penetrate. Any water contacting with these surfaces will run off and be absorbed by the surrounding environment. These surfaces make it easier for rainfall water to carry pollutants into the surrounding soil (NOAA, 2007). Sites with disturbed soil like construction sites are easy to be eroded by precipitation like rain and snow.

Typically, surface runoff through these impervious surfaces tends to pick up pollutants from roads and parking lots, as well as agriculture lawns. Pollutants that usually occur in runoff include sediment, nutrient toxic chemicals like PAH and heavy metal. Roads and parking lots are significant sources of heavy metals like nickel, copper, zinc, cadmium, and lead. Fertilizer use on residential lawns, parks can accumulate in surface runoff when fertilizer is improperly applied (Burton and Pitt, 2001). These contaminants can come from a diversity of sources including sewage sludge, mining works, transportation emissions, fossil fuel combustion, industrial activities and landfills (Leeds et al., 2010).

Runoff can induce heavy metal poisoning into water bodies like river and ocean and creatures in them. When heavy metal is transferred into the ocean through runoff, these metals are ingested by ocean life which cannot be disposed of. As a result the heavy metal accumulates within these animals. Over time, these metals build up to a toxic level, which may lead animal death. The heavy metal poisoning can also influence

human. If people eat a poisoned animal, there will be a chance of getting heavy metal poisoning too.

Considering soil contamination, runoff waters can have two major pathways of concern. Firstly, runoff water can extract soil contaminants and carry them in the water pollution system to even more sensitive aquatic habitats. Secondly, runoff can deposit contaminants on pristine soils, creating health or ecological consequences. In the case of groundwater, the main issue is contamination of drinking water.

Many researchers have studied the relation between pollution and runoff. Zhu et al. (2012) summarized the characteristics of runoff pollution and its control. Researchers regarding specific areas, such as car parks and roads were also illustrated by Revitt et al. (2014). Moreover, Reddy et al. (2014) studied heavy metal pollution along with rainfall runoff process.

2.2.2 Heavy metal pollution in soil and groundwater

The implications associated with heavy metal contamination have considered one of the serious environmental pollutants. Heavy metals remain in the soil for a long time and have a residence time ranging from a few to several hundred years (Wuana and Okieimen, 2011). Rattan et al. (2000) reported that environmental pollution due to heavy metals could broadly be grouped as (i) deficiency of micronutrient cations and (ii) toxicity of the heavy metals. Balkhair and Ashraf (2016) stated that surface layers of the soil might accumulate significant amounts of heavy metals, which subsequently affect sensitive plants growing in the soil.

Heavy metals indirectly affect soil enzymatic activities by shifting the microbial community which synthesizes enzymes (Khan et al., 2007). Heavy metals manifest toxic effects towards soil biota by affecting key microbial processes and decrease the number and activity of soil microorganisms. Chen et al. (1992) suggested that heavy metals produced a reduction in bacterial species richness and a relative rise in soil actinomycetes or even decreases in both the biomass and diversity of the bacterial communities in contaminated soils. Karaca et al. (2010) reported that the enzyme activities are affected in different ways by varying metals due to different chemical affinities of the enzymes of the soil system.

The plant uptake of heavy metals from soils at high concentrations may result in a significant health risk taking into consideration food-chain implications. Utilization of food crops contaminated with heavy metals is a major food chain route for human exposure. Chronic level ingestion of toxic metals has undesirable impacts on humans and the associated harmful impacts become perceptible only after several years of exposure (Khan et al., 2008).

Zinc is considered to be relatively non-toxic, especially if taken orally. However, the excess amount can cause system dysfunctions that result in impairment of growth and reproduction. The clinical signs of zinc toxicosis have been reported as vomiting, diarrhea, bloody urine, icterus (yellow mucus membrane), liver failure, kidney failure and anemia (Khan et al., 2008).

Heavy metals such as mercury (Hg), cadmium (Cd), arsenic (As) as well as lead

(Pb) are the general known heavy metals that may be found in the groundwater. Groundwater is a water body in the internal body of the land that can face contamination using different heavy metals coming from various elements present in the form of elemental rock (Haileslassie and Gebremedhin, 2015). Accessing those heavy metals in the body of people may lead to different health problems such as cancer, kidney problems, nausea, and high blood pressure. In general series health problems will bring to the healthy person as they are cariogenic in small concentrations. For example, the recommended Daily Dietary Allowance of Zn is 15 mg for adults and 20 to 25 mg for pregnant and lactating women (NAP, 2001). Acute Zn toxicity in human includes vomiting, dehydration, drowsiness, lethargy, electrolytic imbalance, abdominal pain, nausea, lack of muscular coordination, and renal failure. The chronic dose of Zn increases the risk of developing anemia, damage to the pancreas and possibly enhances the symptoms of the Alzheimer's disease (Plum et al., 2010). Workers exposed to Zn fumes from smelting or welding have suffered from a short-term illness called mental fume fever.

2.3 Probabilistic Analysis and Risk Assessment

2.3.1 Monte Carlo simulation

Many modeling parameters may have uncertain characteristics in porous media systems. Such uncertainties can be related to deviations in obtaining data, variations in spatial and temporary units, complexities in hydrogeological processes and incomplete or imprecise information (Uusitalo et al., 2015). It is a challenging task for modelers to evaluate the uncertainties accurately because the complexity of the subsurface system

requires a systematic uncertainty analysis method. Such a procedure should not only provide insight into the level of accuracy of modeling predictions but also aid in the assessment of various modeling outputs. Thus, pivotal sources of uncertainty which merit further research should be identified.

The approaches widely applied to determine uncertainties in environmental simulations include interval analysis, probabilistic analysis and fuzzy set theory (Zhang et al., 2016). In the interval analysis approach, each uncertain parameters are assumed to have upper and lower limits without a probability structure. Probabilistic methodologies have also been widely applied in environmental modeling during recent decades and have been regarded as an effective framework for analyzing uncertainties. In these methods, uncertainties associated with modeling inputs are described by probability distributions, with the result that the modeling outputs can be expressed as probabilistic information. In order to produce probability and cumulative distribution curves for the modeling outputs, the Monte Carlo technique is used for repeating generations of pseudo-values for uncertain input parameters with probability distributions (Farrance and Frenkel, 2014). A cumulative probability under which a specific event will happen can thus be derived. This probability information can then be used to indicate uncertainties.

2.3.2 Risk assessment

Thousands of contaminated industrial sites pose significant threats to human health and the natural environments in Canada. Risk assessment is an important procedure in relative decision-making regarding effective remediation actions and management of

these contaminated sites. However, the observation about risks is limited by the real randomness in the natural environment and insufficient information of relative parameters and conditions, as well as the uncertainty of risk occurrence and the potential consequences of such occurrence. As a result, risk assessment is inherently linked with uncertainty (Theodore and Dupont, 2012; Aven, 2016).

Negligence of uncertainty in the assessment procedures may result in adverse consequences. For instance, over design of remediation systems may lead to waste of money and resources; while underestimation of risks may result in no actions or limited actions towards the management of sites, and in fact will severely threaten human health and the natural environments.

Previously, a large volume of literature has been published on methods for implementing risk assessment at contaminated sites under various sources and/or aquifer conditions. For example, Lee et al. (1994) proposed a fuzzy-set-based approach to estimate risk based one human health from groundwater contamination and evaluate possible regulatory actions; Goodrich and McCord (1995) applied Monte Carlo methods to account for parameter uncertainties in modeling of groundwater flow and solute transport processes, and then the modeling results were used for risk assessment; Batchelor et al. (1998) developed a stochastic risk assessment model for a site by representing relevant parameters as probability distribution functions; Aral and Maslia (2003) developed an integrated modeling system for risk assessment by using Monte-Carlo-based contaminant transport simulation results using probability density functions (PDFs); Maxwell et al. (1998) also developed an integrated system of linked

groundwater transport modeling and human exposure assessment. More recently, a hybrid method has been proposed to combine probabilistic and fuzzy-set approaches to represent modeling parameter uncertainties involved in the risk assessment process (Li et al., 2003; Liu et al., 2004). For instance, Guyonnet et al. (2003) integrated the Monte Carlo random sampling of probability distribution functions with fuzzy calculus to represent different uncertainties for estimating the human exposure to soil cadmium in an industrial site; According to the literature review and studies of Chen et al. (2003) and Kentel and Aral (2005), stochastic and fuzzy-set techniques were commonly used to accommodate uncertainties parameters of modeling inputs and associated modeling output and risk assessment. However, most of the previous work has only considered parameter uncertainties in modeling of contaminant transport, while the uncertainties in environmental quality guidelines and health risk evaluation criteria have received less attention (Minsker and Shoemaker, 1998; Chen et al., 2003). As a result, such negligence may result in lack of information and thus improper decision for remediation and management. It is necessary to develop and improve the risk assessment methods based on fuzzy and probability analysis that can effectively handle a variety of uncertainties.

2.4 Summary

In this chapter, the process of transport in soil by runoff have been introduced and the literature review of their modeling methods and analytical solutions. Moreover, the effect of non-point source pollution to the environment has also been analyzed. Through the chapter, we can know though there were quite lots of modeling and analytical

solutions have been developed in the past years, most analytical solutions were developed for each independent process of heavy metal transport. However, rare researchers focused on an integrated system of modeling or analytical solutions combing all the process such as soil erosion and solute transport. Moreover, few analytical systems consider the uncertainty of parameters and relative risk assessment. Therefore, it is imperious to develop an integrated system which can contain both calculations of contaminant transport in soil by runoff and relative risk assessment.

Furthermore, the uncertainty analysis methods including probabilistic and fuzzy set theory methods have rarely been applied to site risk assessment involving multiple processes. Among those environmental risk assessment studies which quantified system uncertainties, they tended to apply stochastic simulation approach alone to analyze the uncertainties of randomness in their systems. Various types of uncertainties need to be considered when the environmental risk assessment is undertaken. The integrated system applied in this study can quantify both probabilistic and fuzzy uncertainties associated with environmental quality guidelines, and health impact criteria, as well as site conditions.

3. METHODOLOGY

3.1 Study Framework

In this study, an integrated ARCTRA system is developed for calculating the transport of heavy metals in soil by rainfall runoff. As shown in Fig. 3.1, the research approach can be divided into four parts: (1) rainfall-runoff determination, (2) soil erosion, (3) solute transport in soil and (4) probability analysis and risk assessment. Meanwhile, for each section of the ARCTRA system, a existing model is selected to compare and verify the corresponding analytical solution results. The rainfall-runoff section was compared with the PCSWMM model and in the soil erosion section, an analytical solution from the Hairsine-Rose model was studied. The HYDRUS model and STANMOD model are employed for contaminant transport in soil.

In the section regarding the formation of surface rainfall, the analytical solution results will show the relative runoff water depth as well as flux rate according to an average rainfall intensity. In the soil erosion section, the concentration of heavy metals dissolved into the surface runoff can be predicted, and their distribution into the subsurface and unsaturated soil is found using the analytical solution and incorporating soil properties such as the dispersivity, the bulk density, the mass transfer coefficient, etc. The analytical solution to calculate the solute transport is based on the advection-dispersion equation (ADE). With parameters such as retardation factors, the contaminant concentration at different soil depths can be obtained. Finally, Monte Carlo simulation is employed to obtain the distribution function of concentration results due

to uncertain parameter in governing equations. The Fuzzy Set risk assessment method was then applied to quantify fuzzy uncertainties and site risk level based on the Monte Carlo Simulation.

Meanwhile, as shown in Fig. 3.1, the accuracy of the ARCTRA system is verified through compassion analysis against existing models. The rainfall-runoff section was compared with the PCSWMM model which simulates the runoff and infiltration formation under given rainfall conditions. The runoff depth and flux can be generated for comparison with the results of the ARCTRA system. In the soil erosion section, an analytical solution from the Hairsine-Rose model was studied to compare the concentration of heavy metal dissolved in the surface runoff. And, the ARCTRA module for analyzing transport of contaminants in the soil is examined against a HYDRUS model. In HYDRUS models, transport and contaminant reaction parameters are required as inputs. The outputs of the model offer the heavy metal concentration profile according to soil depth. The results of the modeling and the ARCTRA system are both also compared with the literature data from the case study.

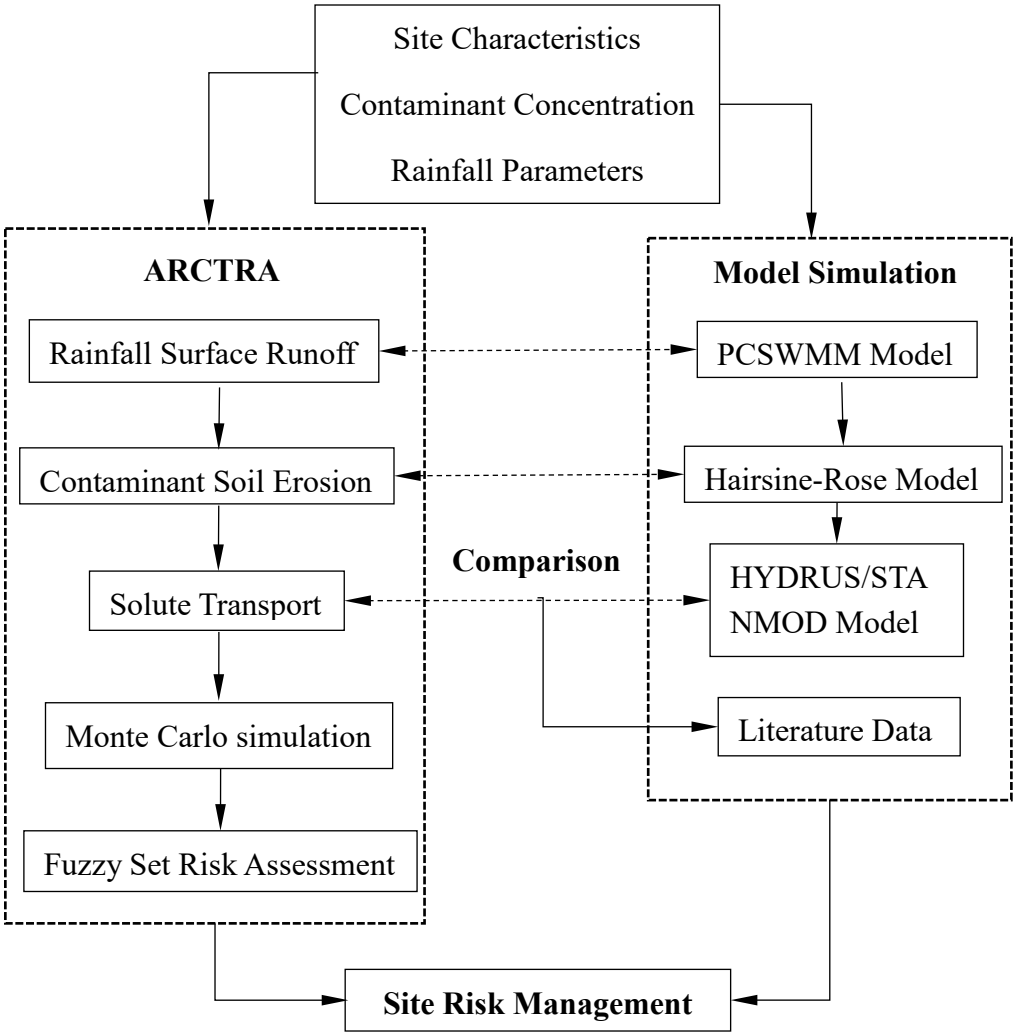

Fig.3.1 Framework of the thesis study

3.2 Integrated ARCTRA System

3.2.1 ARCTRA system framework

The integrated ARCTRA system consists of five sections: rainfall-runoff formation, soil erosion, solute transport, Monte Carlo simulation and Fuzzy Set Risk Assessment. In the calculation section, a governing equation was applied for each process, which will be introduced in detail in the following section. The result of the preceding process will serve as the input of the following section Moreover, the results of solute transport are analyzed by Monte Carlo Simulation considering the uncertainties associated with key

model parameters after model sensitivity analysis. Finally, the Fuzzy Set risk assessment method is employed to quantify incomplete-type uncertainties associated with the site conditions, environmental quality guidelines and health impact criteria based on the Monte Carlo Probability Simulations. Thus, an integrated risk value can be obtained to evaluate and rank the risk level of a contaminated site. The ARCTRA system developed in this study can be used to systematically assess the heavy metal in the unsaturated zone caused by rainfall-runoff process and support effective management of the contaminated site . In the system, parameters such as rainfall rate, infiltration rate, mass transfer coefficient, pore water velocity, retardation factor and distribution coefficient are applied. The framework of the analytical solution is displayed in Fig. 3.2.

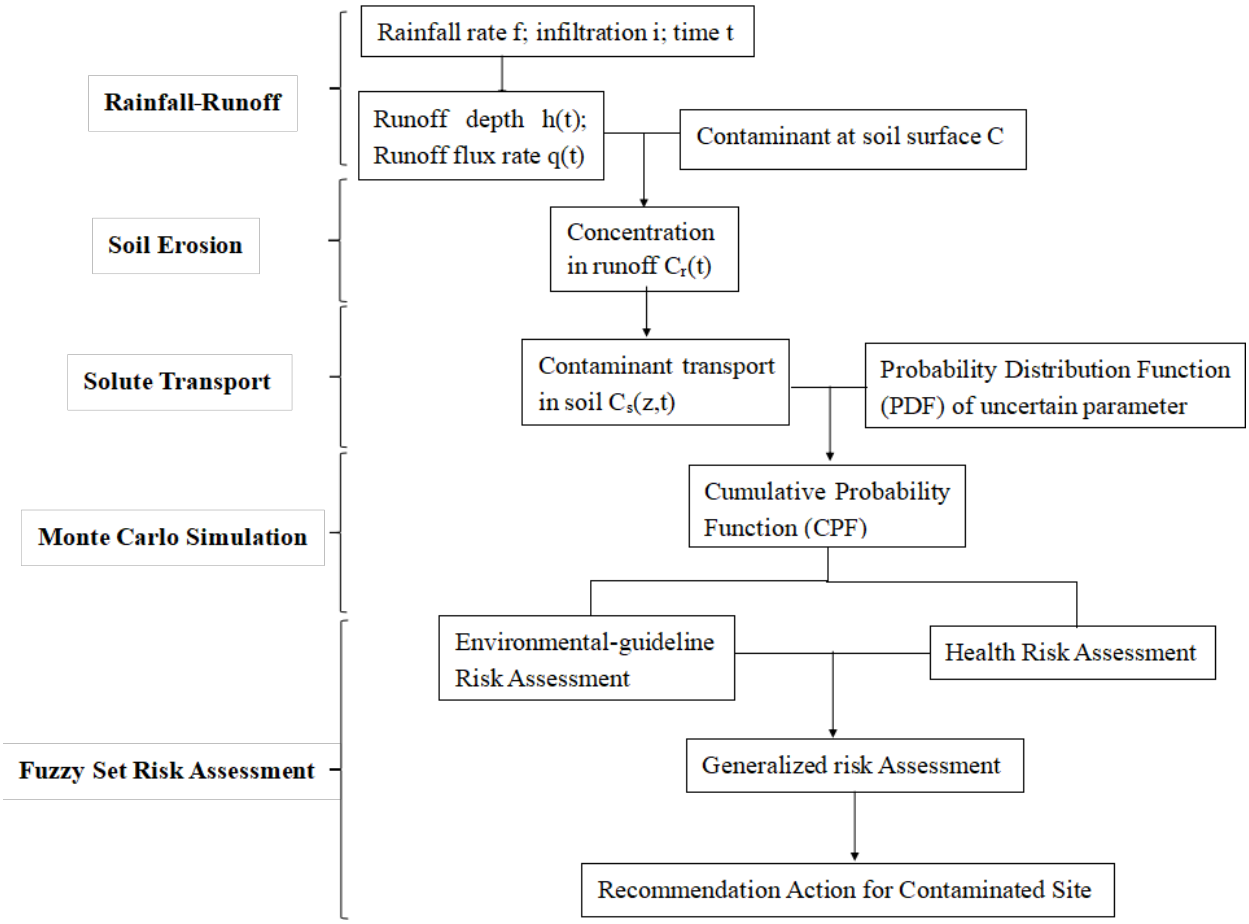

Fig. 3.2 ARCTRA system components

3.2.2 Surface runoff governing equation

For shallow surface runoff flow, the mass balance equation is (Rousseau et al., 2012):

$$\frac{\partial h}{\partial t}+\frac{\partial q}{\partial x}=f(t)-i(x,t) \qquad \text{Eq.(3.1)}$$

where x is the axis along the slope [L], h(x,t) is the depth of the surface runoff [L], q(x,t) is the surface runoff flow rate per unit width [L^2T^{-1}], f(t) is the rainfall rate [LT^{-1}] and i(x,t) is the infiltration rate, [LT^{-1}] (both are assumed to be spatially constant).

The water mass balance equation is function of kinematic-wave equation (Rumyin, 2015):

$$q = \alpha h^m \qquad \text{Eq. (3.2)}$$

where α and m are coefficients which depend on whether the flow regime is laminar or turbulent. For laminar flow (Reynolds' number Re = u/v < 500), m = 3 and $\alpha = 8gs/K_\alpha v$, where s is the uniform soil slope, g is the acceleration due to gravity, v is the kinematic velocity of water and Kr is a parameter related to the soil surface roughness.

Therefore, combining Eq. (3.1) and Eq. (3.2) gives us a kinematic wave equation with a dependent variable:

$$\frac{\partial h}{\partial t} + \alpha m h^{m-1} \frac{\alpha h}{\alpha x} = f - i \qquad \text{Eq. (3.3)}$$

where the boundary and initial conditions for Eq. (3.3) are h(x,0)=h(0,t)=0. The contaminants within the soil surface layer are transferred to the surface runoff by a rate-limited mass transfer process. Dissolved pollutant transport via the surface runoff is described by the following mass conservation equation:

$$\frac{\partial (c_r h)}{\partial t} + \frac{\partial (c_r q)}{\partial x} = k[c(t) - c_r] \qquad \text{Eq. (3.4)}$$

where $c_r(x,t)$ is the dissolved contaminant concentration in surface runoff and c(t) is the dissolved chemical concentration at the soil surface. k is the convective mass transfer coefficient that associates solute flux across the soil surface interface to the variation in concentration of the soil solution at its surface [LT^{-1}].

Combining Eq. (3.4) and Eq. (3.3) yields the following boundary and initial conditions: $c(x,0)=c(0,t)=c_0$.

$$h\frac{\partial(c_r)}{\partial t}+q\frac{\partial(c_r)}{\partial x}=kc(t)-c_r(k+f-i) \qquad \text{Eq. (3.5)}$$

According to Eq. (3.5), the governing equations and analytical solutions of the rising and falling stages can be respectively obtained. For the rising stage, the governing equation is as Eq. (3.6) and the corresponding analytical solution is as Eq. (3.7):

$$\frac{dh}{f-i}=\frac{dx}{\alpha m h^{m-1}}=dt \qquad \text{Eq. (3.6)}$$

$$h=\begin{cases}h(t)=t(f-i), & 0\le t\le t_e\le T\\ h(x)=(f-i)t_e, & t_e\le t\le T\end{cases} \qquad \text{Eq. (3.7)}$$

where t_e is equilibrium time for any point x along the slope.

$$t_e=\left(\frac{x}{\alpha(f-i)^{m-1}}\right)^{1/m} \qquad \text{Eq. (3.8)}$$

For the falling stage, the governing equation is as Eq. (3.8) and the corresponding analytical solution is as Eq. (3.9):

$$\frac{\partial h}{\partial t}+\alpha m h^{m-1}\frac{\partial h}{\partial x}=-i \qquad \text{Eq. (3.8)}$$

$$\frac{dh}{-i}=\frac{dx}{\alpha m h^{m-1}}=dt$$

$$x=\alpha h^{n-1}\left[\frac{h}{r}+n(t-T)\right], \quad t>T>t_e \qquad \text{Eq. (3.9)}$$

3.2.3 Contaminant transport in runoff

The equation of continuity for a single chemical in soil is (Ward and Trimble, 2003)

$$\theta\frac{\partial c}{\partial t}+\rho_b\frac{\partial s}{\partial t}+\frac{\partial J}{\partial z}=0 \qquad \text{Eq. (3.10)}$$

where c and s are the solute concentrations associated with the liquid and solid phases of the soil, respectively; θ is the volumetric content [L^3L^{-3}], ρ_b is the soil bulk density [ML^{-3}], and J is the solute mass flux density given by

$$J = qc - \theta D \frac{\partial c}{\partial z} \qquad \text{Eq. (3.11)}$$

In which D is the dispersion coefficient [L^2T^{-1}] (assumed to be independent of the concentration c).

$$D = D_0 \lambda + \varepsilon v \qquad \text{Eq. (3.12)}$$

where D_0 is the ionic or molecular diffusion coefficient in pure water [L^2T^{-1}], λ is tortuosity factor [], which is estimated using the Millington and Quirk (1961) as $\lambda = \theta^{7/3}/n^2$, where n is the soil porosity ε is the dispersivity, which ranges from about 0.5cm or less for laboratory-scale displacement experiments involving distributed soil to about 10 cm or more for field-scale experiments and v is the average pore water velocity approximated by the relation q/θ.

$$c_r(t) = \frac{1}{Q_r} \int_0^t J_0(t') E(t - t') dt' \qquad \text{Eq. (3.13)}$$

where $J_0(t) = -J(0,t)$ is the solute mass flux from soil to runoff water and Qr is the runoff water flux. During the state flow [L^3T^{-1}], Qr is equal to the difference between the rainfall rate f and infiltration rate i.

The resident time distribution E(t) for the runoff water can be taken as Wallach et al. (1988).

$$E(t) = \frac{1}{\tau}\exp(-t/\tau) \qquad \text{Eq. (3.14)}$$

In which τ is the mean residence time of a runoff water element in the field, approximated by the ratio of the average surface water depth h and the excess rainfall rate f-i. The analytical solution based on the governing equation is as following:

$$\begin{aligned} c_r = \frac{\theta C_0}{2Q_r}\{&\frac{(v+2k)DR}{(v+k)k\tau+DR}\cdot\exp[\frac{(v+k)k\tau}{DR}]erfc[\frac{(v+2k)t}{2(DRt)^{1/2}}] \\ &- v\ erfc[\frac{vt}{2(DRt)^{1/2}}] - \frac{(v+k)k\omega\tau}{(v+k)k\tau+DR}\cdot\exp(-t/\tau)erf[\frac{\omega t}{2(DRt)^{1/2}}] \\ &+ \frac{v(v+k)k\tau-2kDR}{(v+k)k\tau+DR}\exp(-t/\tau)\} \end{aligned} \qquad \text{Eq. (3.15)}$$

where $\omega = v(1-\frac{4DR}{v^2t})^{1/2}$.

3.2.4 Solute transport in soil

Partitioning of solute between the liquid and solid phases of the soil is accomplished but means of isotherm of the form

$$s = K_d c \qquad \text{Eq. (3.16)}$$

The one-dimensional convection-dispersion solute transport equation is shown as (Guerrero et al., 2013):

$$R\frac{\partial c}{\partial t} = D\frac{\partial^2 c}{\partial z^2} - v\frac{\partial c}{\partial z} \qquad \text{Eq. (3.17)}$$

where $R = 1 + \rho K_d/\theta$ is the retardation factor where K_d, is the distribution coefficient of the solute between liquid and solid phases [LT^{-1}]. The solution for the convective-dispersive solute transport in the soil when a rate-limited chemical transfer through a

laminar boundary condition was considered:

$$c(z,t) = C_r\{1 - \frac{1}{2}erfc[\frac{Rz - vt}{2(DRt)^{1/2}}] - \frac{v+k}{2k}\exp(\frac{vz}{D})erfc[\frac{Rz + vt}{2(DRt)^{1/2}}] + (1 + \frac{v}{2k})\exp[\frac{(Rz + vt)(k+v)}{DR}] \cdot erfc[\frac{Rz + (2k+v)t}{2(DRt)^{1/2}}]\} \quad \text{Eq. (3.18)}$$

3.2.5 Monte Carlo simulation and risk assessment

MCS is a conceptually direct approach to dealing with stochastic uncertainties by generating a large quantity of random realizations of inputs, solving certain flow and transport equations for each random parameter and then using the mean and deviation results from across all the realizations to obtain a sample distribution for the solution (Li et al., 2003). It can therefore be used to handle the uncertainties that can be described by PDFs. Monte Carlo techniques utilize the repeated operation of numerical models to simulate the stochastic processes of contaminant transport (Hu and Huang, 2002). Each execution of the model generates a sample output of pseudo-values. As a result, the sampling results can then be evaluated in distributed PDFs. The primary elements of the MCS include PDFs, a random number generator, a sampling rule and deviation estimation and variance reduction techniques (Maqsood et al., 2003; Qin and Huang, 2009). In the Monte Carlo model, there are several types of probability density functions (PDFs) available, such as normal, exponential, Gumbel, triangular, etc. (Cullen and Frey, 1999). The Monte Carlo Simulation can offer the probability function of the modeling results due to uncertain parameters in the modeling process. As an example in Fig. 3.3, the probability of the value at 7.23 to 7.74 is 25%. In this way, the probability of the result over the standard or decided value can be obtained, which

contributes to the risk assessment.

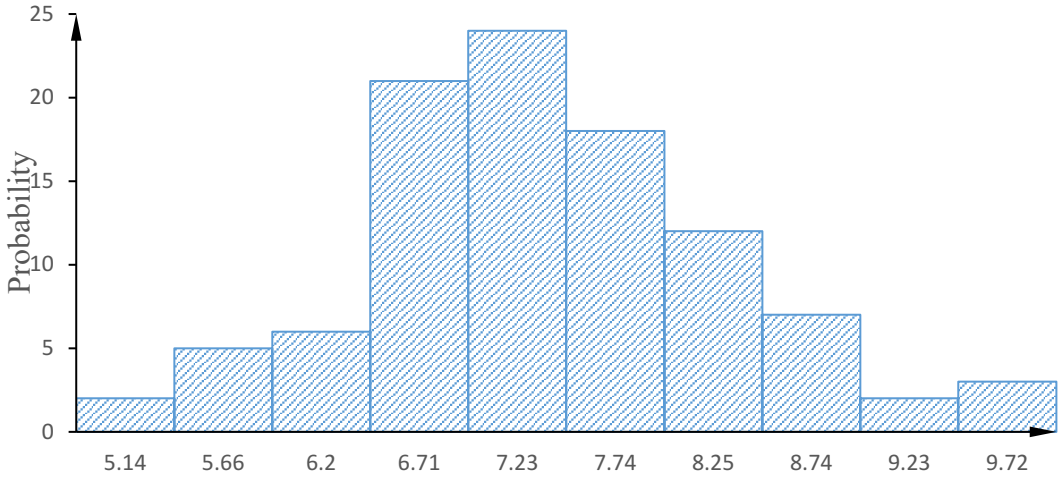

Fig. 3.3 Example of Monte Carlo simulation probability function graph

The modeling of pollutant transport in soil requires inputs for various physical, chemical and biological parameters. The variant parameter in this study was decided by a sensitivity test, which will be explained carefully in the case studies.

Fuzzy-stochastic modeling approach for risk assessment

The detailed risk characterization relative to a contaminated site can usually be regulated through environmental-guideline risk assessment (ERA) and health risk assessment (HRA) (Yang et al., 2010). The environmental-guideline-based risk (ER) is defined as the potential for the violation of environmental regulations, and the health risk (HR) as the risk of health influences due to chronic intake of the contaminant. The ERA approach to contaminant risk assessment is to compare the contaminant concentration with the corresponding quality standard. Using Monte Carlo simulation, the probability (P_F) of the contaminant concentration exceeding the quality standard

can be described as follows (Wu and Chen, 2014):

$$P_F = P(C > C_S) = 1 - F(C_S) \qquad \text{Eq.(3.19)}$$

where C is the contaminant concentration and Cs is the soil quality standard. F(Cs) is the cumulative distribution function (CDF) of the contaminant concentration, which can be obtained from the Monte Carlo simulation results.

Fuzzy environmental quality guidelines

The environmental-guideline-based risk assessment involves a comparison of the contaminant concentration with its corresponding environmental guideline. To facilitate an environmental-guideline-based risk analysis, the guidelines are categorized in this study into three fuzzy sets: “strict”, “medium” and “loose”. The function graph should appear as seen in Fig. 3.4, which illustrates the function of the membership grade (μ) and guidelines.

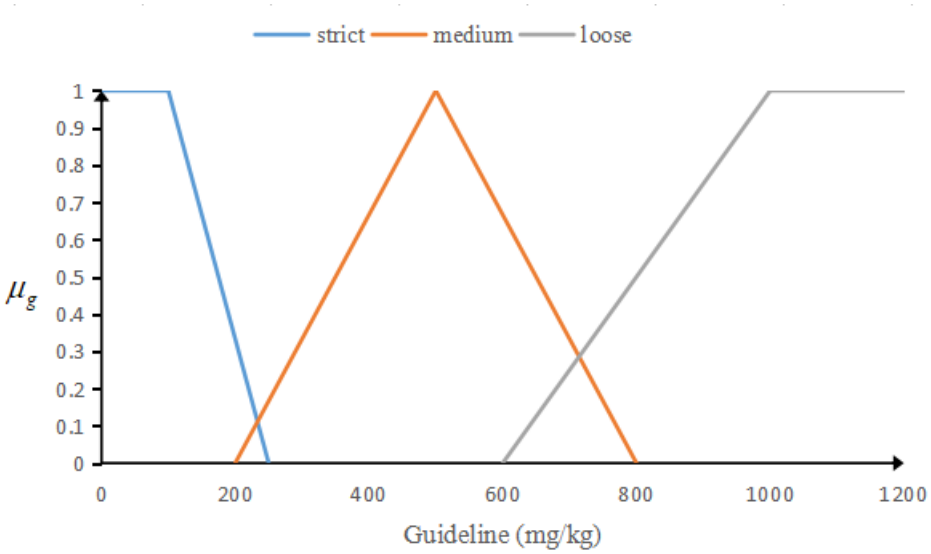

Fig. 3.4 Membership functions of environmental guidelines

The membership function of fuzzy environmental risks associated with the probability (P) of violating soil guidelines with (a) a strict standard, (b) a moderate standard and (c) a loose standard. With the Probability (P) obtained from Eq.(3.19), the environmental-guideline-based risk (ER) graph can be established with a final membership grade for environmental-guideline-based risk (μ_{er}).

Again, according to Cheng (2000) and Chen et al. (1992), the membership functions of the fuzzy sets can be constructed based on investigation results and classified as either “L”, “L-M”, “M”, “M-H” or “H”, representing “low”, “low-to-medium”, “medium”, “medium-to-high” and “high”, respectively. For example, if the Monte Carlo simulation results show the probability of strict-guideline violation is 75%, the related environmental-guideline-based risk can be categorized as partly “M” (with a membership grade of 0.50) and partly “M-H” (with a membership grade of 0.50). A similar membership to environmental quality guidelines is generated for the categories of strict, medium and loose.

Fuzzy health risk assessment

HRAs often appropriate USEPA-published reference doses (RfD) and slope factors (SF) that usually come from laboratory studies on animals. The degree of exposure to a compound is a function of many variables, shown as follows (USEPA, 1989, 1992):

$$\mathrm{CDI}=\mathrm{CW}*\mathrm{IR}*\mathrm{EF}*\mathrm{ED}/(\mathrm{AT}*\mathrm{BW}) \qquad \text{Eq. (3.20)}$$

where CDI is the chronic daily intake (mg/kg per day), CW is the pollutant concentration in the soil (mg/kg), IR is the human ingestion rate (mg/kg-day), EF is the

exposure frequency (days/year), ED is the average exposure duration (year), BW is the average body weight (kg) and AT is the averaging time (AT (365 *ED days). HI can be calculated using the following Eq. (3.21) (Chacko et al., 2016):

$$HI=CDI/RfD \qquad \text{Eq. (3.21)}$$

Fuzzy rules

The generalized risk level is determined by an integrated consideration of environmental-guideline-based and health hazards. Since there are no numerical models that relate to both types of risks, quantification of the generalized risk level can only be achieved based on subjective suggestions rather than through probabilistic analysis. A fuzzy inference process, using fuzzy membership functions and fuzzy rules, will then be used to facilitate this kind of risk quantification. The rules usually consist of a conditional part (e.g., antecedent) and a conclusion part. An antecedent may be a simple clause or an aggregate of several clauses correlated via the fuzzy logical operators AND, OR and NOT.

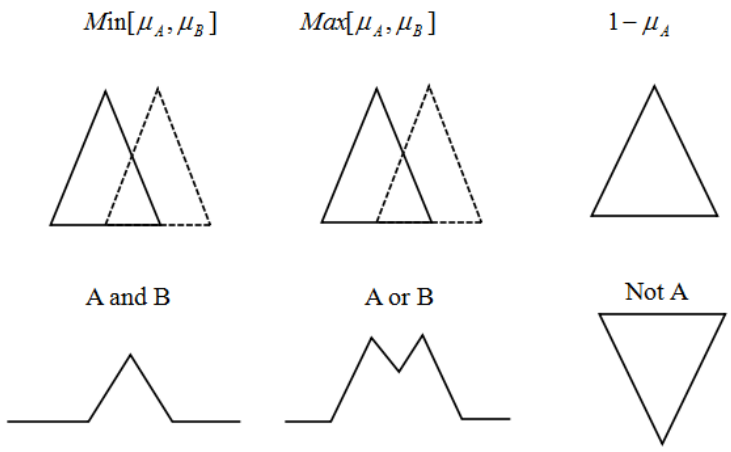

Fig. 3.5 Basic operations in fuzzy logic (Li et al., 2007)

The generalized risk level is derived from an integrated consideration of environmental-guideline-based and health risk. A fuzzy inference process will be introduced for facilitating the risk quantification, by using fuzzy membership functions and fuzzy rules. The generation rule for the GRL is displayed in Table 3.1. For example, ‘‘if environmental-guideline-based risk is M and health risk is H, then the general risk is “M-H”, where the “M” is a fuzzy set of ‘‘environmental-guideline-based risk’’, the ‘‘HIGH’’ is a fuzzy set of ‘‘health risk’’, and the “M-H” is a fuzzy set of ‘‘generalized risk’’. This is a form of fuzzy rules, where the ‘‘environmental-guidelined-based risk’’ and ‘‘health risk’’ are input variables, the ‘‘generalized risk’’ is an output variable.

Table 3.1 Generalized risk level (GRL) generation rule based on environmental-guideline risk (ER) and health risk (HR) (Mohamed and Cote, 1999)

ER	**HR**	**GRL**	**ER**	**HR**	**GRL**
L	L	L	L-M	L	L-M
L	L-M	L-M	L-M	L-M	L-M
L	M	M	L-M	M	M
L	M-H	M-H	L-M	M-H	M-H
L	H	H	L-M	H	H
M	L	M	M-H	L	M-H
M	L-M	M	M-H	L-M	M-H
M	M	M	M-H	M	M-H
M	M-H	M-H	M-H	M-H	M-H
M	H	H	M-H	H	H
H	L	H	H	M-H	H
H	L-M	H	H	H	Very H
H	M	H			

The generalized risk level can be categorized into “low”, “low-to-medium”, “medium”, “medium-to-high”, “high” and “very-high”, and the corresponding membership functions of the fuzzy events can be given according to Chen et al. (1992) as shown, for example, in Fig. 3.5. The scope of the generalized risk levels (i.e., GRL [0, 100]) is given subjectively to the fuzzy sets so that they have single numerical site risk scores (Mohamed and Cote, 1999). The membership grade μ_{gr} is generated based on the environmental guideline risk membership grade μ_{er} and the health risk membership grade μ_{hr}. These numerical values have no direct relationship with the values of the input risk factors (e.g., environmental-guideline-based risk and health risk). However, after establishing the fuzzy sets of generalized risk levels, a numerical site risk score can be obtained from Fig. 3.6 using the fuzzy “AND” or “OR” operations based on the environmental guideline, the probability of guideline violation and the corresponding HI.

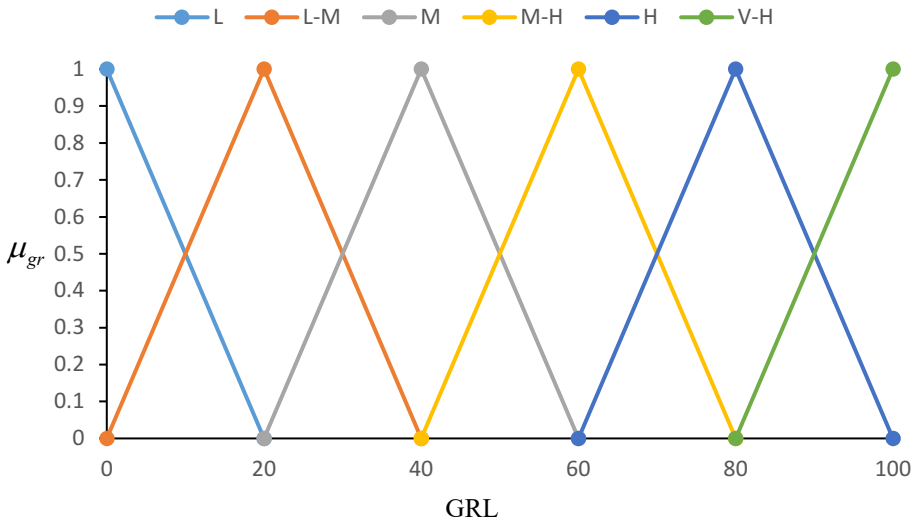

Fig.3.6 Membership functions of fuzzy generalized risk level

3.2.6 Engineering user interface design

In this study, the ARCTRA system was solved using Excel. To ensure the easy use of the analytical solution, a user interface was designed based on the VB editor and inserted into the Excel system. As shown in Fig. 3.6, the system is divided into 3 sections: Rainfall-Runoff, Soil Erosion and Solute Transport. It also later includes analysis such as the comparison of results and the Monte Carlo simulation risk assessment. Users can adopt the whole system for calculation or use a single distinct part according to their needs.

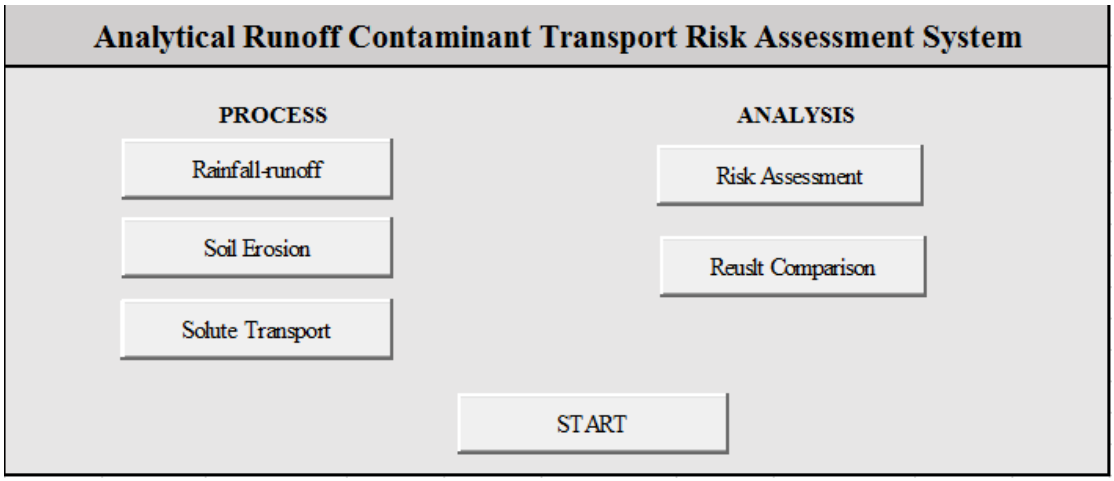

Fig. 3.7 The main interface of the ARCTRA system

An example of the system is displayed in Fig. 3.8. For the calculation of the ‘Solute Transport' section, the user can input the values of the parameters through the interface. These values will be imported into Excel by the VB program code. The results, calculated by Excel, will be displayed in the output section when the user clicks the ‘Calculate' button.

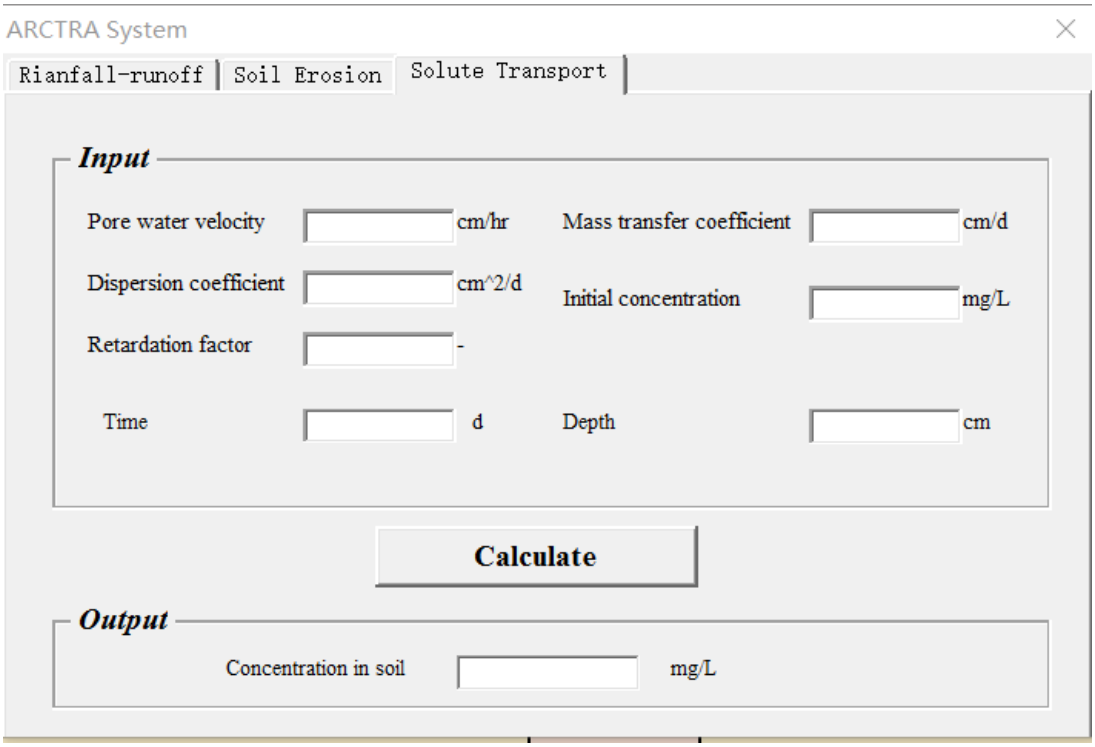

Fig. 3.8 The interface of solute transport process

3.3 Existing Models for Comparison

3.3.1 PCSWMM model

The conceptual view of surface runoff used by SWMM is illustrated in Fig. 3.9 below. Each subcatchment surface is treated as a nonlinear reservoir. Inflow comes from precipitation and any designated upstream subcatchments. There are several outflows, including infiltration, evaporation and surface runoff, as shown in Fig. 3.9.

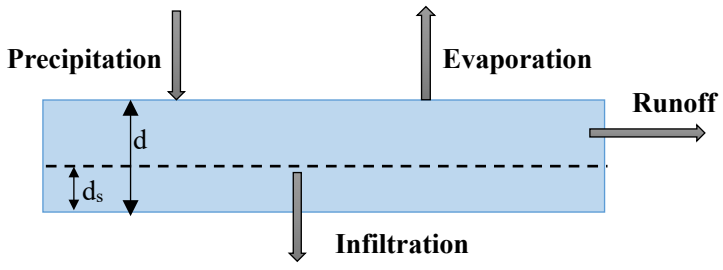

Fig. 3.9 Surface runoff process in PCSWMM

In PCSWMM, the surface runoff per unit area, q, occurs only when the depth of water in the "reservoir" exceeds the maximum depression storage, ds, in which case the outflow is given by Manning's equation. The depth of the water over the subcatchment (d) is continuously updated with the passing of time by the numerical solving of a water balance equation over the subcatchment.

$$Q = \frac{1.49}{n} W (d - d_s)^{5/3} s^{1/2} \qquad \text{Eq. (3.22)}$$

where Q is the runoff volumetric flow rate [L^3T^{-1}], N is Manning's surface roughness coefficient for overland flow, W is the subcatchment width [L], d is the depth of water over the subcatchment [L], ds is the depression storage depth [L], S_0 is the average slope of the subcatchment [] and A is the surface area of the subcatchment [L^2].

3.3.2 Hairsine Rose model

Gao et al. (2004) reexplained the commonly-used expression for the rain-induced soil detachment rate e = ar, where a is the soil detachability [ML^{-3}] and r is the rainfall rate [LT^{-1}] (Sharma et al., 1995; Jayawardena and Bhuiyan, 1999; Gao et al., 2003). The rate of ejection of soil water from the soil during rainfall is generated as shown in Eq.(3.23):

$$e_r = \frac{ar}{\rho_b} \theta \qquad \text{Eq. (3.23)}$$

where e_r is the rainfall-induced water transfer rate [LT^{-1}].

In this model, the rainfall rate controls the transfer between the exchange layer at

the soil surface and the runoff, while diffusion controls the chemical transfer between the underlying soil and the exchange layer. The soil water advection processes are displayed in Fig. 3.10.

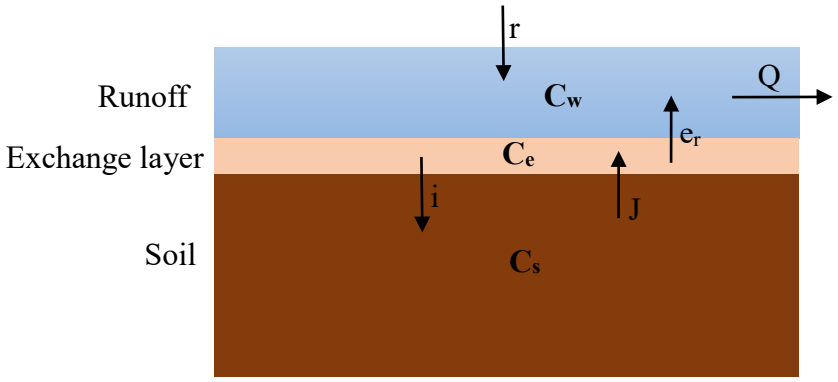

Fig. 3.10 Hairsine-Rose exchange layer model (Gao et al., 2004)

The exchange layer transport processes are controlled by the interactions between the rainfall and the soil surface, and at this layer that chemicals leave the soil and enter the surface runoff. The exchange layer is assumed to be mixed and can be characterized by a single concentration throughout the layer (C_e).

Chemical transport within the soil column below the exchange layer is controlled by both infiltration and diffusion, which can be described by the advection diffusion equation:

$$\frac{\partial \alpha C_s}{\partial t} = \frac{\partial}{\partial z}[D_s \frac{\partial C_s}{\partial z} - iC_s] \qquad \text{Eq. (3.24)}$$

where Cs is the chemical concentration in the soil water below the exchange layer [ML^{-3}], t is time [T], z is the vertical dimension [L], i is the infiltration rate [LT^{-1}], Ds is the dispersivity of chemicals [LT^{-1}] in the soil and α is considered to be the sum of the molecular diffusivity and the mechanical diffusion coefficient (Bear and Bachmat,

1990). Chemical transport in the exchange layer involves raindrop-driven exchange with the runoff water, diffusion into the layer of underlying soil and infiltration-mediated fluxes into the soil below. These processes are incorporated into the following equation:

$$\frac{d(\alpha d_e C_e)}{dt} = J + e_r(\lambda C_w - C_e) + i(C_w - C_e) \qquad \text{Eq. (3.25)}$$

where d_e is the depth of the exchange layer [L], C_e is the solute concentration in the exchange layer [ML^{-3}], C_w is the solute concentration in the runoff water [ML^{-3}], λC_w is the concentration of the water entering the exchange layer ($0 \leq \lambda \leq 1$) and J is the diffusion rate of the solute from the underlying soil to the exchange layer, which is described by Fick's law:

$$J = -D_s \frac{\partial C_s}{\partial z} \qquad \text{Eq. (3.26)}$$

Most processes in the exchange layer depend on rainfall, while the chemical transport into the runoff is most directly controlled by infiltration. The diffusion between the exchange layer and the surface runoff is neglected in this model as the diffusivity, D_s, is much smaller than the raindrop-induced mass transfer rate, e_r. The mass conservation of the chemical solute in the surface runoff can be expressed as shown in Eq. (3.27).

$$d\frac{\partial C_w}{\partial t} + q\frac{\partial C_w}{\partial x} = e_r(C_e - \lambda C_w) - rC_w \qquad \text{Eq.(3.27)}$$

This study uses a simplified analytical solution from the Hairsine-Rose soil erosion model, which can be found under the assumption that $\lambda = 0$, i.e. that the water replacing

the solution ejected from the exchange layer has a chemical concentration similar to rain (chemical-free). The solution can be expressed as:

$$C_w = AC_e - C_0 \exp(-\frac{rt}{d})$$
$$C_e = C_0 \exp(-\beta t) \qquad \text{Eq. (3.28)}$$

where, $A = e_r /(r - d\beta) \square \beta = e_r /(ad_e)$

3.3.3 HYDRUS model

Water flow governing equation

One-dimensional uniform (equilibrium) water transport in a partially saturated inflexible porous medium is described by a modified form of the Richards equation under the assumptions that the air phase plays an insignificant role in the liquid flow process and that the water flow due to thermal gradients can be neglected:

$$\frac{\partial \theta}{\partial t} = \frac{\partial}{\partial x}[K(\frac{\partial h}{\partial x} + \cos\beta)] - S \qquad \text{Eq. (3.29)}$$

where β is the angle between the flow direction and the vertical axis [], and K is the unsaturated hydraulic conductivity function [LT^{-1}] given by

$$K(h,x) = K_s(x)K_r(h,x) \qquad \text{Eq. (3.30)}$$

where K_r is the relative hydraulic conductivity [LT^{-1}] and K_s is the saturated hydraulic conductivity [LT^{-1}].

Solute transport governing equation

The classical equilibrium model for one-dimensional solute transport during

steady-state flow in a homogeneous porous medium can be displayed in the dimensionless form of a CDE as

$$R\frac{\partial C}{\partial T}=\frac{1}{P}\frac{\partial^2 C}{\partial X^2}-\frac{\partial C}{\partial X} \qquad \text{Eq. (3.31)}$$

where C is the dimensionless concentration [], X is the dimensionless distance [], T is the dimensionless time [], and P is the column Peclet number []. The equations for calculating these parameters are as follows:

$$\begin{aligned} &C = c / c_0 \\ &X = z / L \\ &T = vt / L = qt / \theta L \\ &R = 1 + \rho_b k_d / \theta \\ &P = vL / D \end{aligned} \qquad \text{Eq. (3.32)}$$

where k_d is the linear adsorption coefficient [LM^{-3}]. D is the dispersion coefficient [L^2T^{-1}].

3.3.4 STANMOD model

The basic equation used in the 3DADE model is the advection-dispersion equation (ADE), which describes the three-dimensional transport of a non-reactive solute in the soil:

$$R\frac{\partial c}{\partial t}=D_x\frac{\partial^2 C}{\partial x^2}-v\frac{\partial c}{\partial x}+D_y\frac{\partial^2 C}{\partial y^2}-\mu c \qquad \text{Eq. (3.33)}$$

where D_x and D_y are the dispersion coefficients in the x- and y- directions [L^2T^{-1}] respectively and X is the position in the flow direction.

A three-dimensional analytical solution of the ADE equation by Hunt (1978) is

applied in the soil considered as shown in the following equation:

$$C = \exp(-\frac{\mu t}{R}) \frac{M}{8\theta\pi r\sqrt{D_y D_z}} \exp[\frac{(x-r)v}{2D_x}] erfc(\frac{r-vt}{2\sqrt{D_x t}}) \quad \text{Eq. (3.34)}$$

$$r = (x^2 + y^2 \frac{D_x}{D_y} + z^2 \frac{D_x}{D_z})^{1/2}$$

where M is the initial input of contaminant [MT^{-1}].

3.4 Summary

This chapter introduces the methodology of this thesis study. The methodology is divided into two parts: the existing model method and the integrated ARCTRA system. In both methods, three processes were considered: the formation of rainfall-runoff, the dissolution of soil surface contaminant into runoff and the transport of solute in the unsaturated zone. In the existing model method, the PCSWMM model, the Hairsine-Rose model and the HYDRUS model were applied. In the ARCTRA system, Eq. (3.7), Eq. (3.15) and Eq. (3.18) were selected as governing equations and used to calculate the runoff water depth and the concentration in the runoff and the soil.

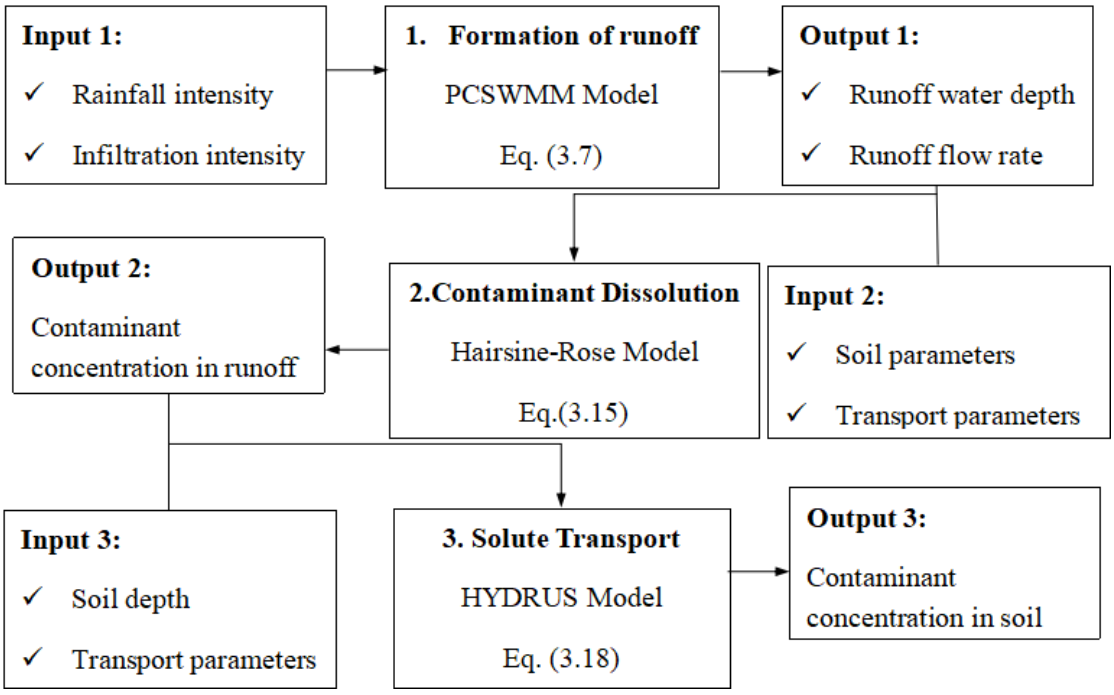

Fig. 3.11 Input and output of modeling and ARCTRA system

The developed ARCTRA system contains a risk assessment method based on fuzzy set theory. The calculation results were analyzed via Monte Carlo Simulation. The cumulative probability function of the results could be generated according to the designed probability density functions (PDFs) of the selected uncertain parameter. In the fuzzy set risk assessment method, the contaminated site was quantified by the generalized risk of the contaminant. The generalized risk level was determined by integrating consideration for both environmental-guideline-based and health risks. In this chapter, the definitions and divisions of environmental guidelines and health risks were explained in detail along with the rules by which the generalized risk score was generated. Finally, in order to ensure easy application of the ARCTRA system, a user interface was designed based on the VB editor and inserted into the Excel system. The system as designed allows users to input the parameters through the interface, which

then displays the results after they are calculated by Excel.

The two methods introduced in this chapter were validated in the subsequent chapters 4 and 5. In chapter 4, the existing models were applied to a case study in Eastern Canada. The results were compared with the literature data. Chapter 5 introduced a case study in France where both the existing models and the ARCTRA system were applied, with the results compared with the literature data.

4. CASE STUDY 1 - EXAMINATION OF EXISTING MODELS

4.1 Study Area

The study area is located in Eastern Canada and encompasses a total area of 12,000 m^2. It is made up of commercial and residential land. The area around the site is home to a transport company, vacation housing, the transport minister, a commercial center, restaurants and an automobile selling and recycling company.

Using the groundwater level data from the Groundwater Information Network (GIN, 2013), a contour map of groundwater levels was generated, and the depth of the groundwater at the study site was estimated to be about 2.72 m. The direction of the groundwater was north-east. The soil surface was covered by the mix packing, which consisted of sand, silt, clay, and gravel (quartz, metal, wood, brick, glass fiber, plaster, plastic bags, asphalt and concrete). The depth range of the mix packing layer was 0 to 1.5 m. The layer below the soil was clay (>1.5m).

In 2004, it was reported that mining waste had been disposed of at the soil surface, which resulted in the presence of heavy metal contaminants such as Pb, Cd, and Zn in the study area. Therefore, an environmental assessment was generated in 2005, analyzing the concentration of related contaminant in the study site. Nine detection points (S1 to S9) were arranged throughout the site as shown in Fig. 4.1.

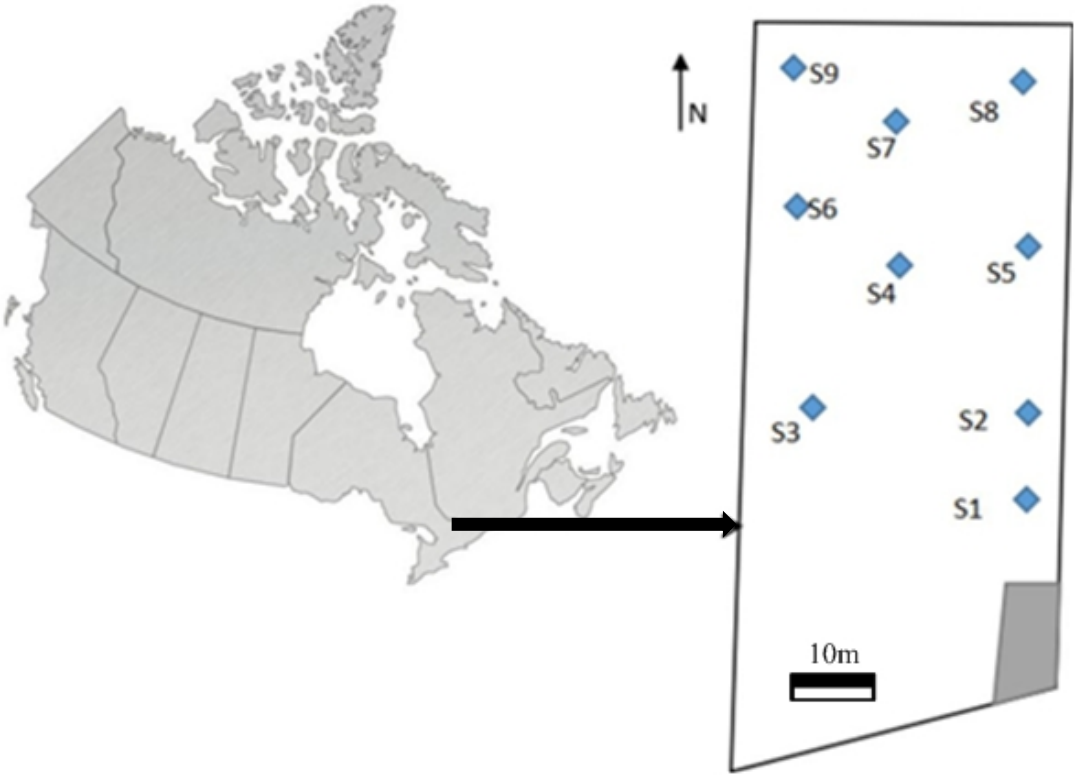

Fig. 4.1 Study area map and sampling point distribution

4.2 Input Data and Parameters

Different pollutants were studied in the environmental assessment report. In the study, lead (Pb) alone was chosen as the pollutant to be explored. The concentrations of Pb at each point measured in the report are displayed in Table 4.1 as shown:

Table 4.1 Pb concentration data from sampling points at different depths (D&G, 2005)

Point	S1	S2	S3	S4	S5	S6	S7	S8	S9
Depth(m)	0-1	0-1.45	0-1.2	0-1.2	0-1	0-1.15	0.6-1.45	0.3-1.5	0-1.8
Concentration(mg/kg)	127	84	106	533	64	252	434	241	36
Depth(m)	1-2	1.45-2	1.2-2	1.2-1.8	1-2.1	1.15-2	1.45-2	1.5-2.4	-
Concentration(mg/kg)	<20	<10	<10	38	<20	<10	<10	38	-

The RPRT (Politique de protection des sols et de réhabilitation des terrains

contaminés) (MDDELCC, 2017) is used as the standard. A contour map was developed as shown in Fig. 4.2 to display the monitored contaminant concentration. In the contour map, the highest concentration of Pb is found at S5 (533 mg/kg) while other relatively high concentrations are shown at S4, S6, and S9. Therefore, it can be indicated that the runoff flow direction was roughly from south to north.

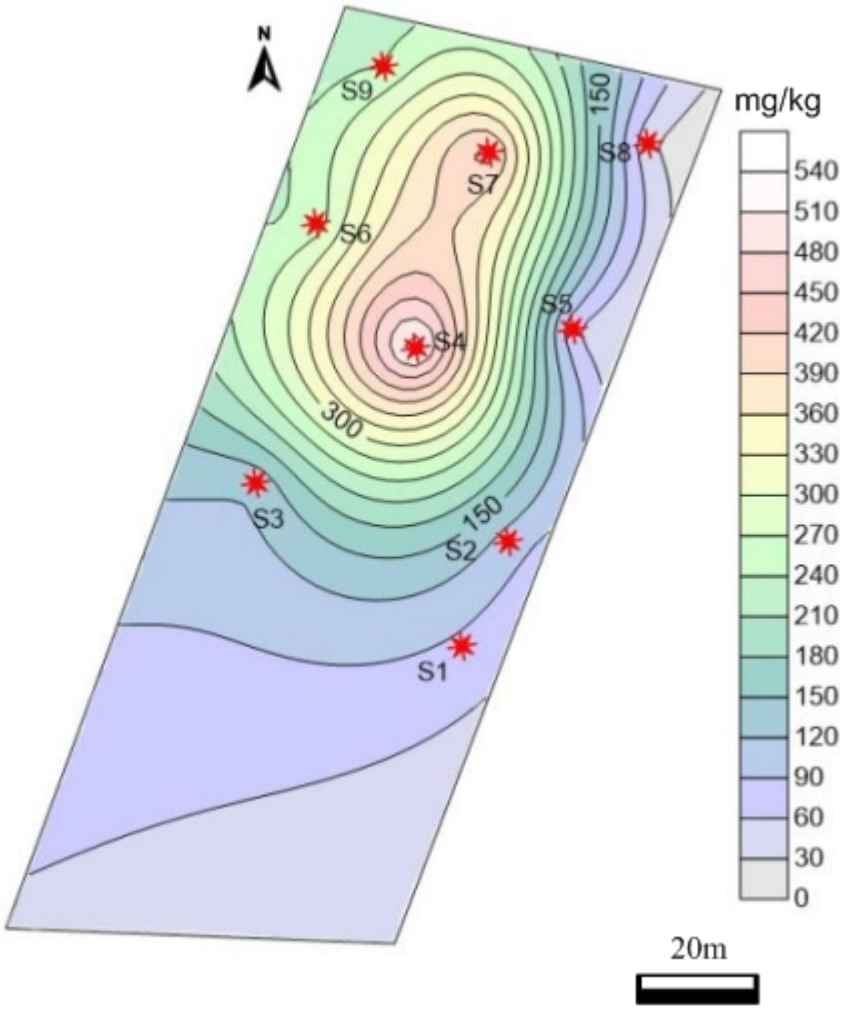

Fig. 4.2 Pb initial concentration contour map at soil surface

For the simulation of the surface runoff formation, an average typical one hour of Quebec rainfall activity was applied in the PCSWMM modeling. The total amount of

rainfall was set at 30 mm and the graph of rainfall intensity over time is displayed in Fig. 4.3 as shown.

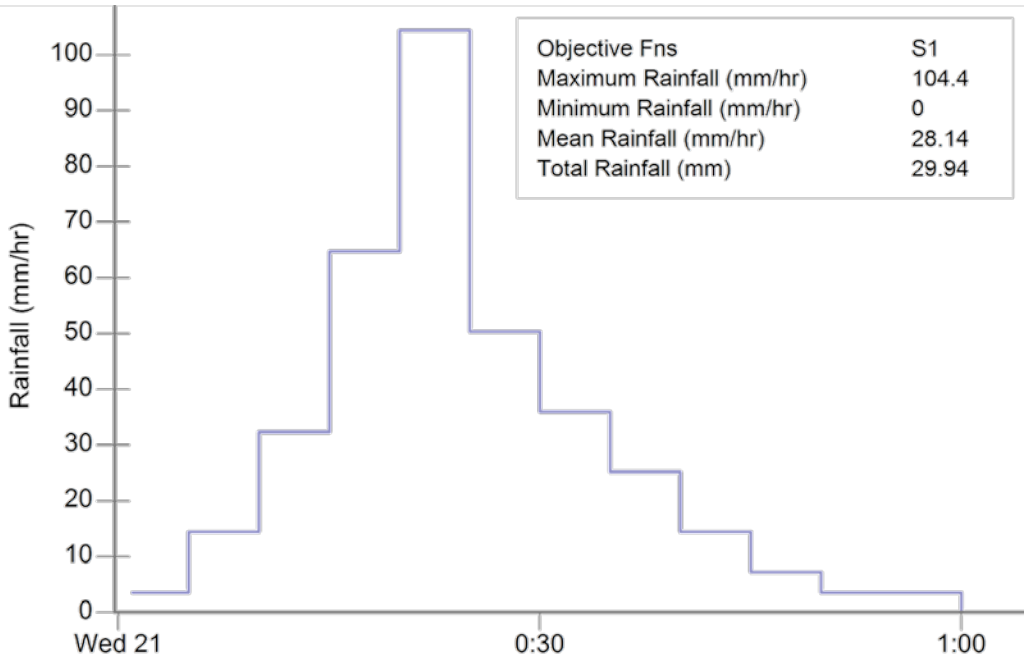

Fig. 4.3 Rainfall intensity graph[1]

Other input parameters for the study area used in PCSWMM are listed in Table 4.2. The subcatchment width and length were subdivided automatically by PCSWMM. The parameters are obtained based on the study area characteristics (D&G, 2005).

[1] The Objective Fns means Objective Functions in the PCSWMM Operation.

Table 4.2 Input data applied in PCSWMM model

Parameters	Values
Subcatchment Width (m)	500
Subcatchment Length (m)	40.242
Slope	5%
Impervious area	25%
Percent of impervious area with no depression storage	25%
Min infiltration capacity (mm/h)	3
Manning's N for impervious area	0.1
Manning's N for pervious area	0.01
Depth of depression storage on impervious area (mm)	0.05
Depth of depression storage on pervious area (mm)	0.05
Max infiltration capacity (mm/h)	0.5

Some parameters applied in the Hairsine-Rose model in this case study were previously published by Gao et al. (2004). This soil mixture has been used in previous soil erosion experiments in which the soil erodibility a=0.40 g/cm^3, and the soil saturated moisture content θ=0.48. Other parameters used in the model are listed in Table 4.3.

Table 4.3 Input data applied in Hairsine-Rose model

Parameters	Values
Bulk density ρ_b (g/cm^3)	1.35
Soil moisture (porosity) θ	0.48
Soil erodibility, a (g/cm^3)	0.4
Diffusivity, Ds (cm^2/ s)	8.6×10^{-6}
Dispersivity, α_L (cm)	0.88
Exchange-layer depth, de (cm)	0.4

According to the results seen in Tables 4.2 and 4.3, the relative input parameters of the STANMOD model are determined as shown in Table 4.4:

Table 4.4 Input data applied in STANMOD model

Parameters	Values
Velocity (m/d)	3.68
Retardation factor	9.44
μ:first-order rate coefficient for decay	0.0034
Dx: dispersion coefficient in the x-direction (cm^2/d)	74.3
Dy: dispersion coefficient in the y-direction (cm^2/d)	74.3

4.3 Model Results

4.3.1 PCSWMM results

With the above parameters, the model calculated the surface runoff activities and generated the flow and infiltration rates of the runoff, which are shown in Fig. 4.4 (a) and (b) as example. As seen in the graph (b), the runoff increased in the first 30 minutes until it reached the maximum flow rate, after which it began to decrease. The average

flow rate of the runoff was 0.0649 m^3/s, and the average depth of the runoff was 28.27 mm. The infiltration rate as calculated by the PCSWMM model is shown in Fig. 4.4 (a), where the average infiltration rate is seen to be 0.4364 mm/h.

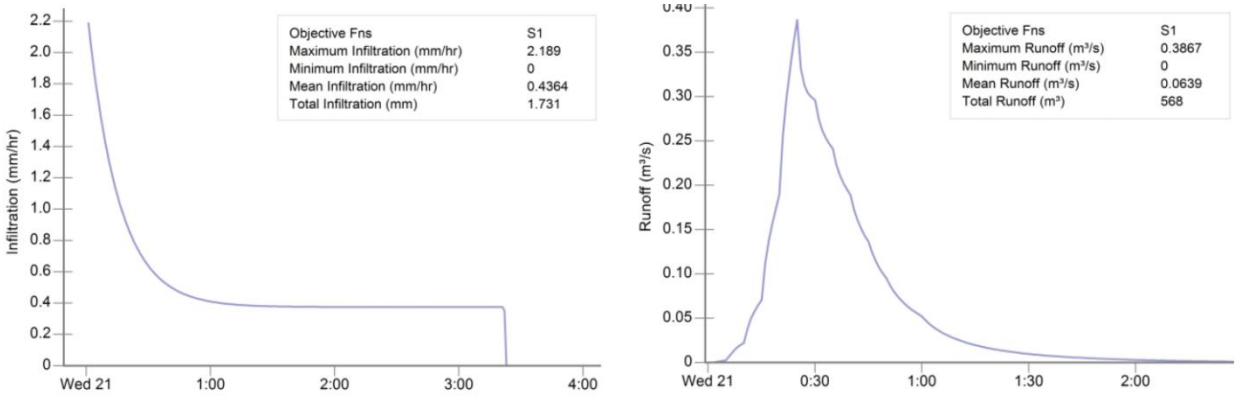

(a) Infiltration Intensity (mm/hr)

(b) Runoff flow rate (m^3/s)

Fig. 4.4 Runoff flow and infiltration rate result

4.3.2 Hairsine-Rose model results

From the results seen in 4.3.1, the depth of the runoff is 28.27 mm, i.e., d_w=28.27 mm and the rainfall r =28.14 mm/h. And the initial concentration of the waste source is 4.5 g/L. With the analytical equation Eq. (3.7), the concentration of Pb in the exchange layer (C_e) can be calculated as 1.853 g/L and the concentration of Pb dissolved into the runoff (C_w) as 0.757 g/L, which can be expressed as 561.1 in mg/kg (based on a dry soil bulk density of 1.35 g/cm^3.

4.3.3 STANMOD model and analytical solution results

About 380 days were therefore simulated, with the resulting profiles of solute transport distribution in the soil at 0 m and 1.5 m in 2005 being displayed in Fig.4.5 (a) and (b) respectively. The contaminant mainly transported in the X direction due to the pore

water flow and also transferred to the Y direction by dispersion. The value of the spectrum stands for the equivalent relative concentration. Fig. 4.5 (a) illustrates the concentration of contaminants at the soil surface after 380 days and most contaminants transported at the soil surface. For the highest concentration, at S4, the concentration decreased in the X transport direction. A profile was also generated at 1.5 m (Fig. 4.5 (b)) showing that only a small amount of contaminant transported and exited in the vertical direction. The concentration at 1.5 m of depth in the soil was less than 1/10th of the initial source concentration.

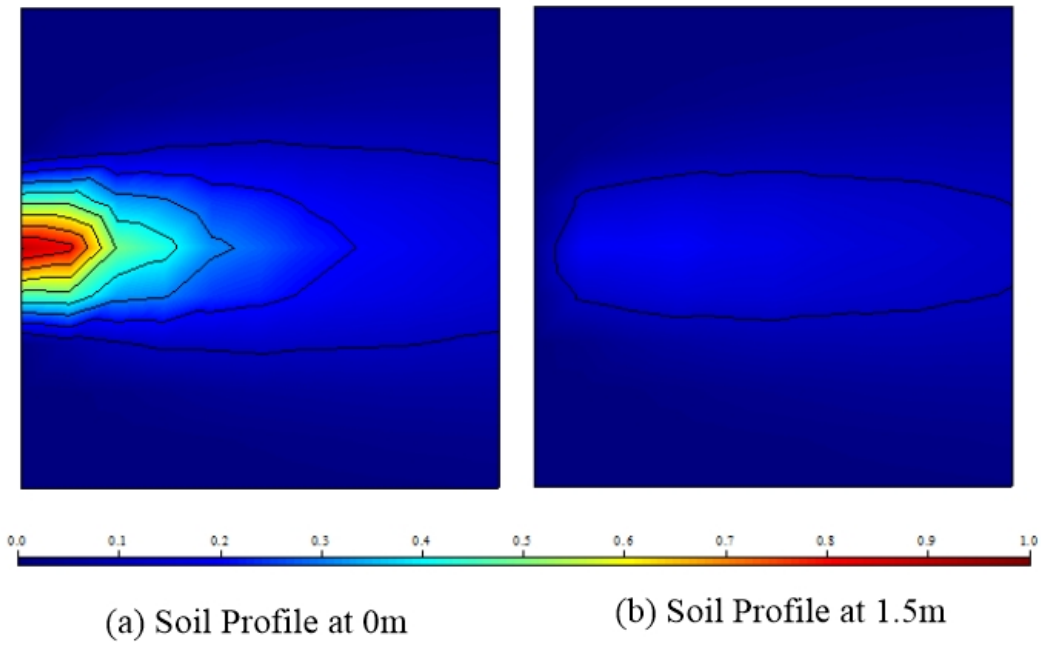

Fig. 4.5 Pb distribution profile in soil at 0 and 1.5 m

4.4 Comparison with Literature Data and Discussion

Assuming S4 has x and y values of 0 at the soil surface, the coordinates of S5, S6, S7, S8, and S9 can be inferred. Using the coordinates, the relative equivalent concentrations can be obtained at these detecting points, and the results can be compared with the real

literature data from the environmental assessment report as seen in Table 4.5. The results in Table 4.5 show a substantial similarity to the literature data. The deviation percentage between the two series of results is lower than 10% at most points except S8.

Table 4.5 Comparison of STANMOD, analytical solution results and literature data of surface layer

Point	S4	S5	S6	S7	S8	S9
STANMOD result	1.0	0.12	0.5	0.8	0.4	0.08
STANMOD concentration [a] (mg/kg)	561.1	67.33	280.55	448.88	44.89	224.44
Analytical result (mg/kg)	644.7	70.14	305.24	501.06	49.71	254.74
Literature data (mg/kg)	533	64	252	434	36	241
Deviation 1[b]	5.27%	5.2%	11.33%	3.43%	24.69%	6.87%
Deviation 2[c]	20.95%	9.59%	21.13%	15.45%	38.03%	5.7%

a. The values are transformed from the relative concentration of STANMOD results.

b. The results present the deviation percentage between STANMOD results and literature data.

c. The results show the deviation percentage between analytical solution results and literature data.

In order to validate the veracity of the model, an analytical solution was also applied in this study. Using Eq. (3.11) in 3.2.4, the results for points S4 to S9 were obtained and listed in Table 4.5. the results of STANMOD are shown as relative concentration to the initial concentration and transferred into mg/kg in Table 4.5. A comparison shows that the results of the analytical solution are similar in value to those obtained using the STANMOD model as well as those found in the literature data, which proves the veracity of the STANMOD model.

In Table 4.5, the values of deviation 2 are greater than those of deviation 1, which means that the modeling results show a higher validity than the analytical solution results when compared with the literature data. Some explanations for this phenomenon have been theorized through comparison of the analytical solution equations of the STANMOD (Leij et al., 1991) model with the analytical solution used in this study. A comparison shows that, with the exception of the primary solute movement by advection and dispersion, the STANMOD model considers solute retardation, first-order decay, and zero-order production, while the analytical solution only accounts for the first-order decay. Therefore, the Pb concentrations found using the analytical solution are higher than those seen in the STANMOD modeling results, especially at the source point S4 and the nearby points S6 and S7.

The transport of Pb in the soil in the vertical direction was also simulated. In the vertical direction, the infiltration velocity obtained by PCSWMM was adopted as the pore water velocity, i.e., v=10.5 mm/day. The other parameters are the same as seen in the previous part. The profile of Pb transport in the soil is shown in Fig. 4.6.

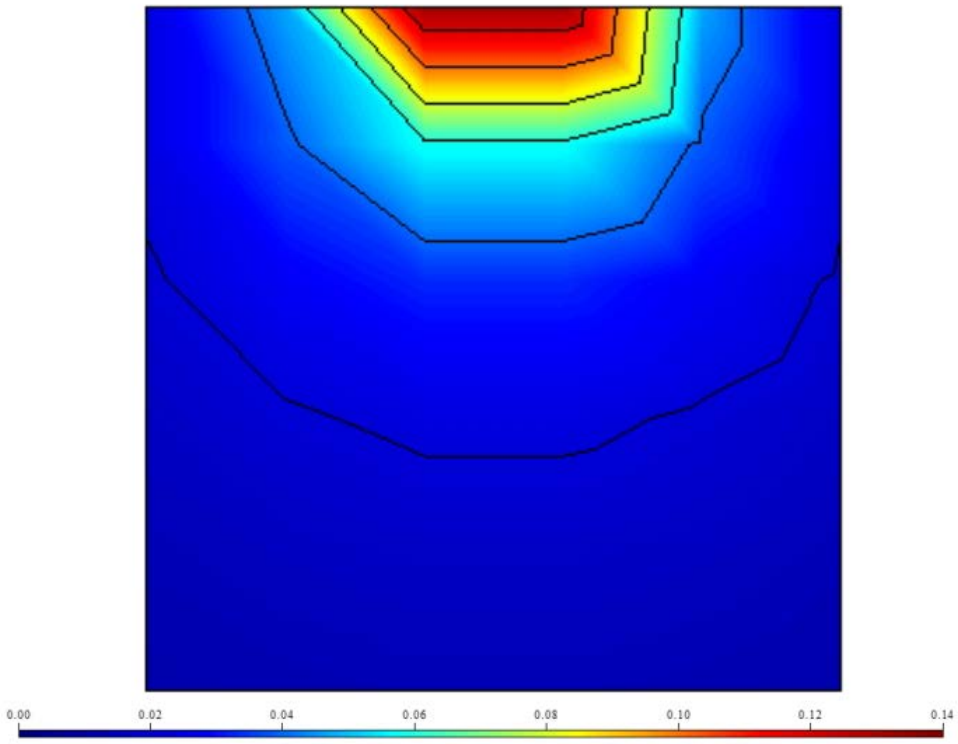

Fig. 4.6 Pb concentration profile in vertical direction in soil

In the environmental assessment report, the concentration of Pb at a 1.2 m depth at the source point S4 was estimated to be 38 mg/kg. In the STANMOD model, the relative equivalent concentration is 0.08 at a 1.2 m depth, which means the concentration is 0.08*561.1 mg/kg = 44.89 mg/kg. The result calculated by the analytical solution is 0.0711, i.e., 51.11 mg/kg. A detailed comparison is shown in Table 4.6.

Table 4.6 Comparison of Pb concentration results at 1.2m of point S4

Point S4	Relative concentration result	Concentration in mg/kg[a]
STANMOD	0.08	44.89
analytical solution	0.0711	39.89
Literature data	-	38
Deviation 1[b]	18.13%	
Deviation 2[c]	4.97%	

a. The values are transformed from the relative concentration of STANMOD and analytical solution results.

b. The results show the deviation percentage between STANMOD result and literature data.

c. The results show the deviation percentage between analytical solution result and literature data.

Using the simulation results of the STANMOD model, a contour map of the concentration of Pb in three different depths of soil (<1 m, 1-2 m, and > 2 m) was generated as shown in Fig. 4.7. From Fig. 4.7, we can see most contaminants transported at the soil surface (soil depth <1.0 m). Pb transported from S5 in a northerly direction due to water flow and dispersion. Meanwhile, in the vertical direction, the contaminant Pb transported through the infiltration from the source at S4. At the depth level of 1 to 2 m, the concentration of Pb at S4 is 44.89 mg/kg. Pb also transported in the horizontal direction. As a result, Pb was also detected at S5, S6, S7, and S8 with concentrations of around 10 mg/kg. Furthermore, only a small amount of Pb transported more deeply than 2 m into the soil. The concentration of Pb at depths of more than 2 m at the detection points was less than 10 mg/kg, which is considered minimally harmful to humans and the environment. The results also illustrate that the quantity of Pb

transported into the groundwater was much too small to seriously affect the quality of the groundwater and nearby surface area.

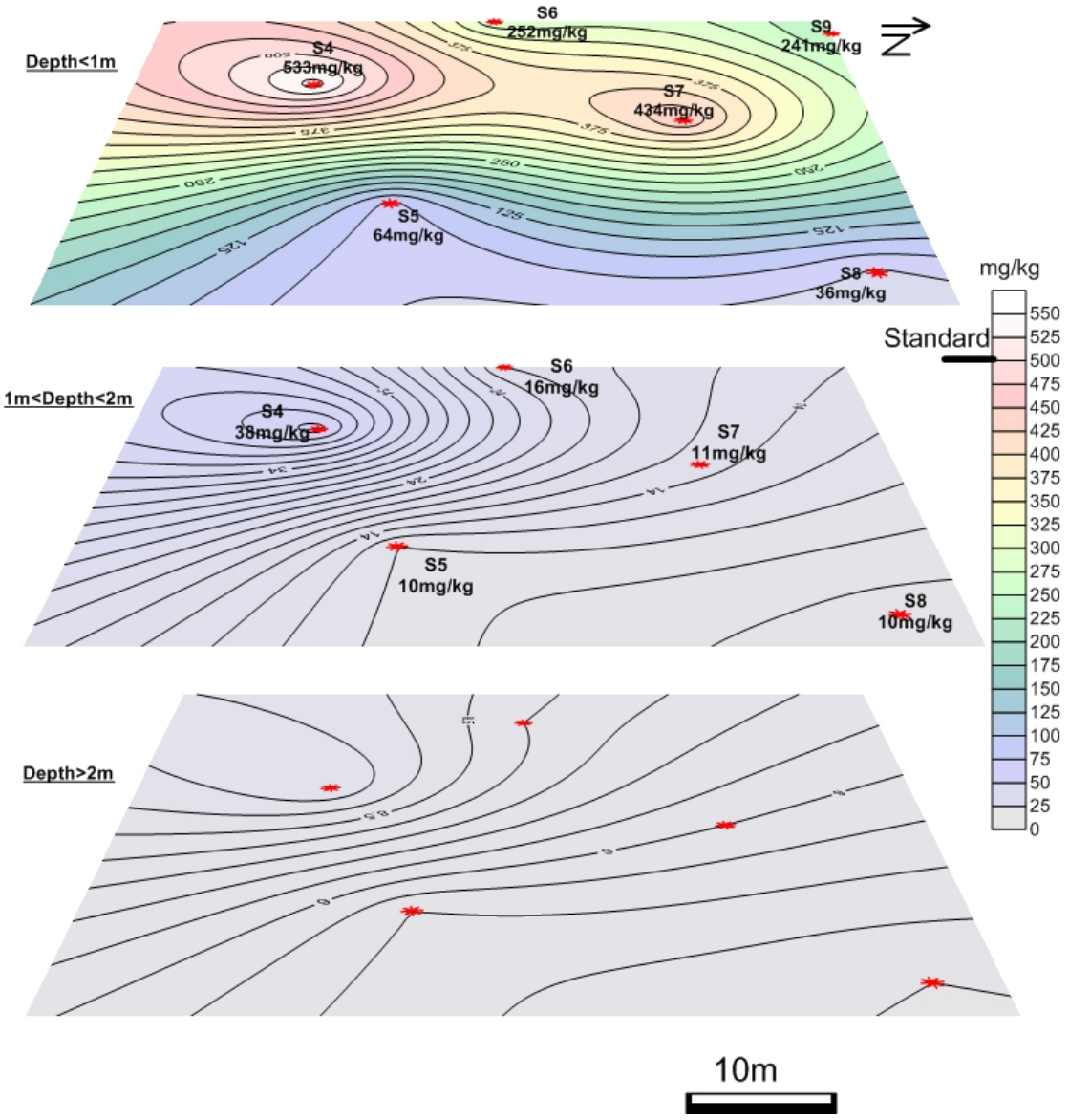

Fig. 4.7 Pb concentration contour results at different soil depths

4.5 Monte Carlo Simulation Analysis and Risk assessment

In this study, soil porosity was selected as the uncertain parameter. With the soil types ranging from sand to clay, the range of soil porosity values was set at 0.36 to 0.58. The PDF of the soil porosity was generated using the Monte Carlo analysis. The triangular

technology was applied as the distribution method. The detailed parameter values are listed in Table 4.7.

Table 4.7 Variant and parameter value for PDF generation

Soil porosity	Mean	Minimum	Maximum	Variance	Distribution
Input	0.48	0.36	0.58	0.01	
Generated	0.478	0.363	0.574	0.00215	

The PDF for the soil porosity found using Monte Carlo simulation was generated as shown in Fig. 4.8. In the simulation, the number of Monte Carlo iterations performed for the variant was 100.

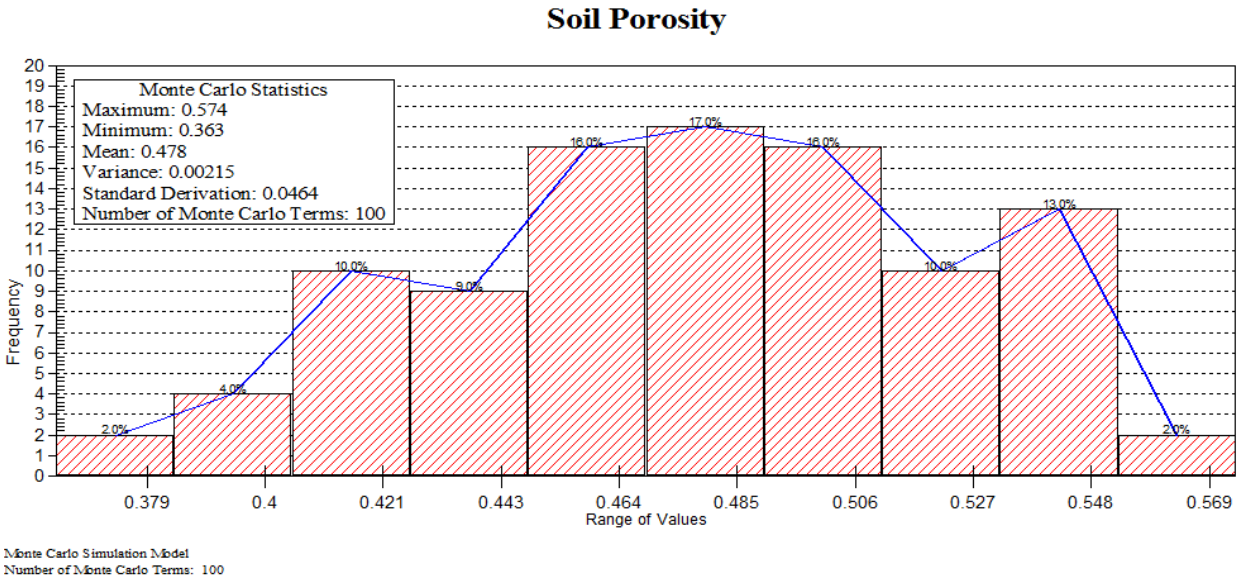

Fig. 4.8 Probability density function generated for soil porosity

With the PDF for soil porosity, we can calculate the uncertain concentration results for pollutant transport in the soil. The result is a range of relative concentration values due to the range of soil porosity. As illustrated in the methodology section, the uncertain parameter is associated with both the soil erosion model and the transport part, i.e., Eq. (3.7) and (3.11). In Eq. (3.7), the value of soil porosity affects the value of concentration

dissolved into the runoff, while in Eq. (3.11) it affects the amount of contaminant transported into the soil.

In this study, S4 was selected as the study point at the site, and the value variation of the relative concentration of Pb was calculated. As shown in the previous results, the relative concentration is 1 when the soil porosity θ is 0.48. As the range of soil porosity is 0.36 to 0.58, the upper limit and the lower limit of the parameter was set as 0.58 and 0.36 respectively. As a result, the range of relative concentration values can determined, which is from 0.765 to 1.208, and the range of Pb concentration in runoff is from 112.84 to 934.631 mg/kg.

A complementary cumulative probability function of the range of relative concentration can, therefore, be generated as shown in Fig. 4.9. We can thus obtain the probability of a range of porosity values. In cases where the exact values of bulk destiny and soil porosity are unknown in the actual modeling, we can estimate the range of concentration values with an infinite range of soil porosity values. For example, if we assume the soil type is clay, the typical bulk density of clay soil is within the range of 1.1 and 1.3 g/cm^3, which gives a porosity value between 0.58 and 0.51. With the range of soil porosity, we can determine the value range of the final concentration in mg/kg as 850 to 1000 mg/kg and also conclude the probability of the value range is about 18% as shown in Fig. 4.9.

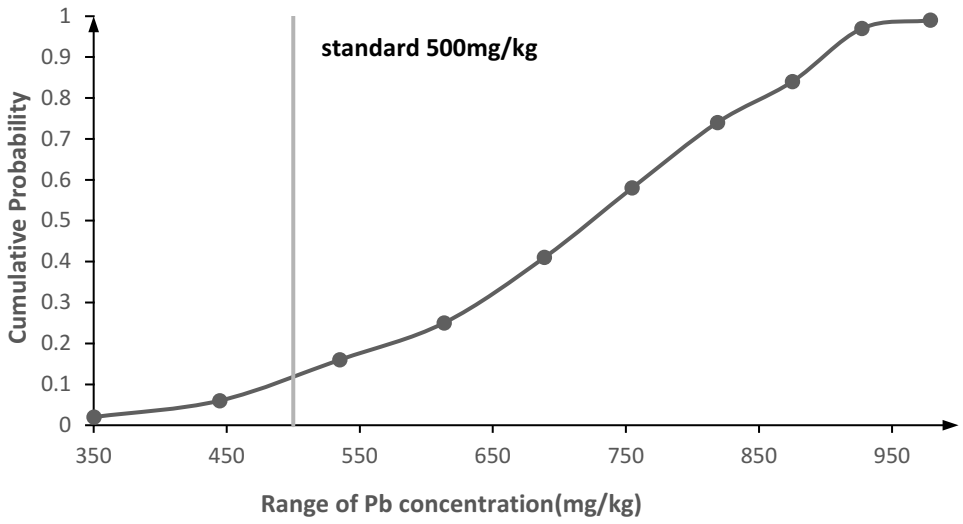

Fig.4.9 Cumulative probability function of Pb concentration

With analysis of the Monte Carlo simulation, we can assess the risk posed by the contaminant to the environment. Taking the case study as an instance, the standard for Pb in the soil is 500 mg/kg according to RPRT (Politique de protection des sols et de réhabilitation des terrains contaminés). Therefore, when the concentration of Pb is over 500 mg/kg at detection point S4, the contaminant is considered to be harmful to humans and the environment. In this case study, the probability of Pb over the standard at 500 mg/kg is around 87%, as shown in Fig. 4.9. Furthermore, if the value of the soil porosity is over 0.41, the concentration of Pb transported at detection point S4 will violate the RPRT environmental guidelines. In other words, with soil porosity selected as the uncertain parameter, 87% of over 500 mg/kg of Pb transports to point S4, which has a hazardous effect on humans and the environment.

4.6 Summary

In this chapter, a case was applied to examine the methodology explained in Chapter 3.

The process framework is concluded in Fig. 4.10. Heavy metal wastes dissolve into runoff due to rainfall and transport into the soil after being released in the environment. Therefore, the existing models were applied to each process respectively. For example, the formation of rainfall-runoff was simulated using the PCSWMM model. The amount of heavy metal dissolved into the runoff from the soil surface was calculated using the Hairsine-Rose model based on the simulation results from the PCSWMM model. Afterwards, the STANMOD model based on the ADE equation was used to simulate the transport of heavy metal solute in the soil in both the horizontal and vertical directions. Moreover, a three-dimension analytical solution of ADE was also applied in the case study. Through comparison with the literature data, the accuracy of the existing models has been validated. The Monte Carlo Simulation was also used to consider the uncertainty parameters in the study process.

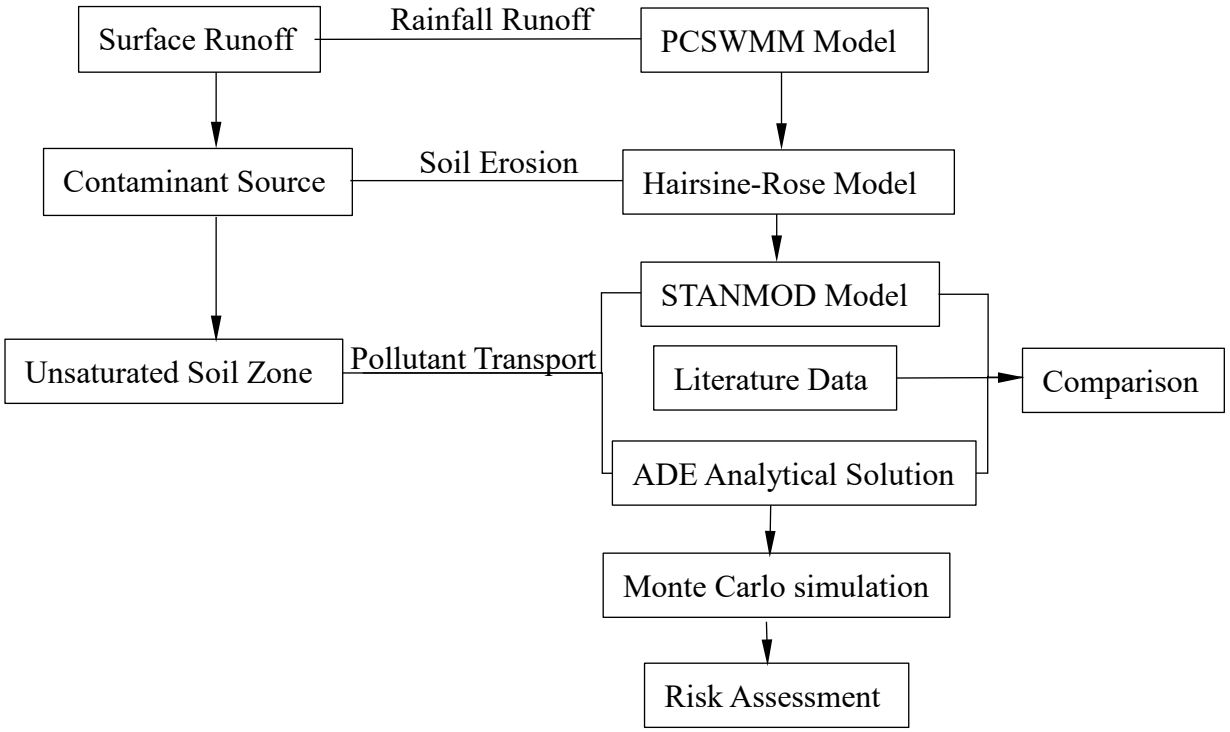

Fig. 4.10 Framework of ARCTRA system implementation

In conclusion, this case study validates the feasibility of the existing models. Moreover, the ADE analytical solution and Monte Carlo Simulation were also examined in this chapter, which could accumulate the experience and reliability for the following development and operation of ARCTRA system.

5. CASE STUDY 2 - TEST AND VALIDATION OF THE ARCTRA SYSTEM

5.1 Study Area

The sampling site is a small public park, called Peru Park, located in the city of Auby (Northern France) and situated close to the Zn smelter Nyrstar (Fig. 5.1), one of the largest factories in Europe and still in activity. Founded in 1869, it produces nowadays approximately 220,000 t of Zn per year. The atmospheric metal emissions released in the past by this factory have contributed to a severe contamination of the surrounding soils. The Peru Park has the particularity of combining an outdoor playground in its north part and a protected area in the South due to the presence of calamine grassland. Contaminated topsoil was indeed partially removed in the North and replaced to accommodate a playground area whereas the rest of the park remains highly contaminated. The contaminated soil can be defined as loamy soil with a quite neutral pH (mean of 7.1) containing an average 20% clays, 31% sands and 49% silt.

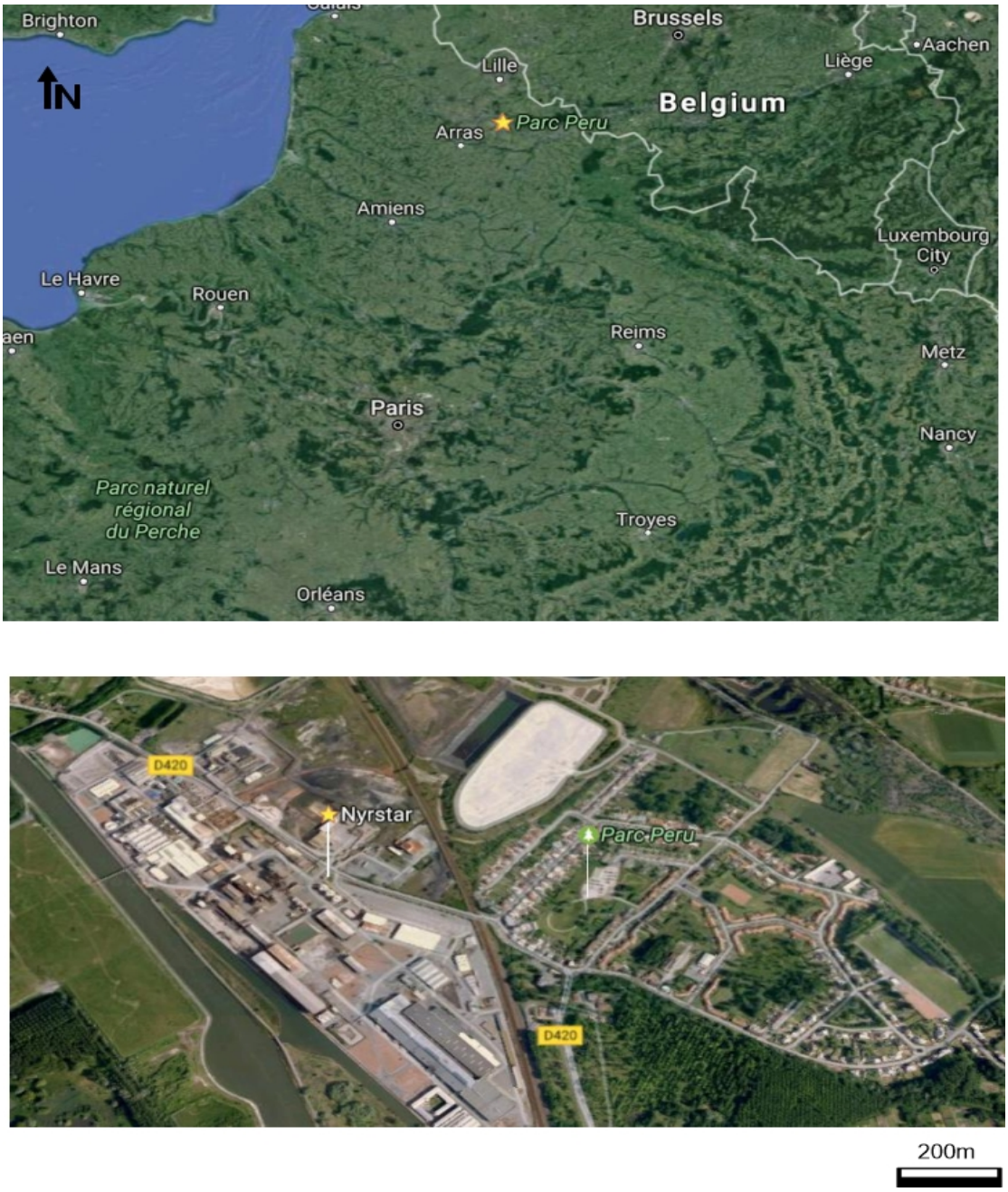

Fig. 5.1 Location of the study area

Several sampling campaigns were scheduled from 2012. The first one took place on 04 April 2012 to map the contamination of the park's topsoil (Fig. 5.2). For that purpose, 22 samples of soils were collected in the study area using a manual six cm-internal diameters stainless steel auger that permits collecting approximately the first 20 cm of the soils.

Fig. 5.2 Location of the study site peru park

5.2 Input Data and Parameters

The literature measured concentration of the samples is listed in the following Table 5.1 and the contour map of Zn concentration with topsoil in this area are generated as Fig. 5.3:

Table 5.1 Zn concentration at sampling points (Dumoulin et al., 2017)

Point	Zn (mg/kg)	Point	Zn (mg/kg)
1	14767	12	11625
2	15913	13	6572
3	6845	14	4665
4	5228	15	4184
5	9736	16	12977
6	2524	17	5922
7	3981	18	7002
8	6338	19	5038
9	11452	20	9597
10	12868	21	3977
11	21020	22	6177
	Mean		8564
	Max		21020
	Min		2524

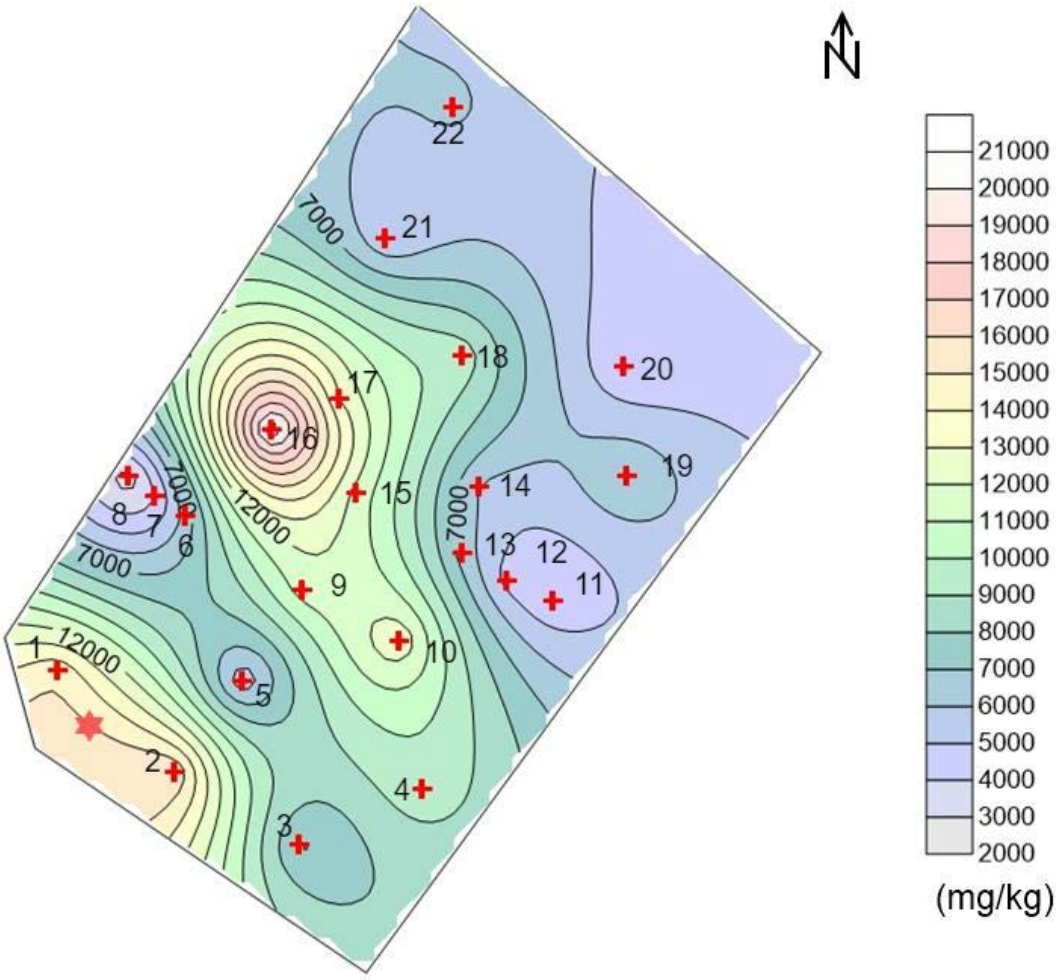

Fig 5.3 Contour map of Zn concentration of sampling point

A third campaign was organized on 20 June 2012. Two small soil pits were dug at the stared point in Fig. 5.3, and the porous candles were inserted in duplicate at two depths: close to the surface (around 0-5 cm) and more deeply in the soils (around 25-30 cm). Afterwards, pore water sampling was periodically performed several times under vacuum in July 2012, October 2012, April 2013 and October 2013. The average values of sampling data at pit 1 and pit 2 are listed in Tables 5.3 and 5.2 respectively. In Table 5.2, the Zn concentration decreased by depth. While considering the Zn concentration in pore water, Zn transports with the rainfall-runoff infiltration. As a

result, the concentration at soil surface was lowest and increased by depth. The concentration was highest at 25 cm depth and decreased at 30 cm. In the studied four dates, the Zn concentration was different; thus we can infer that the transport of Zn is related to rainfall amount and period.

Table 5.2 Zn concentration at sampling pit at different soil depths

Pit Depth (cm)	Zn Concentration (mg/kg)
2.5	9628
7.5	8585
12.5	6953
17.5	6965

Table 5.3 Zn concentration in pore water at different soil depth

DEPTH (cm)	Zn Concentration (mg/L)	DEPTH (cm)	Zn Concentration (mg/L)
July 2012		**April 2013**	
0	8	0	5.05
5	12.1	5	5.8
25	31.7	25	14.5
30	25.1	30	16.2
October 2012		**October 2013**	
0	5.55	0	5.3
5	7.35	5	7
25	20.75	25	17.85
30	20.7	30	20

Weather

In order to simulate the runoff by rainfall, the rainfall data from July 2012 to October 2013 are generated as follows (World Weather Online, 2013):

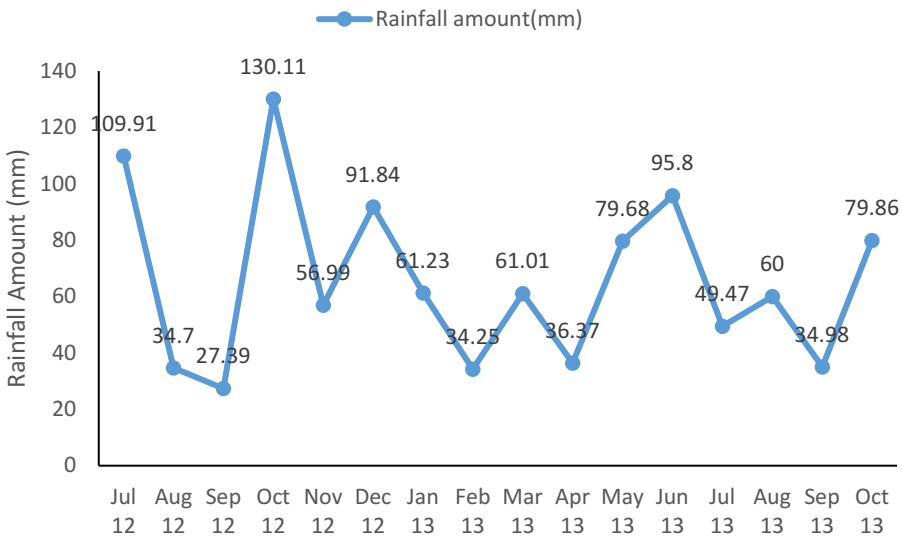

Fig. 5.4 Monthly rainfall data for the study site in 2012-2013

5.3 Model Results

5.3.1 PCSWMM model results

For the simulation of the surface runoff formation, a typical 6 h, 24 h, 4 h and 5 h rainfall activities were applied in PCSWMM modeling for July 2012, Oct 2012, April 2013 and Oct 2013, respectively. The total amount of rainfall was set at 50 mm, 65 mm, 40 mm and 45 mm and the rainfall intensity graphs by time for the four dates are displayed in Fig. 5.5 as follows:

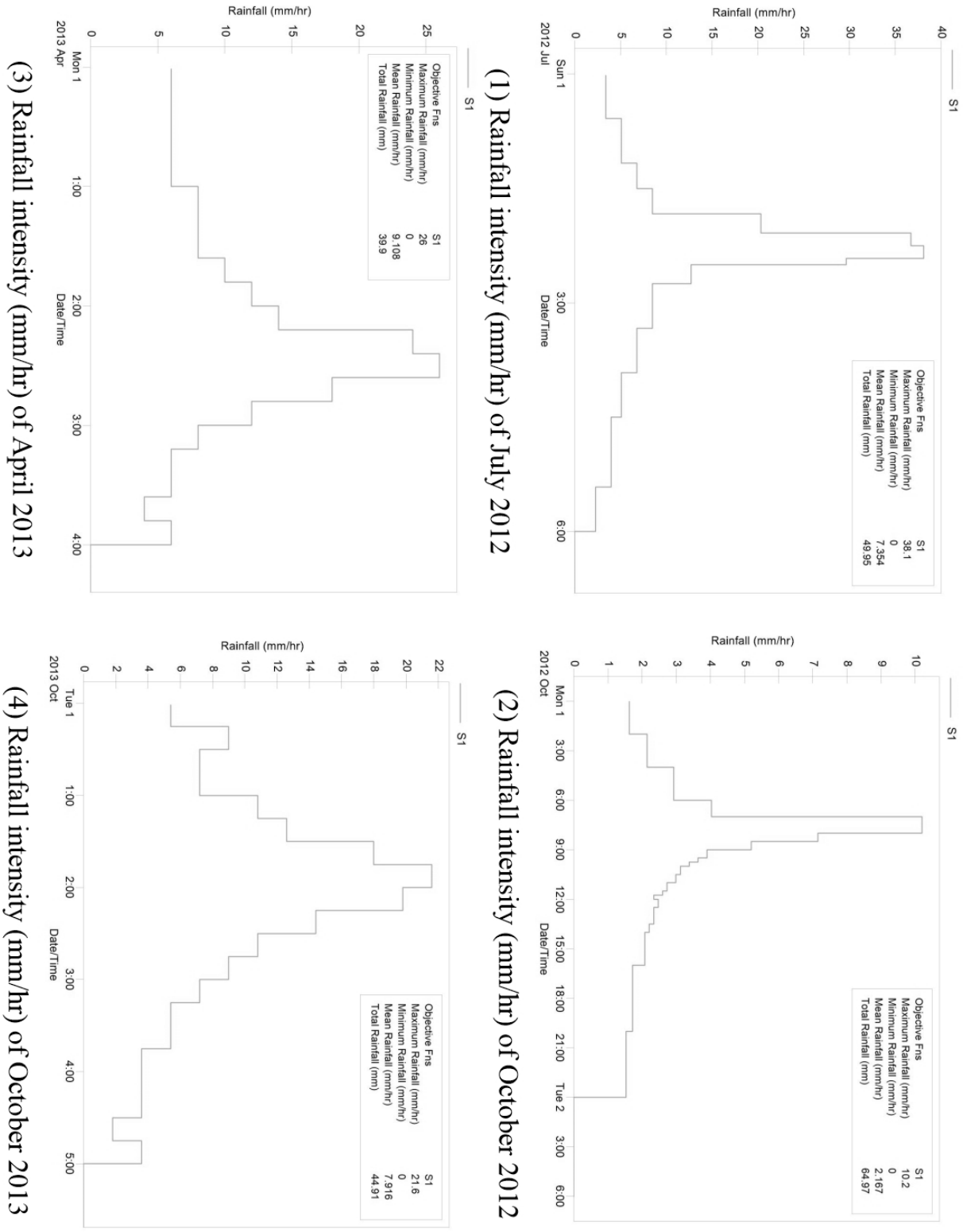

Fig. 5.5 Rainfall intensity for the study period at the study site

Other input parameters for the study area used in PCSWMM are listed in Table 5.4,

in which the subcatchment width and length were subdivided automatically by PCSWMM. The parameters applied in the model are obtained from experimental results and literature data.

Table 5.4 PCSWMM model parameters

Parameters	**Values**
Subcatchment Width (m)	500
Subcatchment Length (m)	62.748
Slope	5%
Impervious area	25%
Percent of impervious area with no depression storage	25%
Min infiltration capacity (mm/h)	4
Manning's N for impervious area	0.1
Manning's N for pervious area	0.02
Depth of depression storage on impervious area (mm)	0.05
Depth of depression storage on pervious area (mm)	0.05
Max infiltration capacity (mm/h)	0.5
Decay constant for Horton infiltration curve (/h)	4

With the above parameters, the model calculated the surface runoff activities and generated the flow rate and infiltration rate of the runoff, which is shown in Fig. 5.6 and Fig. 5.7 respectively for the selected dates.

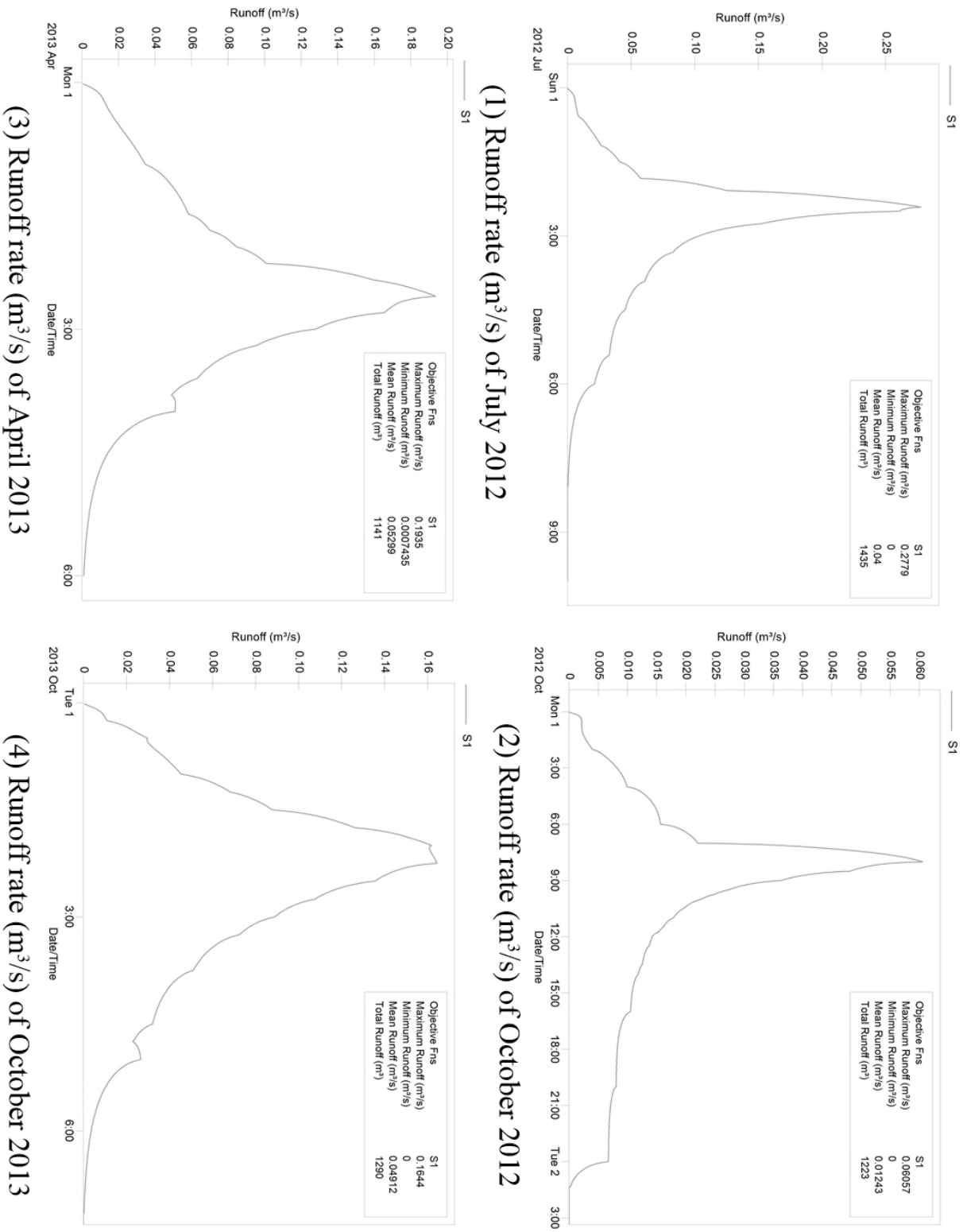

Fig. 5.6 PCSWMM rainfall-runoff results for the study period at the study site

In Fig. 5.6, the flow rate of the rainfall-runoff rose in the first half of rainfall activity

and reached the maximum value at about half of the rainfall activities. In the second half part of the activities, the flow rate began to decrease but remained when the rainfall activities ended. The remaining runoff was transferred into the soil through infiltration. While in Fig. 5.7, the penetration graph of the rainfall-runoff activities were generated. At the beginning of the rainfall, the infiltration intensity was high, but after the soil gets saturated, the infiltration rate decreased to the minimum value according to the soil capability until the end of the runoff activities.

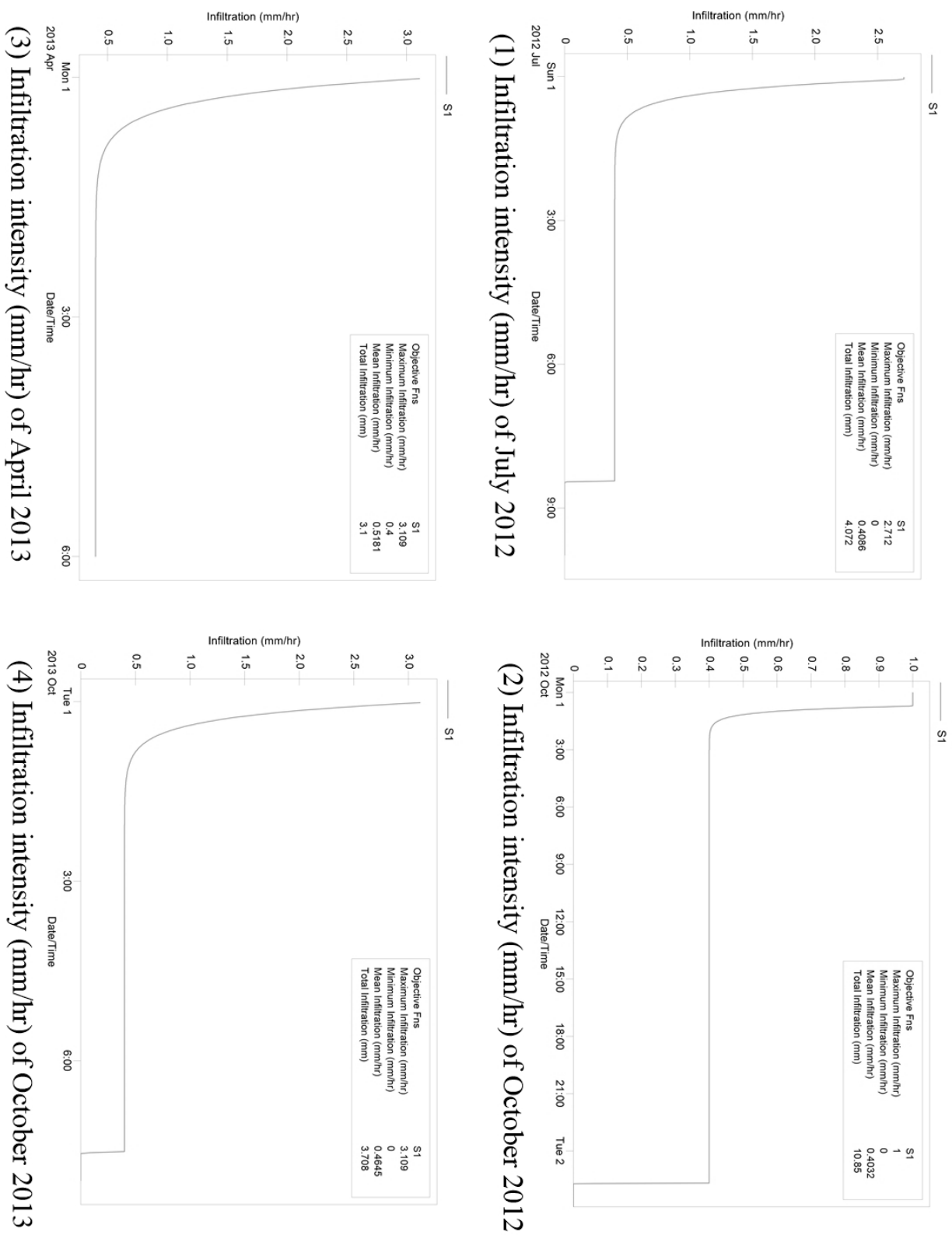

Fig. 5.7 Infiltration intensity of runoff activities for the study period at the study site

The PCSWMM modeling results for the four study dates are concluded in the

following Table 5.5, including the rainfall amount, average runoff depth, rainfall rate, infiltration intensity and rainfall duration.

Table 5.5 PCSWMM model results

Date	July 12	Oct 12	April 13	Oct 13
Rainfall (mm)	110	130.11	80	86
Runoff depth (mm)	45.94	54	36.54	41.29
Rainfall rate (mm/h)	7.354	2.167	9.108	8.18
Infiltration (mm/h)	0.4086	0.4032	0.5181	0.4645
Duration (h)	6	24	4	5

5.3.2 Hairsine-Rose model results

In the Hairsine-Rose model, some parameters applied in this case study were previously published by Gao et al. (2004). All parameters used in the model are listed in Table 5.6.

Table 5.6 Hairsine Rose model parameters

Parameters	Values
Bulk density ρ_b (g/cm^3)	1.56
Soil moisture(porosity) θ	0.4161
Soil erodibility, a (g/cm^3)	0.38
Diffusivity, D_s (cm^2/ s)	1.26×10^{-6}
Exchange-layer depth, de (cm)	0.5

where soil erodibility a [ML^{-3}] is obtained by previous experiments (Gao et al., 2003) and the diffusion constant, Ds [L^2T^{-1}] was based on the published Zn aqueous diffusion coefficient $0.673*10^{-5}$ cm^2/ s (Mills et al., 1985).

The initial concentration for the study point is 16000 mg/kg. Therefore with Eq. (3.28), the concentration of Zn dissolved into runoff can be calculated and concluded in Table 5.7.

Table 5.7 Hairsine Rose model results

Study Period	Zn Concentration (mg/L)
July 2012	11.79
October 2012	19.52
April 2013	8.34
October 2013	10.45

5.3.3 HYDRUS model results

The transport of Zn in soil was simulated by the STANMOD model. The parameters applied are listed as follows, which are obtained based on the soil characteristics and some parameters are assumed based on the experimental value (Kandpal et al., 2005) .

Table 5.8 STANMOD model parameters

Parameters	Values
Velocity (m/d)	3.5
Retardation factor	12.247
μ:first-order rate coefficient for decay	0.005
Dx: dispersion coefficient in the x-direction (cm^2/d)	74.3
Dy: dispersion coefficient in the y-direction (cm^2/d)	28

A soil profile of relative concentration of Zn in the vertical direction can be generated as Fig. 5.8, which displays the concentration transport mainly in the X direction and at 2.5 cm, 7.5 cm, 12.5 cm as well as 17.5 cm the relative concentration

of Zn is 0.5, 0.47, 0.42 and 0.37 respectively.

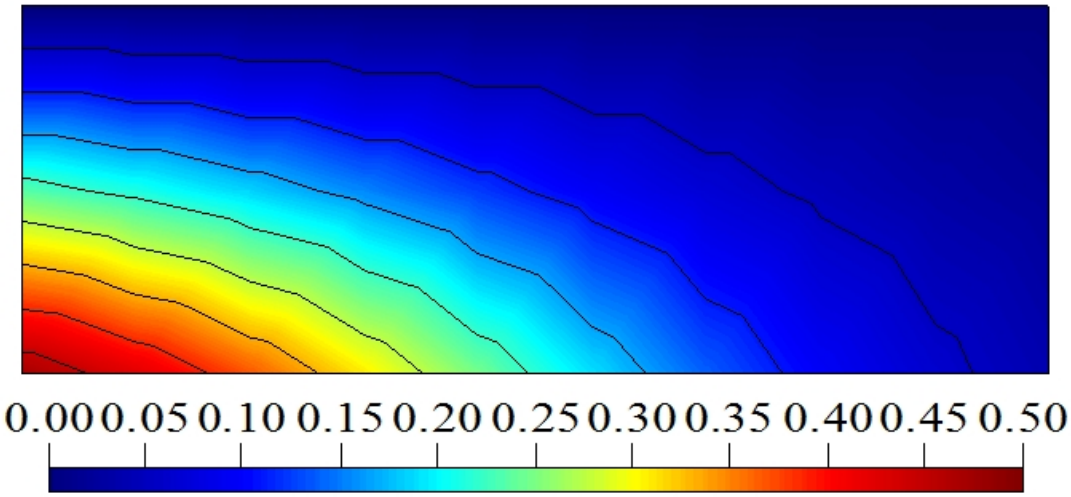

Fig. 5.8 STANMOD model results

Moreover, Eq. (3.18) can also be used to do a simple analytical solution calculated. The results of analytical solution, STANMOD results, as well as the literature data, are compared in Table 5.9. The STANMOD results in Table 5.9 are in the unit mg/kg, which is transformed from the relative concentrations.

Table 5.9 Analytical solution results

Pit Depth (cm)	Literature data (mg/kg)	Analytical solution	STANMOD results	Deviation 1[a] (%)	Deviation 2[b] (%)
2.5	9628	10473.67	8000	16.9%	8.78%
7.5	8585	8755.75	7520	12.5%	2%
12.5	6953	7941.65	6720	3.35%	14.22%
17.5	6965	6221.18	5820	16.44%	10.68%

a. The results present the deviation percentage between STANMOD results and literature data.

b. The results show the deviation between analytical solution results and literature data.

Through the simple calculation of Zn transport in soil, the results of the analytical

solution and modeling results are similar with the literature data, but there is a relative difference between the results of these two methods. Therefore, in order to simulate the solute transport by runoff more accurately, the HYDRUS model was applied. The parameters required in HYDRUS are concluded as follows in Table 5.10:

Table 5.10 HYDRUS model parameters

Parameters	**Values**
D_L (cm)	1
Distribution coefficient K_d (mg/L)	3000
μ:first-order rate coefficient for decay	0.005
D_w (cm^2/d)	1
D_a (cm^2/s)	0.3
Henry constant	0.02

where D_L [L] is longitudinal dispersivity, Dw [L^2T^{-1}] is molecular diffusion coefficient in free water, Da [L^2T^{-1}] represents molecular diffusion coefficient in soil air. And Henry constant is the Equilibrium distribution constant between liquid and gaseous phases, [].

The Zn concentration profile is generated by HYDRUS for the four study dates, which are shown in Fig. 5.9.

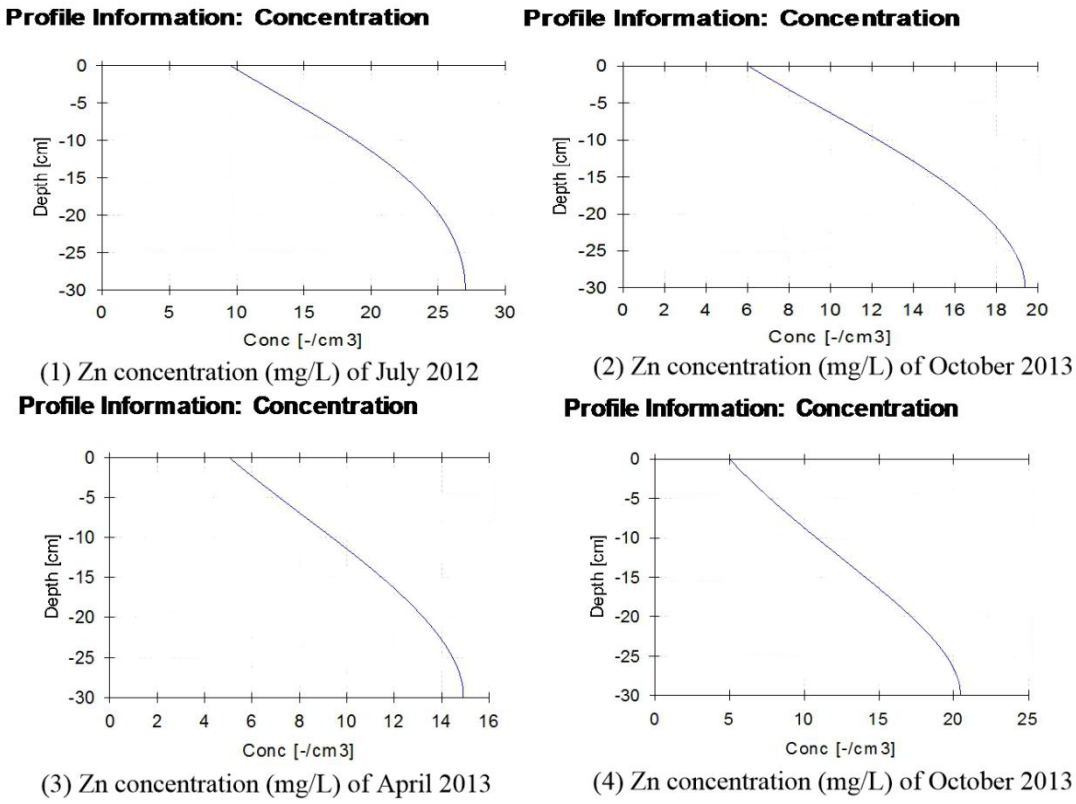

(1) Zn concentration (mg/L) of July 2012

(2) Zn concentration (mg/L) of October 2013

(3) Zn concentration (mg/L) of April 2013

(4) Zn concentration (mg/L) of October 2013

Fig. 5.9 HYDRUS model results

In the transport activities, the concentration of Zn was lowest at the soil surface and increased with higher depths and kept stable after 25 cm. The full value of Zn concentration at different soil depth are listed in Table 5.11 and compared with the literature data.

Table 5.11 HYDRUS model results

JULY 2012			
DEPTH (cm)	Literature data (mg/L)	HYDRUS result	Deviation (%)
0	8	9	12.5%
5	12.1	13.5	11.57%
25	31.7	27	14.83%
30	25.1	27.5	9.56%
OCT 2012			
DEPTH (cm)	Literature data (mg/L)	HYDRUS result	Deviation (%)
0	5.55	6	8.11%
5	7.35	9	22.45%
25	20.75	19	8.43%
30	20.7	19.5	5.8%
APRIL 2013			
DEPTH (cm)	Literature data (mg/L)	HYDRUS result	Deviation (%)
0	5.05	5	1%
5	5.8	7	20.69%
25	14.5	14.5	0%
30	16.2	15	7.41%
OCT 2013			
DEPTH (cm)	Literature data (mg/L)	HYDRUS result	Deviation (%)
0	5.3	5.5	3.77%
5	7	7.5	7.14%
25	17.85	19	6.44%
30	20	21	5%

From the above table, the results present a fine dependency, expected some specific

points, the deviation between modeling and literature data are less than 10%, which could validate the accuracy of the modeling results.

5.4 ARCTRA System Results

5.4.1 Surface runoff results

With Eq. (3.15) and Eq.(3.18), the runoff depth and flow rate due to the rainfall activities can be calculated in the study dates. The results and comparison with modeling results are listed in Table 5.12. Through the comparison, there is some difference between the runoff depth and runoff rate results of modeling and ARCTRA system results. The reason can be concluded as the runoff results of PCSWMM are generated mathematical functions intricately, while in ARCTRA system only runoff duration and amount were considered.

Table 5.12 Runoff results of ARCTRA system

JULY 2012			
Result	PCSWMM result	ARCTRA result	Deviation (%)
Runoff depth (mm)	45.94	47.28	2.92%
Rainfall rate (mm/h)	7.354	8.33	13.27%
Runoff rate (m^3/s)	0.04437	0.05151	16.09%
OCT 2012			
Result	PCSWMM result	ARCTRA solution	Deviation (%)
Runoff depth (mm)	54	56.19	4.05%
Rainfall rate (mm/h)	2.167	2.7083	19.98%
Runoff rate (m^3/s)	0.01737	0.01632	6.04%
APRIL 2013			
Result	PCSWMM result	ARCTRA solution	Deviation (%)
Runoff depth (mm)	36.54	37.93	3.8%
Rainfall rate (mm/h)	9.108	10	9.79%
Runoff rate (m^3/s)	0.053	0.05486	3.51%
OCT 2013			
Result	PCSWMM result	ARCTRA solution	Deviation (%)
Runoff depth (mm)	41.29	42.6775	3.36%
Rainfall rate (mm/h)	8.18	9	10.02%
Runoff rate (m^3/s)	0.04912	0.0463	5.74%

5.4.2 Heavy metal transport with runoff

With Eq. (3.15) the concentration of Zn dissolved from soil to runoff can be calculated.

The parameters required in Eq. (3.15) are listed in Table 5.13.

Table 5.13 Parameters for soil erosion section

Input parameter	Value	Input parameter	Value
Volumetric water content θ	0.4161	Initial soil solution concentration C_0 (mg/kg)	16000
Mass transfer coefficient k (cm/h)	0.083	Pore water velocity v (cm/h)	3.5
Bulk density ρ	1.56	Dispersion coefficient D (cm^2/h)	0.09
Retardation factor R	12.247	Distribution coefficient K_d (mg/L)	3000

With the above parameters, the results calculated in the four study dates are concluded in the following Table 5.14. Through the comparison with modeling results, except the results in July 2012, the results are quite similar and show a goof correlation with the modeling results.

Table 5.14 Soil erosion results of ARCTRA system

Date	July 12	Oct 12	April 13	Oct 13
Analytical solution (mg/L)	9.86	20.4	8.28	11.04
Modeling result (mg/L)	11.79	19.52	8.34	10.45
Deviation (%)	16.37%	4.51%	0.72%	5.65%

5.4.3 Solute transport in soil

With the results obtained in 5.1 and 5.2, the Zn concentration transported in the soil can be calculated by Eq. (3.18). The results of different dates and comparison with modeling results and analytical solution are listed in Table 5.15.

Table 5.15 Results of Zn transport analysis in soil

JULY 2012					
DEPTH (cm)	Literature data (mg/L)	HYDRUS result	ARCTRA result	Deviation 1[a] (%)	Deviation 2[a] (%)
0	8	9	7.483	6.46%	12.5%
5	12.1	13.5	11.013	8.98%	11.57%
25	31.7	27	30.01	5.05%	14.83%
30	25.1	27.5	27.06	7.81%	9.56%
OCT 2012					
DEPTH (cm)	Literature data (mg/L)	HYDRUS result	ARCTRA result	Deviation 1 (%)	Deviation 2 (%)
0	5.55	6	6.07	9.37%	8.11%
5	7.35	9	8.94	21.63%	22.45%
25	20.75	19	24.35	17.35%	8.43%
30	20.7	19.5	21.95	6.04%	5.8%
APRIL 2013					
DEPTH (cm)	Literature data (mg/L)	HYDRUS result	ARCTRA result	Deviation 1 (%)	Deviation 2 (%)
0	5.05	5	5.07	0.4%	1%
5	5.8	7	7.4	21.62%	20.69%
25	14.5	14.5	16.57	14.28%	0%
30	16.2	15	18.18	12.22%	7.41%
OCT 2013					
DEPTH (cm)	Literature data (mg/L)	HYDRUS result	ARCTRA result	Deviation 1 (%)	Deviation 2 (%)
0	5.3	5.5	5.77	8.87%	3.77%
5	7	7.5	8.49	21.28%	7.14%
25	17.85	19	18.21	2.02%	6.44%
30	20	21	20.86	4.3%	5%

a. The results show the deviation percentage between analytical solution results and literature

data.

b. The results show the deviation percentage between HYDURS results and literature data.

In this part, the Zn concentration transported in various soil depth were calculated. And the results are similar with literature data and modeling results, which could prove the accuracy of the analytical results.

As discussed above, the ARCTRA system has been validated. Therefore, it was also applied to other sampling points to simulate the contaminant level of the whole study site. In this study, two soil depth, 7.5 cm and 17.5 cm were analyzed by ARCTRA system, and the results displayed in the contour map as in Fig. 5.10.

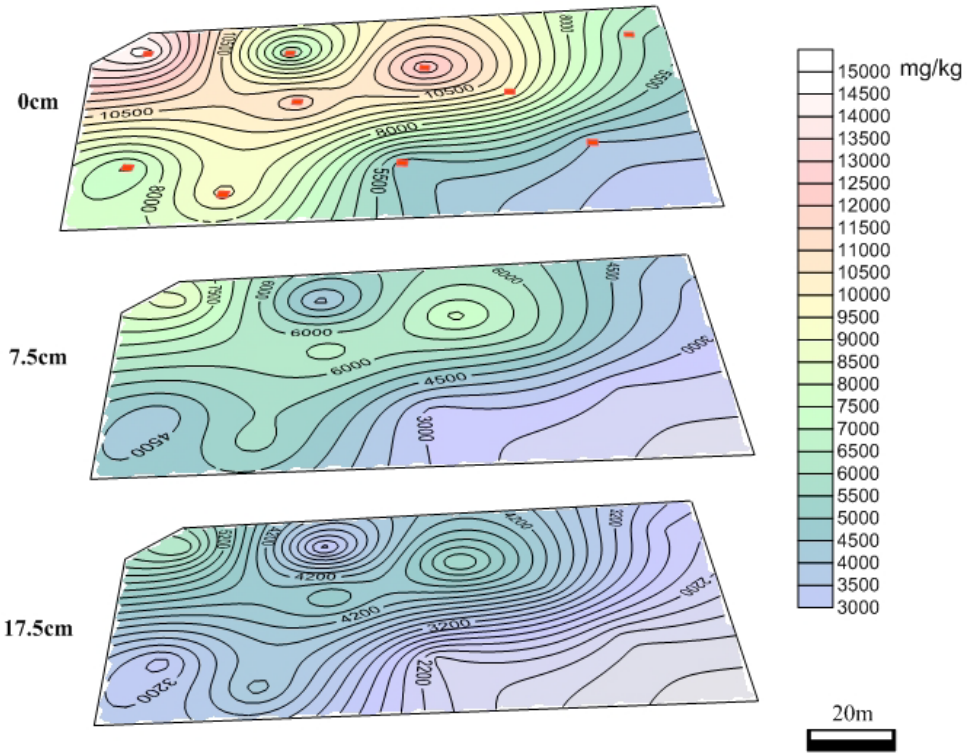

Fig. 5.10 Zn concentration contour map at the study site

Fig.5.10 indicates the concentration of Zn becomes lower in deeper soil. At soil surface, the average Zn concentration is around 9000 mg/kg, while decreases to 3000

mg/kg at 17.5 cm. The change of concentration can be contributed to the advection and diffusion in the transport process.

5.4.4 Application of designed system interface

As explained in Chapter 3, a user-friendly interface has been developed for the calculation system. Therefore, when users input the values of the parameters in each process, the relative results can be obtained. An example of the 'Soil Erosion' has been presented in Fig. 5.11.

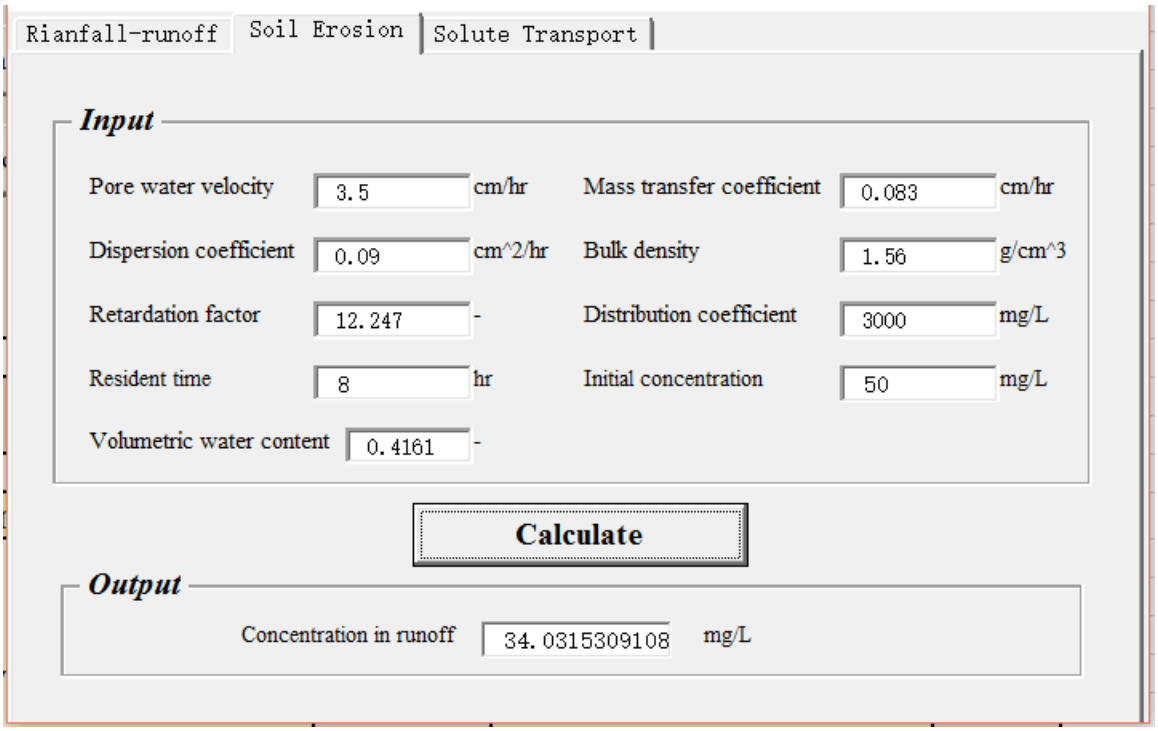

Fig.5.11 ARCTRA system interface with data for soil erosion analysis

5.5 Result Comparison and Discussion

5.5.1 Result comparison

The modeling and analytical solution results of each process are compared in the

following Table 5.16, where in the solute transport process, results at depth 0 cm are selected. In Table 5.16, the result of simulation and analytical solutions are quite similar, where most the deviations are lower than 10%.

Table 5.16 Comparison analysis for ARCTRA system and existing models

JULY 2012			
Result	Modeling result	ARCTRA result	Deviation (%)
Runoff rate (m^3/s)	0.04437	0.05151	16.09%
Concentration in runoff (mg/L)	11.79	9.86	-16.37%
Concentration at 0 cm (mg/L)	9	7.483	-16.09%
OCT 2012			
Result	Modeling result	ARCTRA result	Deviation (%)
Runoff rate (m^3/s)	0.01737	0.01632	-6.04%
Concentration in runoff (mg/L)	19.52	20.4	4.51%
Concentration at 0 cm (mg/L)	6	6.07	1.17%
APRIL 2013			
Result	Modeling result	ARCTRA result	Deviation (%)
Runoff rate (m^3/s)	0.053	0.05486	3.51%
Concentration in runoff (mg/L)	8.34	8.28	0.72%
Concentration at 0 cm (mg/L)	5	5.07	1.4%
OCT 2013			
Result	Modeling result	ARCTRA result	Deviation (%)
Runoff rate (m^3/s)	0.04912	0.0463	5.74%
Concentration in runoff (mg/L)	10.45	11.04	5.65%
Concentration at 0 cm (mg/L)	5.5	5.77	4.91%

5.5.2 Propagate deviation analysis and discussion

In order to analyze the detailed reasons that cause the deviation in the whole calculation process, the propagation of the difference was analyzed. In the analysis, the value of runoff rate was assumed to be same as the value used in the existing models and the results of Zn concentration in runoff and soil were calculated based on this value, so that the deviation percentage can be obtained between the new results and the original results, which is considered as the propagate deviation by the different value of runoff rate in the first process. The original difference and the propagated deviation are listed in Table 5.17. Through Table 5.17, it can indicate that the most deviation in the calculation process is due to the runoff flow rate difference. For example, in the results of July 2012, the deviation caused by the difference of runoff rate is 13.86%, while after removing the propagate deviation, the difference between the concentration results by two methods is only at about 2%. As mentioned before, the rainfall and runoff activities are simulated numerically and dynamically according to the typical situation of the study area in PCSWMM model. While for the analytical solution, the rainfall is set as a constant and the equation is solved simply, which makes the difference between the modeling and analytical solutions.

Table 5.17 Propagate deviation analysis for ARCTRA results

JULY 2012			
Result	Actual deviation (%)	Propagate deviation (%)	Difference (%)
Runoff rate (m^3/s)	16.09%	-	-
Concentration in runoff (mg/L)	-16.37%	-13.86%	2.51%
Concentration at 0 cm (mg/L)	-16.09%	-13.86%	2.23%
OCT 2012			
Result	Actual deviation (%)	Propagate deviation (%)	Difference (%)
Runoff rate (m^3/s)	-6.04%	-	-
Concentration in runoff(mg/L)	4.51%	6.43%	1.92%
Concentration at 0 cm(mg/L)	1.17%	6.43%	5.26%
APRIL 2013			
Result	Actual deviation (%)	Propagate deviation (%)	Difference (%)
Runoff rate (m^3/s)	3.51%	-	-
Concentration in runoff(mg/L)	-0.72%	-3.34%	2.62%
Concentration at 0 cm(mg/L)	-1.4%	-3.34%	1.94%
OCT 2013			
Result	Actual deviation (%)	Propagate deviation (%)	Difference (%)
Runoff rate (m^3/s)	5.74%	-	-
Concentration in runoff (mg/L)	-5.65%	-5.43%	0.22%
Concentration at 0 cm (mg/L)	-4.91%	-5.43%	0.52%

Subsequently, through comparing the governing equations of the existing models

and analytical solutions, the reason for remaining deviations can be estimated. In the HYDRUS model (Šimůnek et al., 2013), molecular diffusion, adsorption, dispersion and first-order decay are considered. As a result, parameters such as longitudinal dispersivity, adsorption isotherm coefficient, diffusion coefficient and first order coefficient for decay are applied in the governing equations. On the other hand, the analytical solution, i.e., Eq. (3.15) and (3.18) in this research, only considered dispersion and first-order decay. Absolutely, there are also allowable deviations between the analytical solution calculation and modeling results, which occupy a small proportion of the total deviation.

From the propagate analysis (Table 5.17), the deviation between ARCTRA system and existing models are due to the deviation in rainfall-runoff flow rate primarily. Furthermore, in Table 5.13, the deviation percentage of rainfall intensity is over 10%, which is the main factor affecting the calculation results of rainfall runoff flow rate. Therefore, the value of rainfall intensity applied in ARCTRA is speculated as the main reason for the result difference. In order to optimize the results, a new method to calculate the rainfall intensity was applied.

According to ARR 2016, an Intensity-Frequency-Duration (IFD) was designed to calculate the rainfall intensity in designed rainfall activity. In this method, time of concentration, return period, and an IDF relationship is used to calculate design rainfall intensity. The designed rainfall intensity is the intensity of a constant intensity design storm with a specified design return duration equivalent to the time of concentration for the drainage area. Once results for the design return period are available, the design

rainfall intensity can be determined from an appropriate intensity-duration-frequency curve or equation for the drainage area location, which is applied in this case study. Therefore, in this case study, the rainfall activity in June 2012 was selected for improvement. The rainfall duration is 6 h, and rainfall amount is 50 mm, so according to the IFD graph, the rainfall intensity can be estimated as 7.54 mm/hr, which is quite close to the modeling results 7.33 mm/hr. Moreover, the results for other processes based on this rainfall intensity values were calculated and concluded in the following Table 5.18.

Table 5.18 Improved results for ARCTRA system

Result	Improved result	Modeling result	Deviation (%)	Original deviation (%)
Rainfall intensity (mm/hr)	7.54	7.354	2.53%	13.27%
Runoff depth (mm)	42.79	45.94	6.86%	2.92%
Runoff flow rate (m^3/s)	0.04649	0.04437	4.78%	16.09%
Concentration in runoff (mg/L)	11.272	11.79	4.39%	16.37%
Concentration at 0 cm (mg/L)	8.35	9	7.22%	16.09%

From the above table, we can indicate the deviation of improved results and modeling results are much better than that of original analytical results. The deviation percentage of each process is at only about 5%, which can be accepted in deviation range. Therefore, the value of rainfall intensity could be proved as one factor which influences the ARCTRA system. An improved analytical solution for calculation of rainfall intensity should be developed for the ARCTRA system in the further study.

5.6 Monte Carlo Simulation Analysis and Fuzzy set Risk assessment

5.6.1 Sensitivity analysis

In the current analysis, the unsaturated zone model evaluation for the transport and fate of heavy metal by runoff , the model input parameters include the mass transfer coefficient k, the pore water velocity v, the dispersion coefficient, D and retardation factor R. The model output of interest is chosen as the concentration in the soil at depth 0 cm.

Table 5.19 Sensitivity analysis for key model parameters

Parameters	-10% Initial value +10%	Concentration results at 0 cm
k	0.0747	7.492
	0.083	7.483
	0.0913	5.413
v	3.15	6.942
	3.5	7.483
	3.85	7.974
D	0.081	6.301
	0.09	7.483
	0.099	8.566
R	11.022	**6.0565**
	12.247	**7.483**
	13.472	**8.861**

5.6.2 Monte Carlo simulation

After the sensitivity analysis of the above parameters, the retardation factor R presents the highest sensitivity to the Zn concentration results. As a result the retardation factor R is used as the uncertainty parameter for the Monte Carlo Simulation. The mean value is 12.247, which is the R value applied in this case study as above. And the range of R is set as 10 to 15, which is about ± 20% fluctuate of the mean value. As a result, a PDF is generated by EXCEL as shown in Fig. 5.12.

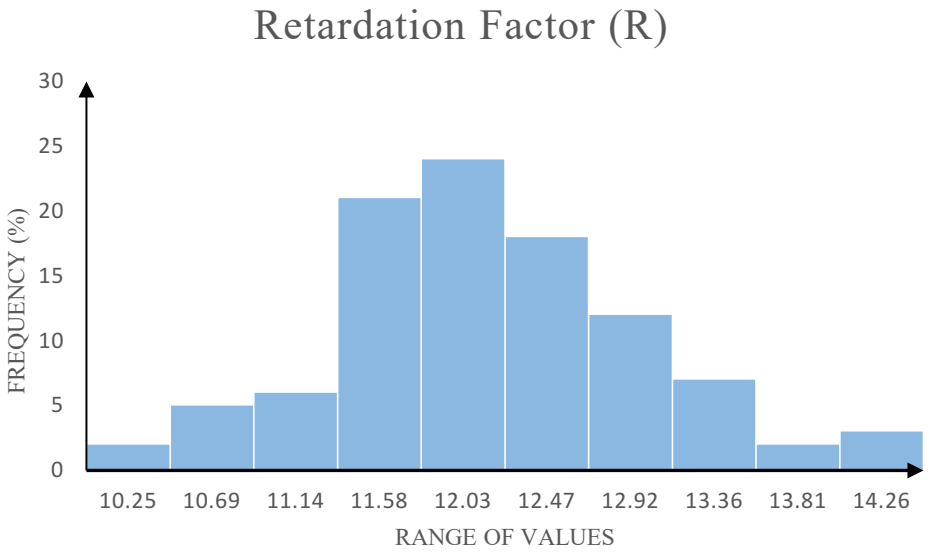

Fig.5.12 Probability density function of retardation factor

The result of Zn concentration at 0 cm for June 2012 is used for Monte Carlo Simulation. The probability distribution and normal distribution graph are shown as following in Fig. 5.13. Fig. 5.13 offers the calibrated concentration as 7.483 mg/L; the mean concentration is 7.4615 mg/L and the standard deviation is 1.5414 mg/L. Moreover, through the normal distribution analysis to the probability function graph, P_{10}=5.4 mg/L; P_{50}=6.454 mg/L and P_{90}=9.474 mg/L, which means the probability of

the concentration less than 5.4 mg/L is 10%, for example.

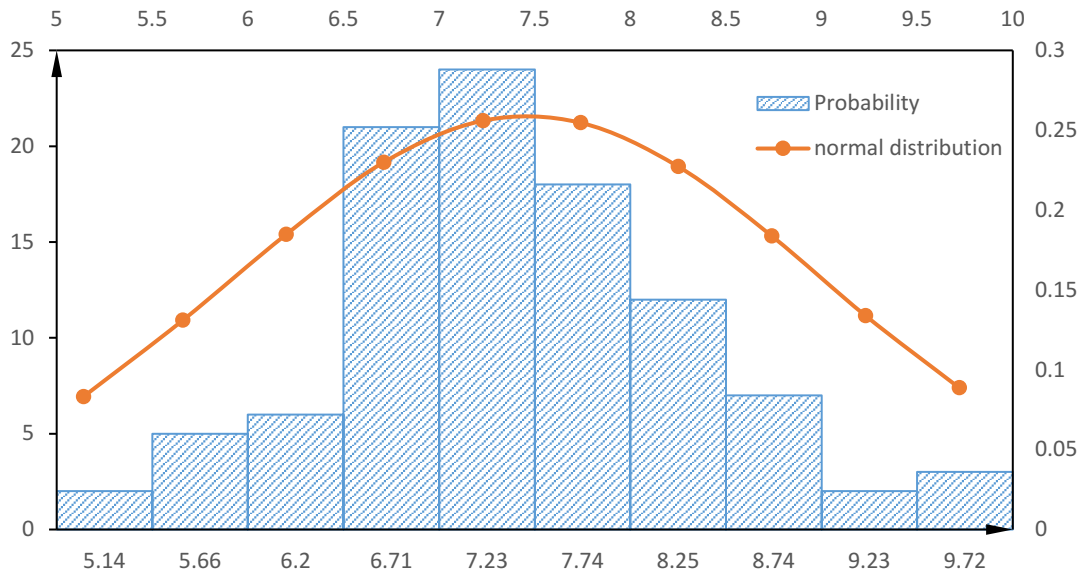

Fig. 5.13 Probability distribution and normal distribution for Zn concentration

Afterwards, the concentration results are transformed to unit mg/kg, and a Cumulative Probability Function of Zn Concentration is generated as following, which is applied to the fuzzy set risk assessment.

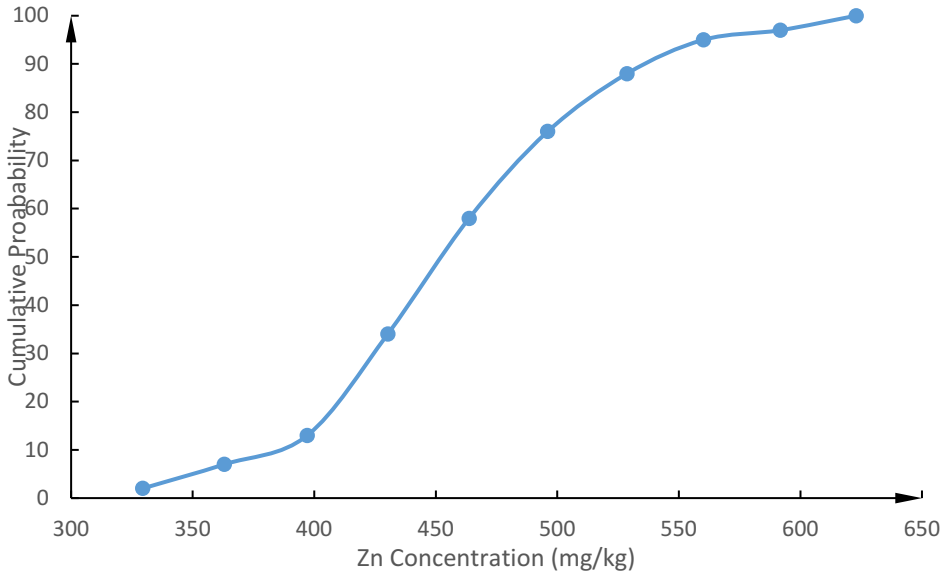

Fig. 5.14 Cumulative probability function for Zn concentration

5.6.3 Fuzzy Set risk assessment

In this study, zinc was selected as the contaminant of interest. To facilitate a guideline-based environmental risk analysis, the guidelines were categorized into three fuzzy sets in this study, namely “strict”, “medium” and “loose”. The membership function set is designed according to the standard in Canada, EU, and China as in Fig. 5.15 and the detailed explanation is as following:

Table 5.20 Zn standard for soil in Canada, EU and China

Canada (CCME, 1999)	Agricultural 200	Parkland 200	Commercial/Industrial 360
EU (MEF, 2007)	Threshold 200	Lower guideline 250	Higher guideline 400
China (GB-15618, 1995)	1st level 100	2nd level 250	3rd level 500

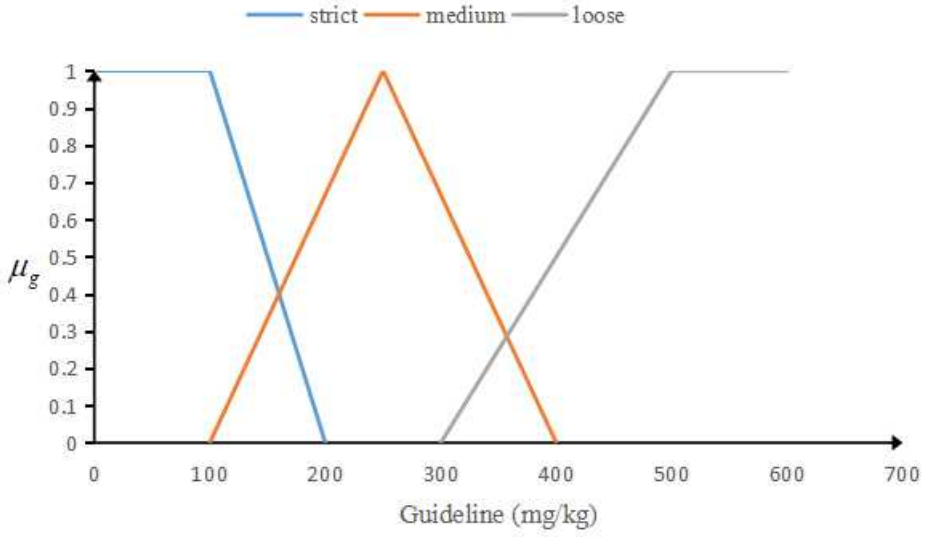

Fig. 5.15 Fuzzy membership functions of soil quality guidelines

The membership function for Fig. 5.15 are listed as follows.

(1)
$$\begin{aligned} &when\ 0 \le c \le 100,\ \mu_g = 1; \\ &when\ 100 \le c \le 200,\ \mu_g = -0.01c + 2; \end{aligned} \qquad \text{Eq. (5.1)}$$

(2)
$$\begin{aligned} &when\ 100 \le c \le 250,\ \mu_g = 0.0067c - 0.67; \\ &when\ 250 \le c \le 400,\ \mu_g = -0.0067c + 2.67; \end{aligned} \qquad \text{Eq. (5.2)}$$

(3)
$$\begin{aligned} &when\ 300 \le c \le 500,\ \mu_g = 0.01c - 4; \\ &when\ \mathrm{c} \ge 500,\ \mu_g = 1. \end{aligned} \qquad \text{Eq. (5.3)}$$

Similarly, according to the methodology in Chapter 3, the membership functions of fuzzy environmental-guideline-based risks under the strict, medium and loose guidelines can be established according to the questionnaire survey results as shown in Figs. 5.16 (a), (b) and (c), respectively.

(a)Strict

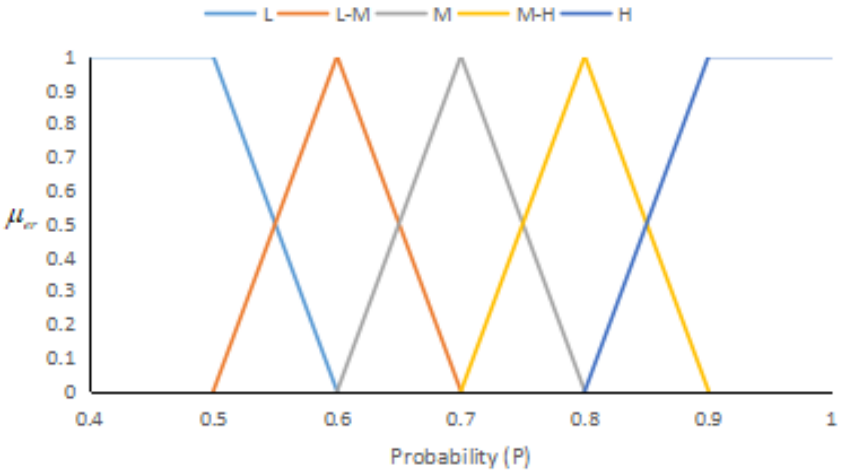

(b)Medium

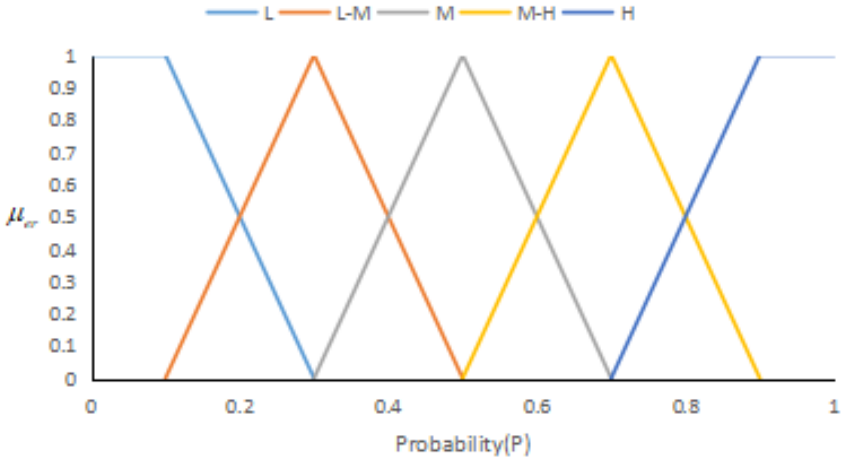

(c)Loose

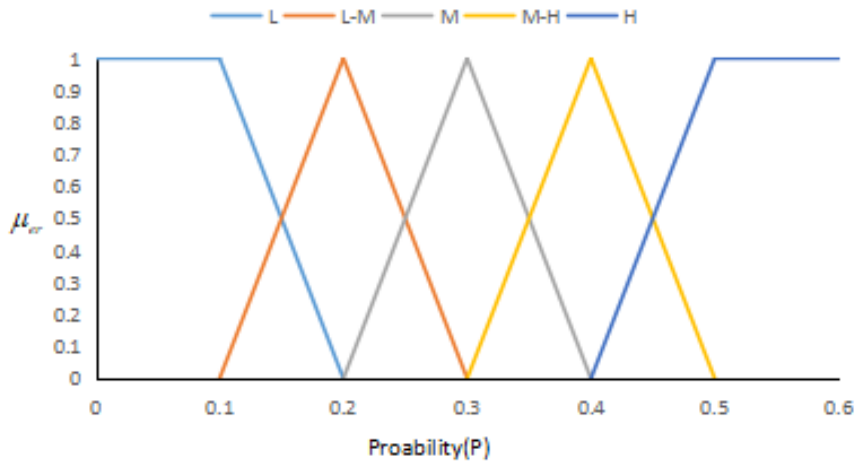

Fig. 5.16 Fuzzy membership functions of different levels of fuzzy set

From USEPA (1998), the RfD value for Zn is 0.3 mg/kg day. According to (Javed and Usmani, 2016), the estimated IR of Zinc for male and female is 6.37×10^{-2} and 7.26×10^{-2} mg/kg body-weight/day, respectively. Therefore, the average CDI is 6.82×10^{-2} mg/kg body-weight/day. Therefore, according to the different standard values applied in Eq. (3.35), some possible HI results are listed in Table 5.21.

Table 5.21 Heath Index (HI) analysis result of Zn standard

Standard value (mg/kg)	**HI result**	**Log10(HI)**
100	22.73	1.357
200	45.47	1.658
250	56.83	1.746
350	79.56	1.9
400	90.93	1.959
500	113.67	2.056

Moreover, the membership function is generated according to the range of Log10 (HI) value. In this study, the range of Log10 (HI) is selected as 1 to 2.2, and the levels are divided into “low” “low to medium”, “medium”, “medium to high”, “high”, which is shown in Fig. 5.17.

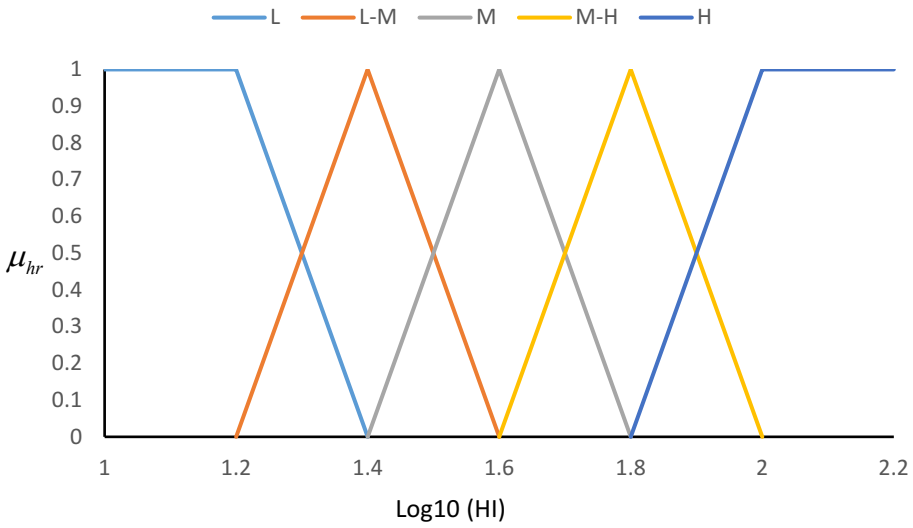

Fig. 5.17 Fuzzy membership function of health risks associated with hazard index

Finally, the membership function of fuzzy generalized risk level are generated according to the fuzzy rules in Chapter 3 as in Fig. 5.18, which is used to quantify the risk of contaminated site.

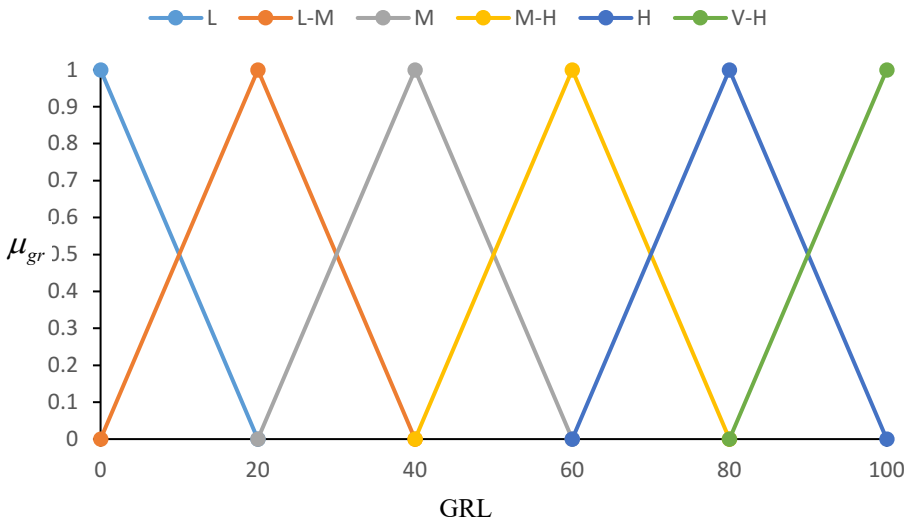

Fig. 5.18 Membership functions of generalized fuzzy risk levels

In this case study, 200 mg/kg for the parkland (CCME, 1999) is selected as the assessment standard. The guideline is at the “Medium” category with a membership

grade μ_g 0.67. When 200 mg/kg is applied, P_F (200) = 1 - F (200) = 1. As a result, the environmental-guideline-based risk (ER) would be ‘‘H’’ with a membership grade μ_{er} 0.67 according to Fig. 5.15 (b) when the probability was 1.0, and the generated graph is illustrated in Figs.5.19 (1) and (4). The associated HI can be calculated as 1.658. It could then be found from Fig. 5.18 that the corresponding health risk (HR) would be partly “M-H” (with a membership grade of 0.29) and partly “M” (with a membership grade of 0.71), as shown in Figs. 5.19 (2) and (5), respectively. Therefore, two combinations of antecedents exist (i.e., two rules have to be analyzed) including: (a) if ER is “H” and HR is “M-H”, and (b) if ER is “H” and HR is “M”.

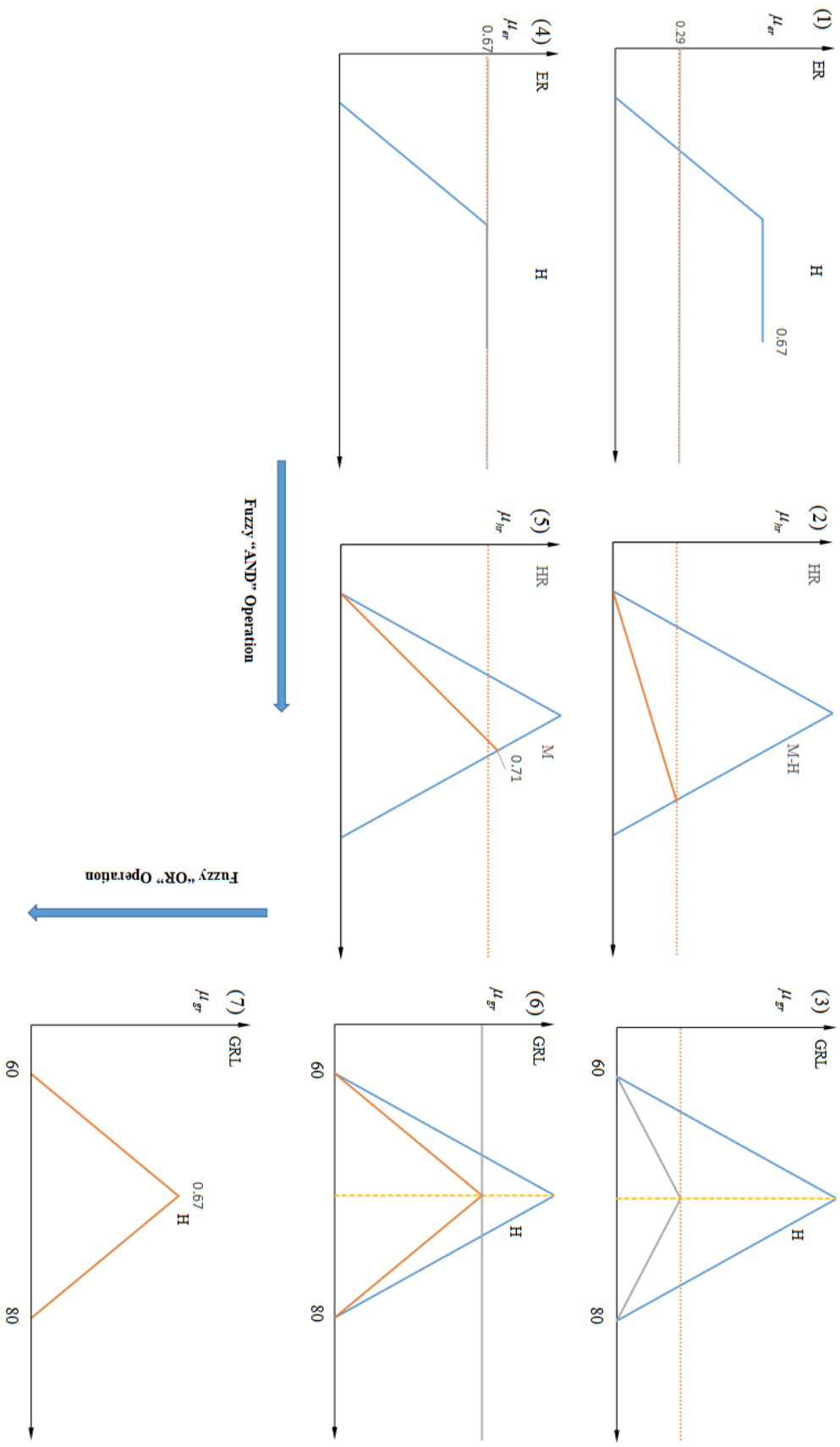

Fig. 5.19 Integrated fuzzy risk assessment of study site

With the Fuzzy set rue “OR”, the final graph of GRL is shown in Figs. 5.19 (7) combing Figs. 5.19 (3) with a membership grade μ_{gr} =0.29 and (6) with a membership grade μ_{gr} =0.67. The final graph of GRL is shown in Figs. 5.19 (7).The crisp final GRL value was then obtained by calculating the centroid of the fuzzy GRL value as 70. The site management decisions can then be made based on the calculated site scores that describe the generalized risk level. Table 5.22 lists the relationship between site scores and suggested management actions.

Table 5.22 Recommendation action for contaminated sites (Mohamed and Cote, 1999)

Site score by risk assessment	**Risk management action**
90-100	The site should be immediately cleaned up
70-90	Take full action to treat the site
50-70	Contain the site and restrict groundwater use
30-50	Take interim control measures and limit access to the site
10-30	The site should be monitored
0-10	No actions are required

As a result, according to Table 5.22, the site is regarded as heavily contaminated, and the suggested risk management action should be “take full actions to treat the site”.

5.7 Summary

According to Fig. 5.23, a score of the contaminated site can be obtained as the final result for the ARCTRA system in this case study.

This section is summarized as follows:

By applying the whole ARCTRA system to this case study, the precise operation

and all the functions in the system are illustrated and tested.

By examining the modeling results, the processes of fate and transport of heavy metal in porous media by runoff are studied, such as advection and diffusion.

Through the comparison of results by ARCTRA system, existing models, and literature data, the ARCTRA system was validated. Moreover, the deviation of results of each process in existing models and ARCTRA system are discussed in this chapter, and some reason and deficiency have been concluded according to the analysis.

In addition to the calculation result of analytical solution, the risk assessment method based on the fuzzy set theory is applied in this section. In this case study, the operation of Monte Carlo Simulation, and quantify of site risk score based on fuzzy rules are also illustrated in detail.

Moreover, through applying the analytical solution in ARCTRA system, the parameters which affect heavy metal transport in soil can be analyzed. For example the mass transfer coefficient k, the dispersion coefficient, D and retardation factor R have a great impact on the results of heavy metal transport in runoff and runoff.

6. CONCLUSION AND FURTURE STUDY

6.1 Conclusion

In the present thesis study, the mechanisms of heavy metal transport by runoff in porous media were formulated. Depending on the process theory, an ARCTRA system was developed to simulate the main operations in this contaminant transport activity. Moreover, several existing models were applied in order to simulate the corresponding processes of environmental contaminant transport. For example, the formation of rainfall-runoff was simulated using the PCSWMM model, which calculated the depth, flux rate and infiltration rate of the runoff due to precipitation. The amount of heavy metal dissolved into the runoff from the soil surface was calculated using the Hairsine-Rose model based on the simulation results from the PCSWMM model. Afterwards, the HYDRUS model based on the Richard equation was used to simulate the transport of heavy metal solute in porous media. The integrated ARCTRA system was developed in this thesis study for the processes of contaminant transport activity, rainfall-runoff formation, soil erosion and contaminant transport in soil. In each process, a governing equation was applied to calculate the runoff depth and the contaminant concentration in the runoff and the soil.

In order to consider the uncertainty in the natural process, the Monte Carlo Simulation was also applied in this thesis study. The retardation factor, which was chosen by a sensitive test, was selected as the variant parameter and the change of the corresponding concentration results was then analyzed. Finally, a risk assessment

method based on fuzzy set theory was employed to quantify the environmental risk of the contaminated site. This method took into consideration both the general environmental risks and the health hazards. Thus, an integrated risk value can be obtained to evaluate and rank the risk level of a contaminated site and relative management actions were recommended according to the different scores.

In order to validate both the modeling and analytical solutions, two real cases were studied in this thesis. Pb and Zn were studied in the case studies. The results of the ARCTRA and other existing models were obtained based on the real case data and compared with monitoring data. The model verification and validation indicate the developed ARCTRA system is useful in assessing the risks of heavy metals in the soil caused by the rainfall-runoff process.

Finally, a user interface was developed for the analytical solution system based on the VB program code in Excel in order to facilitate technology transfer and provide a user-friendly system to help the processing of input and calculation of results.

6.2 Research Contribution

In addition to the conclusion in section 6.1, the research contributions for the present thesis study are summarized below:

1. An integrated ARCTRA system was developed as a package to calculate the determination of rainfall runoff, soil contamination erosion in to runoff and relative pollutant transport in soil. The ARCTRA system can be used to systematically assess the heavy metal in the unsaturated zone caused by rainfall-runoff process.

2. A comparison modeling framework including existing models was constructed to systematically support and verify the development of ARCTRA system, for simulating the rainfall-runoff formation, soil erosion and contaminant transport in soil.

3. Two real case studies were conducted in this thesis study. Through comparison of the results of both theARCTRA system and the existing models together with the literature data, the developed systems were systematically tested and validated.

4. A non-classical risk assessment method including Monte Carlo Simulation and fuzzy set theory was incorporated to quantify both random and incomplete-type uncertainties associated with the site conditions, environmental quality guidelines and health impact criteria, to support effective management of the contaminated site.

6.3 Future Studies

The following future studies are recommended:

1. Contaminant transport in porous media like unsaturated zones is quite a complicated process, including dissolution, advection, diffusion, etc. Only a limited set of factors was considered in this thesis study, with some processes being selectively ignored. Future studies can try to integrate all possible factors, such as decay and chemical reaction.

2. Some parameters, like the diffusion and mass transfer coefficients in the soil, were estimated using empirical or relative references. These estimates may thus

contribute to a degree of imprecision, and more examination methods are thus recommended.

3. A simple system user interface was developed in this study. In future studies, the interface and the function of the system could be improved. For example, an independent system could be programmed using relative software such as MATLAB.

4. In the present uncertainty analysis, only one parameter was considered in the Monte Carlo Simulation. In nature, the majority of the parameters are uncertain. Therefore, several parameters should be considered simultaneously for uncertainty analysis and risk assessment.

References

Aral M.M., and Maslia M.L., 2003. A*pplication of Monte Carlo simulation to analytical contaminant transport modeling probabilistic approaches to groundwater modeling*. Symposium at World Environmental and Water Resources Congress, Philadelphia, Pennsylvania.

ARR, (Australian Rainfall and Runoff), 2016. *Intensity–Frequency–Duration*. Retrieved 21 August, 2017 from http://www.bom.gov.au/water/designRainfalls/ifd/.

Aven T., 2016. Risk assessment and risk management: Review of recent advances on their foundation. *European Journal of Operational Research,*253 (1): 1-13.

Balkhair K.S., and Muhammad A.A., 2016. Field accumulation risks of heavy metals in soil and vegetable crop irrigated with sewage water in western region of Saudi Arabia Saudi. *Journal of Biological Sciences,* 23 (1): 32-44.

Batchelor B., Valdés J., and Araganth V., 1998. Stochastic risk assessment of sites contaminated by hazardous wastes. *Journal of Environmental Engineering,* 124: 380–388.

Bear J., and Bachmat Y., 1990. *Introduction to Modeling of Transport Phenomena in Porous Media*. Springer Netherlands, Kluwer Academic Publishers, Series 4.

Burton G.A., and Pitt Jr. R., 2001. *Stormwater effects handbook: A toolbox for watershed managers, scientists, and engineers.* CRC/Lewis Publishers, New York. ISBN 087371924-7. Chapter 2.

Carlier E., El K.J., and Potdevin J.L., 2006. Solute transport in sand and chalk: A probabilistic approach. *Hydrological Processes,* 20 (5): 1047-1055.

CCME (Canadian Council of Ministers of the Environment), 1999. *Interim Canadian environmental quality criteria for contaminated sites*. The National Contaminated Sites Remediation Program, Report No. CCME EPC-CS34. Winnipeg.

Chacko B.K., Zhi D.G., Darley-Usmar V. M., and Mitchell T., 2016. The bioenergetic health index is a sensitive measure of oxidative stress in human monocytes. *Redox Biology,* 8:

43–50.

Chen S.J., Hwang C.L., Beckmann M.J., and Krelle W., 1992. *Fuzzy multiple attribute decision making: Methods and applications*. Springer, New York.

Chen Z., Huang G.H., and Chakma A., 2003. Hybrid fuzzy-stochastic modeling approach for assessing environmental risks at contaminated groundwater systems. *Journal of Environmental Engineering*, 129: 79–88.

Cheng S., 2000. *Development of a fuzzy multi-criteria decision support system for municipal solid waste management*. M.Sc. thesis, University of Regina, Regina, Canada.

Chung E.T., Fendiev A.E., Leung W.T., and Ren J., 2015. Multiscale Simulations for coupled flow and transport using the general multiscale finite element method. *Computation,* 3: 670-686.

Cullen A.C., and Frey H.C., 1999. *Probabilistic techniques in exposure assessment.* Plenum Press, New York.

Darbra R.M., Eljarrat E., and Barcelo D., 2008. How to measure uncertainties in environmental risk assessment. *Trends in analytical Chemistry*, 27 (4): 377-385.

Dumoulin D., Billon G., Proix N., Frérot H., Pauwels M., and Saumitou-Laprade P., 2017. Impact of a zinc processing factory on surrounding surficial soil contamination. *Journal of Geochemical Exploration,* 172: 142 –150.

D&G Enviro-Group Inc., 2005. *Evaluation Environmentale de Site Phase II Demantelement d'un Deservoir Restauration de Sols.* Technical Report, Montreal, Quebec.

Essaid H.I., Barbara A.B., and Isabelle M.C., 2015. Organic contaminant transport and fate in the subsurface: Evolution of knowledge and understanding. *Water Resources Research,* 51 (7): 4861–4902.

Farrance I., and Robert F., 2014. Uncertainty in Measurement: A review of Monte Carlo simulation using Microsoft Excel for the calculation of uncertainties through functional relationships, including uncertainties in empirically derived vonstants.

The Clinical Biochemist Reviews, 35 (1): 37–61.

Frazer L., and Paving P., 2005. The peril of impervious surfaces. *Environmental Health Perspectives*, 113 (7): 456–462.

Gao B., Walter M.T., Steenhui T.S., Parlange J.Y., Nakano K., Hogarth W. L., and Rose C.W., 2003. Investigating ponding depthand soil detachability for a mechanistic erosion model using a simple experiment. *Journal of Hydrology,* 277 (1–2): 116–124.

Gao B., Walter M.T., Steenhuis T.S., Hogarth W.L., and Parlange, J.Y., 2004. Rainfall induced chemical transport from soil to runoff: theory and experiments. *Journal of Hydrology,* 295 (1-4): 291–304.

GB-15618, 1995. *Environmental quality standard for soils.* Ministry of Environmental Protection, China.

GIN (Groundwater Information Network), 2013. Retrieved 21 August, 2017, from http://gin.gw-info.net/service/api_ngwds:gin2/en/gin.html.

Godongwana B., Solomons D., and Sheldon M.S., 2015. A Finite-Difference Solution of Solute Transport through a Membrane Bioreactor. *Mathematical Problems in Engineering,* 2015.

Goodrich M.T., and McCord J.T., 1995. Quantification of uncertainty in exposure assessments at hazardous waste sites. *National Ground Water Association (NGWA),* 33 (5): 27-732.

Govindaraju R.S., Morbidelli R., and Corradini C., 2001. Areal infiltration modeling over soil with spatially-correlated hydraulic conductivities. *Journal of Hydrological Engineering,* 6: 150– 158.

Guerrero J.S.P., Pontedeiro E.M., M.Th.van Genuchten, and Skaggs T. H., 2013. Analytical solutions of the one-dimensional advection–dispersion solute transport equation subject to time-dependent boundary conditions. *Chemical Engineering Journal,* 221 (1): 487-491.

Guyonnet D., Bourgine B., Dubois D., Fargier H., Côme B., and Chilès J.P., 2003. Hybrid approach for addressing uncertainty in risk assessments. *Journal of Environmental*

Engineering, 129: 68-78.

Haileslassie T., and Gebremedhin K., 2015. Hazards of heavy metal contamination in groundwater. *Intentional Journal of Technology Enhancements and Emerging Engineering Research*, 3 (2) ISSN 2347-4289.

Hairsine P.B., and Rose C.W., 1991. Rainfall detachment and deposition: sediment transport in the absence of flow-driven processes. *Soil Science Society of America Journal,* 55 (2): 320–324.

Hjelmfelt A.T., 1981. Overland flow from time-distributed rainfall. *Journal of the Hydraulics Division*, 107 (2): 27–238.

Hu B.X., and Huang H., 2002. Stochastic analysis of reactive solute transport in heterogeneous, fractured porous media: a dual-permeability approach. *Transport in Porous Media,* 48 (1): 1–39.

Hunt B.W., 1978. Dispersion sources in uniform groundwater flow. *Journal of Hydraulics Division*, 104 (1): 75-85.

Jayawardena A.W., and Bhuiyan R.R., 1999. Evaluation of an interrill soil erosion model using laboratory catchment data. *Hydrological Processes,* 13(1): 89–100.

Javed M., and Usmani N. 2016. *Accumulation of heavy metals and human health risk assessment via the consumption of freshwater fish Mastacembelus armatus inhabiting, thermal power plant effluent loaded canal.* Springer Plus, 5:776.

Kabata-Pendias, and Adriano D.C., 1995. Trace meals. In: Rechcigl. J.E. Ed. Soil Amendments and Environmental Quality. *Lewis Publishers,* 139-167.

Kandpal G., Srivastava P.C., and Bali Ram, 2005. Kinetics of desorption of heavy metals from polluted soils: Influence of soil type and metal source. *Water, Air, and Soil Pollution,* 161 (1-4): 353–363.

Karaca A., Sema C.C., Oguz C.T., and Ridvan K., 2010. Effects of heavy metals on soil enzyme activities. *Soil Biology,* 19: 237-262.

Kentel E., and Aral M.M., 2005. 2D Monte Carlo versus 2D fuzzy Monte Carlo health risk

assessment. *Stochastic Environmental Research and Risk Assessment,* 19: 86–96.

Khan S., Cao Q., Hesham A.E., Xia Y., and He J.H., 2007. Soil enzymatic activities and microbial community structure with different application rates of Cd and Pb. *Journal of Environmental Sciences,* 19: 834–840.

Khan S., Cao Q., Zheng Y.M., Huang Y.Z., and Zhu Y.G., 2008. Health risks of heavy metals in contaminated soils and food crops irrigated with wastewater in Beijing. *China Environmental Pollution,* 152 (3): 686–692.

Lee Y.W., Dahab M.F., and Borgardi I., 1994. Fuzzy decision making in ground water nitrate risk management. *Water Resources Research,* 30 (1): 135-148.

Leeds R., Brown L.C., and Watermeier N.L., 2008. *Food, agricultural and biological engineering*. Ohio State University Extension Fact Sheet.

Leij F.J., and Bradford S.A., 1994. *3DADE: A computer program for evaluating three-dimensional equilibrium solute transport in porous media.* Research Report No. 134, Riverside, Cal.: USDA-ARS U.S. Salinity Laboratory.

Li J.B., Huang G.H., Chakma A., Zeng G.M., and Liu L., 2003. Integrated fuzzy-stochastic modeling of petroleum contamination in subsurface. *Energy Sources,* 25: 547–563.

Li M.H., Cheng H.P., and Yeh G.T., 2005. An adaptive multigrid approach for the simulation of contaminant transport in the 3D subsurface. *Computers & Geosciences*, 31 (8): 1028-1041.

Liu L., Cheng S.Y., and Guo H.C., 2004. A simulation-assessment modeling approach for analyzing environmental risks of groundwater contamination at waste landfill sites. *Human and Ecological Risk Assessment,* 10:373–388.

Liu C. L., Wang M. K., Chang T. W. and Huang C. H., 2006. Transport of cadmium, nickel and zinc in Taoyuan red soil using one-dimensional convection-dispersion mode. *Geoderma,* 131(1-2): 181-189.

MacKenzie L.D., and Susan J.M., 2008. *Principles of environmental engineering and science*. Mcgraw-Hill Higher Education, New York.

Maqsood I., Li J.B., and Huang G.H., 2003. Inexact multiphase modeling system for the management of uncertainty in subsurface contamination. *Practice Periodical of Hazardous, Toxic and Radioactive Waste Management (ASCE)*, 7(2): 86–94.

Markstrom S.L., Regan R.S., Hay L.E., Viger R.J., Webb R.M.T., Payn R.A., and LaFontaine J.H., 2015, *PRMS-IV, the precipitation-runoff modeling system, version 4: U.S. Geological Survey Techniques and Methods.* Book 6, Chap. B7, 158 p., http://dx.doi.org/10.3133/tm6B7.

Maxwell R.M., 1998. *Understanding the effects of uncertainty and variability on groundwater-driven health risk assessment.* Ph.D. dissertation, University of California.

McLaughlin M.J., Hamon R.E., McLaren R.G., Speir T. W., and Roger S.L., 2000. Review: a bioavailability-based rationale for controlling metal and metalloid contamination of agricultural land in Australia and New Zealand. *Australian Journal of Soil Research,* 38 (6): 1037–1086.

MDDELCC (Ministère du Développement durable, de l'Environnement et de la Lutte contre les changements climatique), 2017. *Politique de protection des sols et de réhabilitation des terrains contaminés.* Quebec, Canada.

MEF (Ministry of the Environment, Finland), 2007. *Government decree on the assessment of soil contamination and remediation needs* (214/2007, March 1, 2007).

Millington R.J., and Quirk J.M, 1960. Transport in porous media. *Transactions International Congress of Soil Science, Adelaide, S.A.,* 7(1): 14-24.

Mills A.W., and Thomas G.W., 1985. Rainfed retention probabilities computed for different cropping-tillage systems. *Agricultural Water Management,* 15: 61–7.

Minsker B.S., and Shoemaker C.A., 1998. Quantifying the effects of uncertainty on optimal groundwater bioremediation policies. *Water Resources Research,* 34, 2626–3615.

Mizumura, K., 1992. *Nonlinear analysis of rainfall and runoff process: Catchment runoff and rational formula.* Water Resources Publications, Highlands Ranch, CO, 128–144.

Mizumura, K., 2006. Analytical solutions of nonlinear kinematic wave model. *Journal of Hydrologic Engineering*, 11 (6): 539–546.

Mohamed A.M.O., and Cote K., 1999. Decision analysis of polluted sites—a fuzzy set approach. *Waste Management,* 19: 519–533.

Morbidelli R., Corradini C., Govindaraju R.S., 2006. A field-scale infiltration model accounting for spatial heterogeneity of rainfall and soil saturated hydraulic conductivity. *Hydrological Processes,* 20 (7): 1465– 1481.

NAP (National Academy Press), 2001. *Dietary reference intakes for vitamin A, vitamin K, arsenic, boron, chromium, copper, iodine, iron, manganese, molybdenum, nickel, silicon, vanadium, and zinc*. Washington, D.C..

NOAA (National Oceanic and Atmospheric Association), 2007. *Nonpoint source pollution*. Washington D.C..

NSC (National Safety Council), 2009. *Lead poisoning*. Retrieved 21 August, 2017, from http://www.nsc.org/news resources/Resources/Documents/Lead Poisoning.pdf.

Plum L.M., Lothar R., and Hajo H., 2010. The Essential Toxin: Impact of Zinc on Human Health. *International Journal of Environmental Resource and Public Health,* 7 (4): 1342–1365.

Qin X.S., and Huang G.H., 2009. Characterizing uncertainties associated with contaminant transport modeling through a coupled fuzzy-stochastic approach. *Water, Air & Soil Pollution,* 197 (1-4): 331–348.

Rattan R.K., Datta S.P., and Chhonkar P.K., 2000. *Annual report on the ICAR AP Cess Fund Scheme on heavy metals in sewage effluent –irrigated soils and their utilization by crops.* Division of Soil Science and Agricultural Chemistry, IARI, New Delhi.

Reddy K.R., Tao X., and Sara D., 2014. Removal of heavy metals from urban stormwater runoff using different filter materials. *Journal of Environmental Chemical Engineering,* 2: 282–292.

Revitt M.D., Lian L., Frédéric C., and Martin F., 2014. The sources, impact and management

of car park runoff pollution: A review. *Journal of Environmental Management,* 146: 552-567.

Rousseau M., Olivier C., Olivier D., Fabrice D., and Francois J., 2012. *Overland flow modeling with the Shallow Water Equation using a well balanced numerical scheme: Adding efficiency or just more complexity.* HAL.

Rumynin V. G., 2015. *Overland Flow Dynamics and Solute Transport.* Springer International Publishing Switzerland.

Shackelford C.D., and Lee J.M., 2005. Analyzing diffusion by analogy with consolidation. *Journal of Geotechnical and Geoenvironmental Engineering,* 13 (11): 1345-1359.

Sharma P.P., Gupta S.C., and Foster G.R., 1995. Rindrop-induced soil detachment and sediment transport from interrill areas. *Soil Science Society of America Journal,* 59: 727–734.

Shigaki F., Sharpley A., and Prochnow L.I., 2007. Rainfall intensity and phosphorus source effects on phosphorus transport in surface runoff from soil trays. *Science of The Total Environment,* 373 (1): 334-43.

Šimůnek J., Šejna M., Saito H., Sakai M., and M. Th. van Genuchten, 2013. *The Hydrus-1D Software Package for Simulating the Movement of Water, Heat, and Multiple Solutes in Variably Saturated Media, Version 4.17, HYDRUS Software Series 3.* Department of Environmental Sciences, University of California Riverside, Riverside, California, USA, 342.

Smith R.E., and Goodrich D.C., 2000. Model for rainfall excess patterns on randomly heterogeneous area. *Journal of Hydrological Engineering,* 5: 355–362.

Srinivasan V., Clement T.P., and Lee K.K., 2007. Domenico solution-is it valid? *Ground Water,* 45 (2): 136-146.

Theodore L., and Dupont R.R., 2012. *Environmental health and hazard risk assessment: Principles and calculations.* CRC Press, Boca Raton, FL.

Tong J., Hu B.X., Yang J., and Zhu Y., 2016. Using a hybrid model to predict solute transfer

from initially saturated soil into surface runoff with controlled drainage water. *Environmental Science and Pollution Research,* 23 (12): 44-55.doi: 10.1007/s11356-016-6452-4.

UNESCO, 1975. *A hydrologic model with physically realistic parameters*. Bratislava Symposium, International association of hydrological science, 115.

USEPA (US Environmental Protection Agency), 1989. Risk Assessment Guidance for Superfund, vol. I: Human Health Evaluation Manual (Part A). Office of Emergency and Remedial Response, EPA 540/1-89/002, Washington, DC.

USEPA (US Environmental Protection Agency), 1992. *Guidelines for Exposure Assessment.* USEPA 600Z-92/001, Risk Assessment Forum, Washington, DC.

USGS (U.S. Geological Survey), 2008. *Runoff*. Retrieved 21 August, 2017, from URL: http://water.usgs.gov/edu/runoff.html.

Uusitalo L., Annukka L., Inari H., and Kai M., 2015. An overview of methods to evaluate uncertainty of deterministic models in decision support. *Environmental Modelling & Software,* 63: 24-31.

van Genuchten M.Th., 1981. Analytical solutions for chemical transport with simultaneous adsorption, zero-order production and first-order decay. *Journal of Hydrology,* 49 (3-4): 213-233.

Wallach R., William A.J., and William F.S., 1988. Transfer of chemical from soil solution to surface runoff: a diffusion-based soil model. *Soil Science Society of America Journal,* 52: 612–617.

Ward A.D., and Stanley W. T., 2003. *Environmental Hydrology.* Second Edition CRC Press, Boca Raton, FL.

World Weather Online, 2013. Retrieved 21 August, 2017 from https://us.worldweatheronline.com/auby-weather-averages/nord-pas-de-calais/fr.aspx.

Wu H., and Chen B., 2014. Using statistical and probabilistic methods to evaluate health risk assessment: A case study. *Toxics,* 2: 291-306. doi:10.3390/toxics2020291

Wuana R.A., and Okieimen F.E., 2011. Heavy metals in contaminated soils: A review of

sources, chemistry, risks and best available strategies for remediation. *International Scholarly Research Notices: Ecology,* 2011.

Yang A.L., Huang G.H., and Qin X.S., 2010.An integrated simulation-assessment approach for evaluating health risks of groundwater contamination under multiple uncertainties. *Water Resources Management*, 24: 3349–3369.

Yang T., Wang Q., Wu L., Zhao G., Liu Y., and Zhang P., 2016. A mathematical model for soil solute transfer into surface runoff as influenced by rainfall detachment. *Science of The Total Environment,* 590-600. doi: 10.1016/j.scitotenv.2016.03.087.

Zhang X., Shia R.L., and Yuk L.Y., 2013. Jovian stratosphere as a chemical transport System: benchmark analytical solutions. *The Astrophysical Journal*, 767 (2): 172-187.

Zhang K.R., Zeng Q.Y., Enrico Ziob, and Li X.Y., 2016. Measuring reliability under epistemic uncertainty: Review on non-probabilistic reliability metrics. *Chinese Journal of Aeronautics,* 29 (3): 571-579.

Zhu H., Xu Y.Y., Yan B.X., and Guan J.N., 2012. Snowmelt runoff: A new focus of urban nonpoint source pollution. *International Journal of Environmental Research and Public Health,* 9 (12): 4333–4345.